UNIVERSITY OF CALIFORNIA,
IRVINE

EEG studies of the human brain motor system--
New insights into learning and plasticity

DISSERTATION

submitted in partial satisfaction of the requirements
for the degree of

DOCTOR OF PHILOSOPHY

in Biomedical Sciences

by

Jennifer Wu

Dissertation Committee:
Professor Steven C. Cramer, Chair
Professor Ramesh Srinivasan
Professor David J. Reinkensmeyer

2015

DEDICATION

To the superheroes.
For being so super.

TABLE OF CONTENTS

LIST OF FIGURES

LIST OF TABLES

ACKNOWLEDGMENTS

Many, many innumerable thanks first to my dissertation advisor and committee chair, Professor Steven C. Cramer for his expert guidance, dedicated mentorship, and for sharing his ever-expanding knowledge which have molded me into the scientist I am today. Your unrelenting enthusiasm for research and passion for improving stroke care are a model that aspire to and hope to emulate in my future career. In addition, many thanks to Professor Ramesh Srinivasan, part two of my advisor dynamic duo; my training would have been wholey incomplete without your invaluable input as UCI's EEG-guru-in-residence.

I would also like to thank Professor David J. Reinkensmeyer who has followed and supported my work throughout these last 4 years. Also, I would like to thank Professors Leif Havton and Frithjof Kruggel for their insights and feedback at my advancement.

Special thanks to the fabulous human beings of the Cramer lab who have provided unending support, laughs, and fun, and served as superb meal companions during this journey. To Erin, Kristin, Franzi, Jessica, Vu, Lucy, Jill Stewart, Jill See, Alison, Renee, Jeff, Robert, Sarvy, Arshie, Nikki, and Kinnari, so many thanks and kudos for your expert knowledge, shrewd advice, sympathetic ear, entertaining dialogue, and endless hours cleaning EEG data files. I am so grateful to have met all of your acquaintances and look forward to our next encounter.

An important thanks also to my fellow graduate students. I've met you all from across campus, including the Medical Scientist Training Program, Interdepartmental Neuroscience Program, and the department of Anatomy & Neurobiology. It has truly been my pleasure to be a peer to all of you wonderful and brilliant brains.

Financial support for these projects were provided by the University of California, Irvine Medical Scientist Training Program, the UC Irvine Dean's Triumvirate Grant, the NIH Center for Research Resources (UL1 TR000153 and TL1 TR000148), the NIH National Institute for Neurological Disorders (R01 NS059909), the NIH Eunice Kennedy Shriver Institute of Child Health and Human Development (K24 HD074722 01), and the Stanley Behrens Public Impact Fellowship.

Finally, I would like to thank my parents, Justin and Joanna Wu, who came to this country with nothing but dreams, who are always available when I need advice, and who quietly deferred their vision for me to become a pharmacist or an electrical engineer, while I continue to seek (apparently) unending education. Thanks for being open arms and open ears when I have struggled through the difficult times. I am forever indebted to you both for the wonderful life you have provided for us.

CURRICULUM VITAE

Jennifer Wu

EDUCATION

2015 Ph.D., Biomedical Sciences, University of California, Irvine; Irvine, CA
2009 B.S., Biomedical Engineering, Washington University; Saint Louis, MO

RESEARCH EXPERIENCE

2010- Graduate student, Department of Anatomy & Neurobiology
University of California, Irvine; Irvine, CA
Research advisor: Steven C. Cramer, MD

2007-2009 Research technician, Mallinckrodt Institute of Radiology
Washington University in Saint Louis School of Medicine; Saint Louis, MO
Research advisor: Joel S. Perlmutter, MD

PUBLICATIONS

Ngo D, Sun Y, Genton MG, **Wu J**, Srinivasan R, Cramer SC, Ombao H. An exploratory data analysis of electroencephalograms using the functional boxplots approach. (In Review)

Wu J, Quinlan EB, Dodakian L, McKenzie A, Kathuria N, Zhou RJ, Ausberger R, See J, Le VH, Srinivasan R, Cramer SC. EEG connectivity measures are robust biomarkers of cortical function and plasticity after stroke. *Brain* (In press)

Wu J, Srinivasan R, Kaur A, Cramer SC. Resting-state cortical connectivity predicts motor skill acquisition. *Neuroimage*. 91: 84-90. PMID: 24473097

Cramer SC, **Wu J**, Hanson JA, Nouri S, Karnani D, Chuang TM, Le V. A system for addressing incidental findings in neuroimaging research. *Neuroimage*. 55(3): 1020-3. PMID: 21224007

Karimi M, Golchin N, Tabbal SD, Hershey T, Videen TO, **Wu J**, Usche JWM, Revilla FJ, Hartlein JM, Wernle AR, Mink JW, Perlmutter JS. Subthalamic nucleus stimulation-induced regional blood flow responses correlate with improvement of motor signs in Parkinson disease. *Brain*. 131(10): 2710-9. PMID: 18697909

PUBLICATIONS IN PREPARATION

Wu J, Srinivasan R, Quinlan EB, Solodkin A, Small SL, Cramer SC. Brain function and neural injury predict early impairment early after stroke.

Knapp F, **Wu J**, Kaur A, Valand K, Srinivasan R, Cramer SC. Connectivity predictors of short-term motor learning demonstrate specificity for training content.

CONFERENCE ABSTRACTS

Wu J, Srinivasan R, Solodkin A, Small SL, Cramer SC. Neurological correlates of brain function after acute stroke-- a dense array EEG study. International Stroke Conference; Nashville, TN, 2015

Wu J, Knapp F, Varzhapetyan N, Srinivasan R, Cramer SC. Cortical connectivity at rest predicts consolidation of a novel motor skill. 44th Annual meeting of the Society for Neuroscience; Washington, DC, 2014

Wu J, Kathuria N, Burke E, Dodakian L, See J, McKenzie AL, Srinivasan R, Cramer SC. Cortical connectivity is a powerful predictor of motor recovery in chronic stroke. American Heart Association Scientific Sessions: Best of Abstracts; Chicago, IL, 2014

Wu J, Cramer SC. Cortical connectivity is a predictor of motor recovery in chronic stroke. Associated Graduate Student Symposium; Irvine, CA, 2014

Wu J, Kathuria N, Burke E, Dodakian L, See J, McKenzie AL, Srinivasan R, Cramer SC. Cortical connectivity is a powerful predictor of motor recovery in chronic stroke. International Stroke Conference; San Diego, CA, 2014

Wu J, Srinivasan R, Kathuria N, Dodakian L, See J, Cramer SC. Cortical connectivity predicts motor impairment and improvement with Telerehabilitation therapy in chronic stroke. 43rd Annual meeting of the Society for Neuroscience; San Diego, CA, 2013

Wu J, Kaur A, Srinivasan R, Cramer SC. Cortical connectivity predicts short-term motor skill acquisition. Annual National MD/PhD Student Conference; Keystone, CO, 2013

Wu J, Kaur A, Srinivasan R, Cramer SC. Cortical connectivity predicts short-term motor skill acquisition. 19th Annual meeting of the Organization for Human Brain Mapping; Seattle, WA, 2013

Liu VB, Winter WR, **Wu JC**, Srinivasan R, Cramer SC. Electrical Neuroimaging in Acute Stroke: a pilot study. 18th Annual meeting of the Organization for Human Brain Mapping; Beijing, China, 2012

Cramer SC, **Wu J**, Hanson JA, Nouri S, Karnani D, Chuang TM, Le V. A system for addressing incidental findings in neuroimaging research. 17th Annual meeting of the Organization for Human Brain Mapping; Quebec City, Canada, 2011

ACADEMIC AND PROFESSIONAL HONORS

2015	Public Impact Fellowship University of California, Irvine/Stanley Behrens Foundation
2014	Graduate Merit Fellowship Center for Cognitive Neuroscience and Engineering, University of California, Irvine
2014	Dean's Prize, School of Medicine Associated Graduate Students Symposium, University of California, Irvine
2013-2015	Pre-doctoral TL-1 Scholars Training Program Institute for Clinical & Translational Science, University of California, Irvine NIH National Center for Advancing Translational Sciences: TL1 TR000148
2009	Alpha Eta Mu Beta, Biomedical Engineering Honor Society Washington University
2005-2009	Calvin M. Woodward Fellowships School of Engineering, Washington University
2005-2009	Mesmer Scholarship Washington University
2005-2009	National Merit Scholarship Washington University
2005-2009	Robert C. Byrd Honors Scholarship Program State of Oregon
2007	Undergraduate Scholarship Samaritan Albany General Hospital Auxiliary
2006-2007	Undergraduate Scholarship Raytheon Corporation
2005-2006	Martina Tesla Award Willamette Chapter, Society of Women Engineers

PROFESSIONAL MEMBERSHIPS

2013- Organization for Human Brain Mapping
2012- American Heart Association
2011- Society for Neuroscience

ABSTRACT OF THE DISSERTATION

EEG studies of the human brain motor system--
New insights into learning and plasticity

By

Jennifer Wu

Doctor of Philosophy in Biomedical Sciences

University of California, Irvine, 2015

Professor Steven C. Cramer, Chair

Stroke is highly heterogeneous, with patients demonstrating variation in infarct characteristics, baseline impairment, degree of spontaneous recovery, and response to treatment. There is ample literature on the neural correlates of post-stroke variation. However previous methods incompletely characterize inter-individual differences and have limitations for clinical adoption. The studies herein examine the use of dense-array electroencephalography (EEG) measures of brain function for predicting response to motor training in non-stroke control and stroke populations. In Chapter 2, a partial least squares regression (PLS) model found resting-state connectivity was a robust predictor of subsequent response to motor training (R^2 = 0.81) in non-stroke individuals. Results in Chapter 2 were confirmed in Chapter 3, and extended when the same resting-state connectivity measure was shown to demonstrate specificity with respect to the content of motor training. Specifically, individuals with increased connectivity between electrodes overlying left primary motor cortex (M1) and left premotor cortex (PM) showed greater improvement with training of the motor sequence learning task, but

lesser improvement with training of the visuospatial learning task. The same EEG methods were applied to a chronic stroke population in Chapter 4. Separate PLS models found baseline resting-state connectivity was related to baseline impairment (R^2 = 0.78) and predicted motor gains across the 4 week arm motor therapy (R^2 = 0.79). Finally, in Chapter 5, similar EEG methods were used to identify the neural correlates of impairment in acute stroke (0 - 12 days). A PLS model showed relative delta power across the brain accounted for a substantial proportion of variance in early post-stroke impairment state (R^2 = 0.72). Furthermore, the neural correlates of acute stroke impairment were found to vary according to infarct size subgroup; the model for small strokes was driven by ipsilesional signals, whereas the model for large strokes was driven by contralesional signals. In sum, the current studies demonstrate that PLS modeling EEG measures of resting brain function provide useful insights into basal differences in brain state which can be used to predict the capacity of an individual brain to undergo plasticity and thus respond to motor training in non-stroke and stroke populations.

INTRODUCTION

Stroke is the leading cause of serious long-term adult disability in the United States[1]. There are an estimated 6,600,000 adults in the United States who have had a stroke[2], and many of these individuals live with persistent physical and cognitive deficits that substantially reduce their quality of life. Over the next 15 years, the combined direct and indirect costs related to stroke care, including inpatients services, rehabilitation, home health care, and productivity loss, are expected to exceed 185 billion dollars[2]. With stroke-related disabilities ranging hemiparesis, cognitive deficits, depression, aphasia, and visual impairment[3], stroke represents a significant psychosocial and economic burden. As a result, there is a pressing need for novel methods that reduce disability and allocate resources after stroke.

After stroke, patients demonstrate significant variability in degree of impairment[4], response to treatment[5], and long-term outcome[2]. For example, in acute stroke, only a portion of patients experience successful recanalization following tissue plasminogen activator (tPA) therapy[6,7]. In chronic stroke, experimental treatments provide highly variable outcomes across patients[8–10]. Although baseline measures and clinical and demographic variables partially inform long-term outcome after stroke[11,12], surrogate measures of neural injury and neural function may be instrumental in elucidating the pathophysiology that underlies stroke heterogeneity, informing treatment decisions after stroke, and maximizing long-term outcome.

Precise measures of neural injury are presently easily obtained with modern CT and MRI. However, the same is not true for measuring brain function. Although functional MRI and PET, and other related methods, are able to assess brain function, these neuroimaging techniques have significant limitations for broad clinical adoption, including cost, accessibility, and safety. As a result, improved methods for measuring brain function that address these limitations are needed.

The studies that comprise the dissertation herein sought to establish a safe, non-invasive, accessible, and inexpensive method for characterizing brain function, particularly in clinical settings that are traditionally difficult, like acute stroke. Specifically, the current studies examine whether dense-array electroencephalography (EEG) measures of brain function provide useful insights into brain function as they pertain to cortical motor system function and plasticity. In addition, several recent studies have shown a multimodal approach accounting for both neural injury and neural function provides a more comprehensive understanding of post-stroke impairment[13–16]. Therefore, studies of acute and chronic stroke patients examined multimodal models of post-stroke impairment that included EEG measures of neural function and MRI measures of neural injury.

The first aim examined whether resting-state EEG measures of neural function, particularly a measure of cortico-cortical connectivity, could be used to predict subsequent motor system plasticity in healthy control subjects who acquire a novel motor skill (Chapter 2). Then, the first aim was extended in a secondary study that

examined whether the same cortico-cortical connectivity predictors of motor skill acquisition demonstrate specificity with respect to the content of motor training (Chapter 3). In the second aim, the same method was used as a marker of baseline arm motor impairment, biomarker of improvement, and predictor of treatment effects in a group of patients with chronic stroke undergoing home-based arm rehabilitation (Chapter 4). Finally, the third aim examined neural correlates of impairment in hospitalized patients who underwent bedside EEG during early stroke recovery (Chapter 5). Together, these studies demonstrate EEG measures of neural function in both healthy control and stroke populations provide useful insight into inter-subject heterogeneity in motor system plasticity. Importantly, these studies demonstrate robust prediction of response to motor training and provide insights into the neural circuits that underlie variable response to motor training. The data from this doctoral work strongly suggest that EEG measures of neural function, particularly in combination with measures of neural injury, provide added-value as part of clinical decision making in post-stroke treatment and long-term planning.

CHAPTER 1

Background

THE HETEROGENEITY OF STROKE

The heterogeneity of stroke remains a major focus of ongoing research. After stroke, patients demonstrating wide ranging variability across multiple domains, including infarct size and location, baseline impairment, response to treatment, and long-term outcomes[2]. For example, in acute stroke, approved treatments mostly involve intervention at the artery or blood clot. However, studies report highly variable rates of clinically significant improvement with these treatments with outcomes dependent on the selected primary behavioral endpoint, time to treatment, age, presence of comorbid conditions, and other baseline factors[17–20]. Experimental interventions that are being examined in the chronic phase of stroke recovery, including pharmacologic intervention[21], novel methods of physiotherapy[22,23], and robotic-assisted rehabilitation[8,10,24], also report significant variability in individual response to treatment. Stroke heterogeneity represents a major obstacle both for clinical decision-making in individual patients and for researchers studying novel therapies in patient cohorts. As a result, methods that are able to predict individual response to treatment or stratify patient cohorts to reduce heterogeneity in study populations may be key to maximizing individual outcomes and resolve treatment effects[25].

Baseline impairment is a commonly cited predictor of spontaneous recovery, response to treatment, and long-term outcome. Overall, greater baseline stroke severity is

associated with poorer outcome, including both increased morbidity and mortality in the long-term[26–28]. In the acute rehabilitation setting, lower baseline impairment has been correlated with greater treatment-related gains[29], shorter length of stay[30], and lower impairment at discharge[31,32]. Similarly, better clinical status at the acute phase is predictive of reduced impairment at 3 months post-stroke[33,34]. Although baseline behavior measures contribute to predictive models of response to treatment and long-term outcome, effect sizes are generally small to moderate[26,33] and therefore, incompletely characterize inter-individual differences.

Other clinical factors, including the presence of comorbid conditions, concomitant diagnoses, age, race, and ethnicity also contribute to stroke recovery and response to treatment. Large-scale retrospective studies report the presence of comorbid conditions, including atrial fibrillation[35] and diabetes mellitus[29,35], were predictive of greater impairment. Concomitant symptoms, including patients who demonstrate impairments in more than one domain and the development of post-stroke depression, show poorer long-term outcome. For example, baseline cognitive deficits are associated with longer recovery and greater impairment[30,32,36], and patients with higher levels of depressive symptoms showed reduced improvement during acute inpatient rehabilitation and longer length of stay[37]. Increased age, Hispanic ethnicity, and African American racial background have also been associated with poorer outcome[35,38]. Specifically, patients younger than 55 years old demonstrate the better recovery compared to their older counter-parts[31]. Although several clinical and demographic characteristics contribute to

variance in post-stroke recovery and response to treatment, similar to baseline impairment status, effect sizes are small.

NEUROIMAGING PREDICTORS OF POST-STROKE RECOVERY

Measures that characterize the structure or function of the biological target of interest, for instance neuroimaging, are likely provide greater insight into the capacity for reorganization compared to bedside measures of behavior[39]. Although neuroimaging measures are not commonly used to inform clinical decision making in rehabilitation care after stroke, such surrogate measures are routinely used in other areas of medicine to inform clinical care. Examples include levels of HIV RNA as a marker of progression to AIDS, blood pressure as a marker of cardiovascular health, levels of hemoglobin A1c for diagnosing and management of diabetes mellitus, and tumor size for prediction of survival. In the acute stroke setting, examples that have recently been advanced include the use of the perfusion-diffusion mismatch[40], the clinical-diffusion mismatch[41], and perfusion imaging to direct acute intervention[42]. In the setting of stroke rehabilitation and recovery, preliminary evidence to date suggests that these surrogate measures may provide an improved picture of neural structure and neural function, and are increasingly being evaluated as potential predictors of response to treatment. Furthermore, neuroimaging based measures are easier to standardize, and as a result provide greater inter-rater reliability compared to behavioral endpoints.

Studies that examine measures of neural injury have found greater degree of neural injury predicts poor prognosis. Among the most commonly examined measure are

lesion volume, in which larger infarcts, and thus a greater degree of neural injury, are associated with both greater impairment and poor long-term outcome[43–45]. However, the these relationships may show inconsistent utility when patients reach rehabilitation and more chronic phases of recovery[9,46].

The brain, as a mass entity, is a combination of many interacting and inter-connected systems, and various stroke injuries likely affect each of these systems differently. Therefore, a system-specific approach for measuring neural injury may improve prediction of an individual brain's potential to respond to a therapy designed to promote neuroplasticity of a specific neural system. As an example, in the motor system, measures that characterize damage to the descending corticospinal tract from M1 demonstrate improved prediction of treatment-induced motor gains in patients with chronic stroke, compared to baseline impairment and infarct volume[15,47,48]. In addition, other structural measures such as gray matter density and gray matter volume in secondary motor regions, have also been successfully used to predict response to treatment[49,50].

Functional measures of brain state have also been used to characterize the post-stroke brain. In general, better recovery has been linked to normalization of brain activation patterns[51]. For instance, in the motor system, greater recovery has been linked to return of activation in the primary sensorimotor cortex[52], while resolution of attentional deficits are linked to restitution of activity in right cortical areas[53,54] and return of language function has been correlated with greater activity in left temporal regions[55,56].

Conversely, persistent deficits after stroke have been negatively correlated with compensatory mechanisms as demonstrated by increased activation in homologous contralateral regions or secondary cortical regions[52].

Although there is a general consensus regarding the neural correlates of recovery after stroke, there is some contention regarding the optimal brain state which predicts greater recovery, particularly in response to treatment. In a study by Cramer et al.[57], individuals who experienced the greatest gains with rehabilitation therapy had relatively decreased motor cortex activation at baseline, suggesting these patients were able to recruit underutilized motor cortex substrate to support behavioral gains during therapeutic intervention. However, in a study of patients undergoing constraint-induced movement therapy, greater baseline activation of sensorimotor cortex was predictive of greater gains[58]. The apparent disparity between these studies may reflect different but synergistic compensatory mechanisms, which are incompletely characterized with focal measure of brain function.

Connectivity-based measures of brain function, as compared to regional assessments of brain activity, are better able to represent inter-regional complexity of neuronal networks. As a result, these measures demonstrate an improved relationship with several types of behavior[59]. To date, the limited studies that have examined connectivity predictors of recovery find increased ipsilesional connectivity is a marker of better outcomes[60,61]. Furthermore, behavioral deficits have been associated with reduced connectivity within the corresponding cortical network[62]. Thus, patients in whom there is

greater ipsilesional connectivity and the cortical network is able to further recruit ipsilesional resources, either ipsilesional motor or ipsilesional sensorimotor cortex, greater behavioral gains are observed.

Several recent studies also make the case for multimodal predictive models that include both structural and functional measures of brain state. In the seminal study by Stinear and colleagues[15], a predictive model that combined both a functional and structural measure of corticospinal tract integrity outperformed models that included either measure alone. Aligned with these results, Carter et al.[14], report both structural damage to the descending motor tracts and upstream cortical dysfunction in bilateral motor cortices contribute to post-stroke motor dysfunction. Furthermore, stroke subtype (lacune compared to non-lacune) was reported to have a significant effect on the relationship between baseline brain state and prediction of therapy-induced gains[13]. Together, the present studies strongly suggest predictive models that include both functional and structural measures of brain state are required in order to optimally characterize post-stroke recovery potential and predict response to treatment.

EEG ASSESSMENTS OF BRAIN FUNCTION AFTER STROKE

As the first method for non-invasive measure of brain function in humans, EEG has been used to characterize the electrophysiologic changes associated with cerebral ischemia for more than five decades[63–68]. Although neuroimaging methods with improved spatial resolution, such as PET and MRI, have largely supplanted EEG for the diagnosis of stroke, EEG is still utilized in several clinical settings that include

localization of seizure focus[69], neuromonitoring during carotid endarterectomy[70], and diagnosis of sleep disorders[71]. Indeed, EEG has several characteristics that are advantageous for rapid, non-invasive, bedside examination of brain function, and recent hardware advances, including dry-electrode, wireless systems, provide vital improvements for brain function assessment during the first minutes to hours of acute stroke. The present review briefly summarizes the major findings from electromagnetic assessments of brain function in settings of stroke, with a focus on EEG studies in the early phase of stroke recovery.

OSCILLATIONS FROM THE BRAIN

Scalp potentials recorded in the electroencephalogram (EEG) provide a macroscopic view of mass neuronal function[72]. Overall, the majority of this scalp electric potential is believed to originate from the cortex, however, there is significant evidence that both cortico-cortical and thalamo-cortical interactions contribute to the observed EEG signal[73,74]. At the microscopic scale, the EEG signal primarily reflects the activity of pyramidal neurons of the cortex. Then, within each layer of the cortex, low frequency portions of the EEG signal are said to derive from layers II-IV of the cortex and faster frequencies from layers IV and V of the cortex[75].

The high temporal resolution of the EEG signal also allows frequency resolution of mass neuronal activity. Overall, the EEG signal is commonly subdivided into 5 broad frequency bands, in increasing frequency: delta, theta, alpha, beta, and gamma ranges. Delta band oscillations, ranging from 1 Hz to 4 Hz, are most often linked to deep sleep

or neural injury or other conditions of compromised neuronal function[76]. Although, recent findings suggest modulation of delta oscillations may also play a role in attentional processes[77,78]. For oscillations that range from 4 – 7 Hz, the theta band has been associated with neuronal processes underlying working memory and consolidation of visuomotor learning[79,80]. Alpha band activity, which include oscillations in the 8 – 12 Hz range, is the predominant rhythm of the awake, resting human brain, and has been associated with numerous cognitive processes[81], including working memory[82], attention[83,84], conscious perception[85], and long-term memory formation[86]. In addition, disruptions of alpha band oscillations have been observed in several neuropsychiatric disorders, such as brain tumors[87,88], schizophrenia[89], Alzheimer's disease[90], and stroke[91,92]. Oscillations of the beta band range from 13 Hz to 30 Hz and are associated with motor production and motor imagery[93,94]. Finally, gamma oscillation, which include all EEG signals at frequencies higher than 30 Hz have been associated with sensory and attentional selection[95].

ISCHEMIC INJURY RESULTS IN GLOBAL CHANGES IN BRAIN FUNCTION

Neuroimaging studies that describe the neurophysiologic differences between the diseased and injured brain and the control, non-injured brain provide insights into the neurobiological changes that underlie dysfunction and elucidate the physiology of specific brain regions. Indeed, the beginnings of neuroanatomy and physiology are closely linked to lesion mapping studies[96]. During stroke, ischemia leads to decreased cerebral blood and downstream neural injury, initiating a cascade of molecular and cellular changes[51]. In addition, reorganization of neural networks may lead to

recruitment of secondary regions to enhance reduced function in stroke-injured brain regions[97–99].

EEG changes associated with acute stroke occur within seconds of ischemic injury, and have been associated with specific thresholds of progressively decreasing cerebral blood flow (CBF)[75]. For example, in a study of 31 patients undergoing continuous EEG monitoring during carotid endarterectomy[100], less severe ischemia was associated with reduced amplitude of faster frequency activity with increased amplitude of slower frequency activity. In contrast, more severe ischemia was associated with reduced amplitude across the frequency spectrum. Furthermore, frequency-specific changes in EEG rhythms may be related to the injury sub-type or location. In a review by Faught[92], the loss of fast rhythm activity was linked to gray matter ischemia, while the loss of slow rhythm activity was linked tied to white matter ischemia leading to functional deafferentation. Conversely, van Putten and colleagues reported that while injury to the left hemisphere resulted in a reduction of fast activity, patients with right hemisphere lesions were more likely to demonstrate both a reduction of fast activity with a relative increase in slow activity[70]. Thus, frequency-specific EEG changes may provide insight into the degree and location of brain injury.

An increase in delta (1-3 Hz) activity is one of the most commonly cited EEG changes during acute stroke[64,101–104]. This increase in delta activity has been described not only as a general increase in both ipsilesional and contralesional delta power[102,105], but also as an increase in delta-alpha ratio[106] and an increase in delta-theta-alpha-beta

ratio[101,107] compared to controls. Although increased delta activity has been described in both ipsilesional and contralesional hemispheres, the degree of delta increase is generally higher in ipsilesional versus contralesional electrodes when compared to control values[101–103,108], with increased ipsilesional delta activity particularly apparent in electrodes that directly overlie ischemic core[66,109,110]. Thus, it unsurprising to note there is some evidence that source localization of delta foci at the scalp may have utility as a method for the localizing cortical infarcts[111].

Changes in background EEG activity, particularly of alpha rhythms, are also widely reported during acute stroke. In patients who were examined within 24 hours of stroke onset, there was a significant decrease in background activity of occipital electrodes overlying the ischemic hemisphere compared to contralesional electrodes[112,113]. Similarly, global inter-hemispheric asymmetry of background activity has also been associated with focal neurologic deficits[65]. However, while changes in background activity are commonly observed in conjunction with ischemic injury, it is important to note that normal background activity has been observed with smaller lesions[114]. More specifically, changes in background activity often are a reference to changes in alpha activity, which is the predominant rhythm of the awake, relaxed human cortex[115]. In the stroke injured brain, there is a relative decrease in alpha activity compared to controls[101,104], with relatively higher alpha activity in the contralesional compared to the ipsilesional hemisphere[108]. In addition, beta activity is also increased in contralesional compared to ipsilesional electrodes[108].

DEGREE OF BRAIN SLOWING CORRELATES WITH IMPAIRMENT STATE

Patients demonstrate huge variability following stroke, beginning with baseline impairment status. Surrogate markers of impairment state can provide insight into the neurobiology that underlies this post-stroke variability. For example, in the motor system, increased corticospinal tract integrity in descending fibers of the precentral gyrus is a marker of reduced motor impairment in patients with chronic stroke[116]. Behavioral motor status has also been associated with activation map size of the ipsilesional motor cortex[117,118]. Likewise, in the language system, degree of injury to dorsal and ventral language pathways was related to performance of repetition or comprehension tasks[119].

The relative degree of brain slowing, as indicated by frequency-specific changes in brain activity, have been correlated with both degree of impairment and severity of neural injury[92,103,120]. However, results are mixed across studies. While delta power was correlated with both NIHSS score and lesion volume in one study by Assenza and colleagues[120], an earlier study by Zappasodi, et al., found delta activity was correlated with lesion volume by not acute clinical status[103]. Although, it is worth noting that these contradictory results across studies may reflect methodological differences as one study examined EEG-derived scalp delta activity while the other study used MEG-derived delta dipole strength. Other frequency-specific measures of brain activity have also been correlated with impairment state after stroke. Individuals with relatively higher alpha power have relatively lesser impairment compared to their counter-parts[106], while greater increased ipsilesional gamma was correlated with both lower NIHSS score and

higher Barthel Index score[102]. Also, a study by Visser, et al., suggested the degree of neural injury was related frequency-band specific changes in brain activity. Where greater cerebral ischemia was indicated by both decreased fast activity and increased slow activity, smaller ischemia was characterized by decreased fast activity without alterations in slow activity[121].

In EEG studies, ratios of activity in limited frequency bands are used to describe the relative predominance of slower frequency activity as a proportion of faster frequency activity. The DTABR is defined as the sum of delta and theta activity divided by the sum of alpha and beta activity. Overall, higher DTABR values have been associated with increased impairment[107,122]. Similarly, higher DAR values, which is a ratio of delta and alpha activity, are also correlated with increased impairment[106]. These ratios of frequency-specific brain activity have also been correlated with severity of injury; patients with a greater degree of brain injury demonstrate proportionately greater brain slowing, as represented by increased DTABR[107].

Impairment status and degree of neural injury have also been correlated with a variety of measures that characterize inter-hemispheric asymmetry of brain function, with greater asymmetry associated with poorer clinical status[123]. The Brain Symmetry Index (BSI) is a frequency-specific measure of inter-hemispheric differences in spectral power across homologous electrodes. Larger BSI values, indicating a greater degree of inter-hemispheric asymmetry have been correlated with both higher levels of impairment[70,124] and a greater degree of post-stroke disability[125]. Additionally, BSI have also been

correlated with severity of neural injury, such that a greater degree of functional asymmetry was observed in patients larger infarcts[68,107]. While both DTABR and BSI demonstrate utility as markers of post-stroke behavioral status and degree of neural injury, in studies that examined both metrics, BSI generally outperforms DTABR in correlations with NIHSS and infarct volume[68,122].

EVOLUTION OF BRAIN FUNCTION IN POST-STROKE RECOVERY

A biomarker is a surrogate measure of disease state, providing insight into molecular or cellular events that are difficult to measure directly[39,126]. Good biomarkers correlate with either clinical state or clinical evolution and reflect biological mechanisms of recovery. Identification of these markers can be useful for understanding variable response to treatment and for identifying promising biological targets in the development of novel interventions. For post-stroke motor impairment, both spontaneous recovery and treatment-induced gains have been associated with a shift of activation from the contralesional motor system to the ipsilesional motor cortex[52,127].

Longitudinal EEG studies of stroke show clinical improvement parallels normalization of EEG measures. In a study by De Weerd, et al., patients underwent serial EEG imaging across a 3 year period[128]. Overall, patients demonstrated the greatest clinical improvement in the first 3 months, and this recovery occurred in parallel with significant improvement in both frequency distribution and inter-hemispheric asymmetry of EEG signals. In contrast, both clinical status and EEG measures remained relatively stable over the subsequent 33 months. Similarly, overall reduction in ipsilesional delta power

with greater symmetry in both delta and theta power from acute measurement to assessment at 3 months post-stroke was observed in conjunction with clinical recovery[108]. Greater improvement has also been associated with normalization of higher frequency signals, with patients demonstrating significantly increased peak alpha frequency during recovery compared to acute stages[123].

Changes in EEG measures can even precede clinical changes. In single subject case studies, continuous EEG monitoring showed progressive deviations in EEG measures from normal values occurred prior to clinical signs of deterioration[129,130]. For example, in two patients with serial EEG and behavioral assessments clinical deterioration and subsequent death were preceded by an evolution of delta activity from an ipsilesional to a contralesional maxima[130]. Furthermore, increases in contralesional delta activity preceded development of DWI abnormalities by 9 hours and clinical signs of decline by > 24 hours. Additionally, a separate study of a patient with progressive cerebral edema found contralesional changes in EEG signals preceded the development of clinical signs of herniation by 6 hours.

Repeated EEG assessments before and after acute stroke interventions demonstrate normalization of EEG measures also parallel clinical improvement even across shorter time frames. As an exemplar case, in a patient who demonstrated significant clinical improvement with tPA injection, delta power (measured within minutes of reperfusion therapy) was significantly reduced compared to pre-reperfusion therapy values[109]. Furthermore, the degree of improvement in EEG parameters have been correlated with

the degree of clinical improvement. Indeed, in a group of patients with continuous EEG during r-tPA treatment, greater increases in the Brain Symmetry Index were correlated with greater improvements in NIHSS score[124].

DISRUPTION OF EEG MEASURES ACUTELY PREDICT POOR CLINICAL OUTCOME

Heterogeneity across stroke patients make prediction of long-term outcome a significant challenge. The ability to predict degree of spontaneous recovery and response to treatment could be useful for individualizing clinical decision making, stratifying patients to appropriate therapies, improving allocation of rehabilitation and financial resources, reducing variance in clinical trial to maximize power, and informing long-term care plans[25,131]. Although, behavioral measures in the acute stage are the most commonly used to predict long-term outcome after stroke, measuring brain function likely provides an improved picture of an individual's capacity of neural reorganization compared to bedside examination.

Patients with EEG measures close to normal values when assessed at baseline tend to demonstrate improved long-term outcome, while patients with wide-spread alterations in brain function typically demonstrate poorer outcomes. In group comparisons, patients with poorer outcomes had higher delta power and lower alpha power globally when assessed at admission[132]. Furthermore, the spatial extent of EEG abnormalities also predicts long-term recovery, with patients demonstrating a more limited focus of EEG abnormalities having better outcomes compared to patients who demonstrate diffuse

slowing and increased delta activity across the entire scalp[112]. Acute EEG assessments of brain function have also been used to predict clinical status. Overall, relatively lower slow rhythm activity, including both delta and theta ranges, is associated with decreased impairment and better function when assessed days and months later[68,106,122,133,134]. Prediction was further improved when a behavioral measure of impairment state at baseline was compared with contralesional delta power to predict 6 month NIHSS score[120]. Greater recovery has also been associated with greater symmetry of EEG signal at baseline, with the Brain Symmetry Index outperforming both baseline impairment status and age for predicting long-term outcome[122,125].

CONCLUSIONS

Electromagnetic measures of brain function after stroke demonstrate utility as biomarkers and predictors of post-stroke impairment state and long-term outcome. The reviewed studies suggest that improved behavioral status and better long-term outcome are associated with normalization of brain function. Specifically, these measures include, decreased slow frequency activity in delta and theta bands, increased faster frequency activity in alpha, beta, and gamma bands, and greater symmetry in EEG signals across all frequencies. However, a number of key limitations still exist. First, traditional, clinical EEG systems, although they demonstrate excellent temporal resolution and permit lengthy continuous assessments of brain function, are cumbersome for both the assessor and the assesse to perform. While recent developments in EEG hardware, including dry electrode and wireless systems[135–137], are promising, further study of these systems in clinical settings are needed. In addition,

although the current studies report moderate correlations between EEG measures and various behavioral measures, a significant proportion of variability remains unaccounted for. Recent studies suggest a multimodal approach, particularly those that include measures of inter-regional connectivity, better characterize stroke heterogeneity[13,14,138]. EEG measures of brain function provide key insights into the neurobiology of post-stroke impairment and variability in long-term outcome.

CHAPTER 2

Resting-state cortical connectivity predicts motor skill acquisition

ABSTRACT

Many studies have examined brain states in an effort to predict individual differences in capacity for learning, with overall moderate results. The present study investigated how measures of cortical network function acquired at rest using dense-array EEG (256 leads) predict subsequent acquisition of a new motor skill. Brain activity was recorded in 17 healthy young subjects during three minutes of wakeful rest prior to a single motor skill training session on a digital version of the pursuit rotor task. Practice was associated with significant gains in task performance (% time on target increased from 24% to 41%, $p < 0.0001$). Using a partial least squares regression (PLS) model, coherence with the region of the left primary motor area (M1) in resting EEG data was a strong predictor of motor skill acquisition ($R^2 = 0.81$ in a leave-one-out cross-validation analysis), exceeding the information provided by baseline behavior and demographics. Within this PLS model, greater skill acquisition was predicted by higher connectivity between M1 and left parietal cortex, possibly reflecting greater capacity for visuomotor integration, and by lower connectivity between M1 and left frontal-premotor areas, possibly reflecting differences in motor planning strategies. EEG coherence, which reflects functional connectivity, predicts individual motor skill acquisition with a level of accuracy that is remarkably high compared to prior reports using EEG or fMRI measures.

INTRODUCTION

Individuals demonstrate significant variability in motor learning[139,140]. The ability to predict an individual's learning skill could have utility in a number of settings, including clinical[141]. Previous studies have identified neural correlates of variability during motor learning[142], and both structural and functional neuroimaging methods have been evaluated as predictors of motor learning[143,144]. However, the ability to accurately predict learning differences, in healthy or diseased populations, remains modest, for example, with fMRI-derived resting-state connectivity accounting for 35%[145] to 66%[146] of inter-individual variability.

Recent resting-state studies have provided new inroads for measuring differences in brain function in relation to behavior across individual subjects[147]. Markers of brain function at rest are influenced by experience[148] and reflect the functional organization of brain networks that are selectively engaged during behavioral tasks. Organization of brain networks at rest has also been correlated with subsequent behavioral performance[149,150]. However, there is limited study of how inter-individual heterogeneity in brain functional connectivity at rest relates to learning and plasticity.

Combined EEG and fMRI studies have reported that specific combinations of EEG rhythms correspond with low frequency activity of specific resting-state networks[151]. Thus, EEG metrics also may be useful for characterizing brain states and relating them to behavioral variance. One potential metric is spectral power, which measures synchronization *within* cortical regions[72]. A recent EEG study found that a regional

measure of spectral power in a frontal electrode (Fz) and a parietal electrode (Pz) obtained early during training predicted 53% of the variance in subsequent motor learning[144]. An alternate EEG-based metric is spectral coherence, which measures synchronization *between* regions and thus can capture cortical connectivity. In various studies of motor function using EEG coherence, changes in brain connectivity have been observed in the beta (20-30 Hz) frequency range[152–154].

Measures of connectivity, as compared to assessments of focal brain regions, have an improved ability to represent complexity in human cortical processing and as a result have a stronger relationship with many types of behavior[59]. Therefore, the present study hypothesized that EEG coherence measures of motor network connectivity in the beta band during wakeful rest would predict subsequent motor skill acquisition in a single motor skill training session. Secondarily, it was hypothesized that a PLS approach for deriving brain-behavior relationships would perform better than an ROI based approach. An additional secondary hypothesis was that beta band coherence during movement (in the training session) would also be a predictor of subsequent motor skill learning.

METHODS

EXPERIMENTAL DESIGN

Healthy subjects, age 18-30 years and right-handed (Edinburgh Handedness Inventory) were recruited. This study was approved by the University of California, Irvine Institutional Review Board. Each subject gave written informed consent.

The experiment took place across a single session. Participants sat in a chair facing a computer monitor atop a desk. In order to minimize variation across participants, awake resting-state EEG was acquired for three minutes (EEG-Rest) at 1000 Hz prior to any description or practice of the motor task. Next, each individual's maximum arm movement speed was measured, standardized instructions for the visuomotor skill task were provided, and a baseline assessment of the motor skill task was obtained (Test 1), during which EEG was again recorded (EEG-Test 1). Next, two blocks of practice and two additional blocks of motor skill task testing with EEG recording were completed in an interleaved manner (Figure 2.1A), from which measures of motor skill learning were obtained. Arm movements were recorded by a USB 8"X6" digitizing pen tablet (Genius MousePen, Taipei, Taiwan).

To measure maximum arm movement speed, two 20-pixel target circles were displayed on the monitor, 1300-pixels apart. Participants were instructed to make horizontal movements between the centers of each circle, as rapidly as possible. The maximum number of targets hit during a 10 second period was recorded, and a maximum movement speed was calculated. The speed test was repeated three times, and the maximum was used to determine the speed that motor task target moved for each individual participant.

The motor skill task used in the current study was a digital version of the classic pursuit rotor task motor learning paradigm[155,156]. Subjects viewed a computer monitor on which a target (a 20-pixel diameter red circle) moved, back and forth, along a fixed arc (yellow,

spanning a 450-pixel wide and 200-pixel long path), at 50% of each individual's maximum movement speed. A cursor (15-pixel diameter white circle) was also present, the position of which was controlled by subjects using the digitizing tablet pen held by the right hand (Figure 2.1B). Subjects were instructed to keep the cursor on the target as the target moved along the arc (Figure 2.1C).

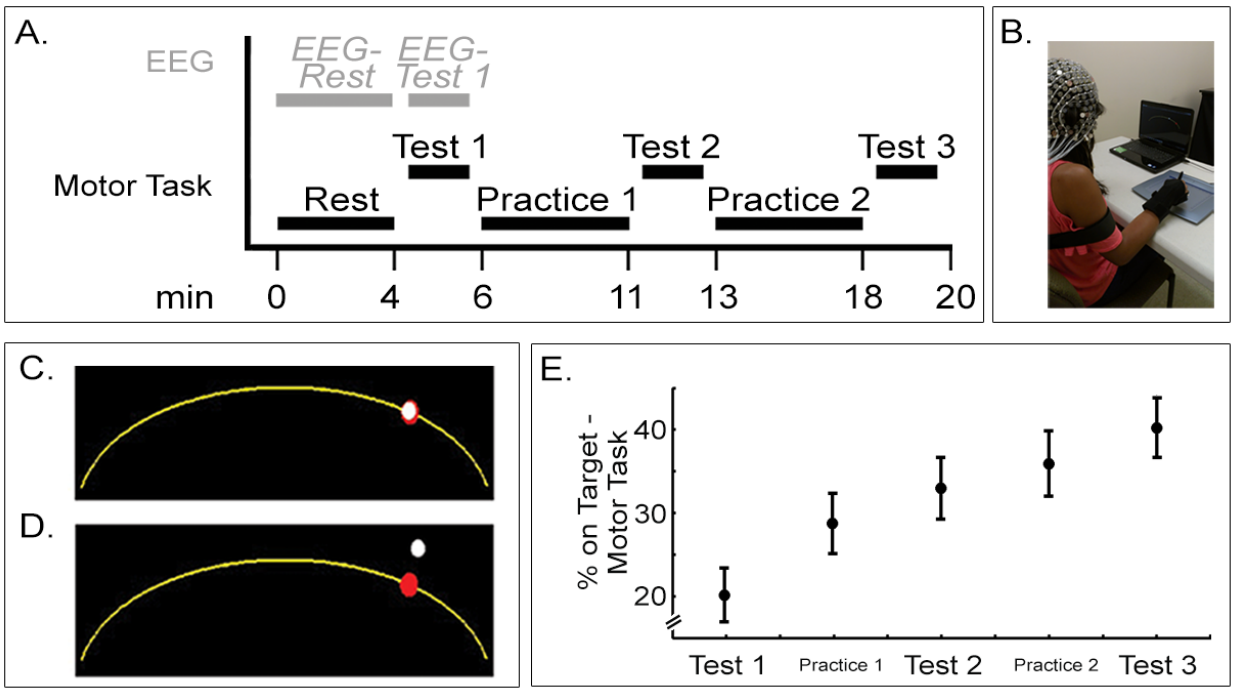

FIGURE 2.1. Experimental setup. **A.** Experiment timeline. **B.** Digitizing pen tablet and presentation laptop. **C.** Example of cursor *on target*. **D.** Example of cursor *off target*. E. The % Improvement (Test 3 - Test 1) on the motor task with practice was statistically significant (mean±s.e.; repeated measures ANOVA, $F(2,15) = 5.05$, $p<0.0001$).

Participants directed cursor movement by moving the pen tip across the surface of the USB digitizing tablet, maintaining contact of the pen tip on the tablet surface at all times during task performance. To insure arm movements were standardized across participants and were restricted to right shoulder internal/external rotation only, a soft strap was placed on the distal part of the right forearm, minimizing shoulder abduction,

and a wrist brace was placed across the distal right arm, minimizing wrist flexion/extension (Figure 2.1B). Subjects sat with both feet flat on the floor and were not permitted to move at other body joints.

Performance was quantified as percent time that the cursor position was >50% overlapping with target position *(% on Target*, Figure 2.1C). A total of three test blocks and two interleaved practice blocks were completed (Figure 2.1A). Each Test block consisted of a 50 second rest period followed by an 80 second task period. Each Practice block consisted of four 20-second task periods interleaved with three 50-second rest periods. Degree of motor skill acquisition was calculated from absolute change in *% on Target* from Test 1 to Test 3 (% Improvement).

EEG ACQUISITION

Dense-array surface EEG was acquired using a 256-lead Hydrocel net (Electrical Geodesics, Inc., Eugene, OR). Awake resting-state EEG was acquired for three minutes. EEG signal was referenced to Cz during recording and re-referenced to the average of all leads for analysis; an advantage of this approach is that it minimizes common reference effects. A ground electrode was not used. EEG signal was recorded raw with no bandpass filter used.

During EEG-Rest, participants were asked to hold still with the forearms resting on the anterior thigh and to direct their gaze at a fixation cross displayed on the computer monitor. During EEG-Test 1, and subsequent recordings (EEG-Test 2 and EEG-Test 3),

participants used their right hand to keep the cursor on the target, as above. Data were collected at 1000 Hz using a high input impedance Net Amp 300 amplifier (Electrical Geodesics) and Net Station 4.5.3 software (Electrical Geodesics).

EEG PREPROCESSING

EEG data were exported to Matlab (7.8.0, MathWorks, Inc., Natick, MA) for preprocessing. The continuous EEG signal was low-pass filtered at 50 Hz, segmented into non-overlapping one-second epochs, and detrended. Visual inspection and independent components analysis were used in combination to remove extra-brain artifacts from the EEG. First, epochs were visually inspected for contamination by overt muscle activity, such as from neck or cheek movements, and removed from further analysis. Next, EEG data underwent an Infomax ICA decomposition (EEGLAB[157]). Components that only occurred in one channel were automatically rejected, as were components attributed to muscle artifact (showing high activity at >35 Hz, and generally accompanied by high activity at 4-15 Hz with visual review consistent with muscle artifact). Of the remaining components, amplitude topography, frequency spectra, and component time series were inspected to identify eye blinks, eye movements, and heart rhythms[158], and were removed. Across EEG-Rest and EEG-Test data, 6.8±5.5 of the top 30 components were removed from each EEG recording. Finally, data were transformed back to channel space, and epochs were again visually inspected to insure absence of artifacts. Of all epochs recorded in EEG-Rest and EEG-Test 1 data sets, 92.1±6.8% were retained for further analyses.

COHERENCE AND POWER

EEG coherence was used to estimate functional connectivity[72,159,160]. At each frequency band, coherence is a measure of phase consistency between signals recorded at two electrodes. It is reported as a squared correlation coefficient, and expresses the fraction of variance at a given electrode in one frequency band that can be linearly predicted by the signal from another electrode. For a given frequency, a coherence value of 1 indicates EEG signals that have exactly the same phase difference and amplitude ratio on each epoch, while a coherence value of 0 indicates EEG signals that have a random difference in phase. Although EEG coherence is here used as an index of cortico-cortical functional connectivity to represent communication between neural sources, it does not exclude the possibility that increased coherence may also represent increased drive from a common source [161,162].

Spectral analysis was performed by submitting the time series to a discrete Fast Fourier transform with the MATLAB *fft* function, and was normalized by epoch length. The frequency resolution was 1 Hz, and no windowing function was used. Average absolute power at each electrode and coherence between each pair of electrodes for beta (20-30 Hz) frequencies, a range associated with motor system function[153,163]. Due to the central role of the contralateral primary motor cortex in movement execution and motor learning[164,165], EEG coherence with a seed region overlying left hand motor area (M1) was used as the primary metric of interest. The M1 seed region included C3 and the six electrodes immediately surrounding C3, with each surrounding electrode being located approximately 1-cm from C3; this seed region may have included some signal from

sensory cortex and other surrounding areas, and so the "M1" label is used to refer to the center of the seed. As a control, a right M1 seed region including C4 and its six immediate neighbors was also examined in separate analyses.

PLS ANALYSIS

A partial least squares (PLS) regression model of the EEG data, focused on M1 connectivity at rest was used to predict motor skill acquisition. PLS analysis is a multivariate method in which an optimal least-squares fit is computed for a partial correlation matrix between the independent and dependent variables. The PLS algorithm then generates a series of models with successively more components that maximally account for variance in the dependent variable. PLS methods have been used to identify patterns of neural activation related to changes in task content[166], and has been found useful for defining relationships between measures of brain function and performance in spatial attention tasks[167].

In the present study, the N-way toolbox[168] was used to generate PLS models of resting EEG coherence predicting % Improvement across practice. As a pre-processing step, data were mean-centered. Direct orthogonal signal correction[169] was then used to remove the component of the predicting data (coherence) that was most orthogonal to the behavioral data (% Improvement). As with previous studies that used PLS[170–173], this step allowed for more efficient PLS models with fewer components. Two separate PLS models were generated for % Improvement with each of the EEG metrics, beta frequency bands during EEG-Rest, and during EEG-Test 1. As in a previous study from

our group using PLS, as many components as were required to explain at least 80% of fitted behavior variance were used to determine the number of components to retain in the model[171].

PREDICTING MOTOR SKILL ACQUISITION

A leave-one-out cross-validation procedure was applied to determine predictive value of each of the four PLS models. With this approach, data from one participant is iteratively removed from the PLS model, then this participant's skill acquisition is predicted from his/her EEG data based on the PLS model and direct orthogonal signal correction generated from the remaining *n-1* participants. The resulting cross-validated R^2 is a measure of prediction accuracy determined from the ratio of prediction error and total variance in the actual behavioral data.

As control analyses, mean power and coherence were also calculated from regions of interest (ROIs), defined a priori via two methods, to predict subsequent motor skill acquisition. Similar to a recent study by Mathewson and colleagues[144], mean beta power and coherence were calculated for single electrodes, including C3 (left M1), F3 (left frontal-premotor, PM), and P3 (left parietal, Pr). Alternatively, and more akin to fMRI studies[145,146], regions in left M1, left PM, and left Pr were outlined across several scalp electrodes. Left M1 was defined as above for left M1 seed region in the PLS analyses. Left PM included F3 and the six electrodes that are immediately proximal, and left Pr included P3 and its six immediate neighbors. For both methods, mean power for each region and mean coherence for each pair of regions were then used to predict %

Improvement in separate bivariate models. In an additional exploratory secondary analysis, separate PLS prediction models were also calculated using coherence in theta (4-6 Hz), mu (11-14 Hz), lower beta (15-19 Hz), and gamma (31-50 Hz) frequency bands.

STATISTICAL ANALYSES

Performance on the motor skill task was subjected to one-way repeated measures ANOVA to establish significance of motor skill acquisition with factor Test. Bivariate analyses of ROI-based brain-behavior relationships used two-tailed parametric linear regression. Statistical significance was set at $p < 0.05$.

RESULTS

Eighteen healthy, right-handed individuals were recruited, one of whom was excluded due to technical problems during data collection, leaving 17 participants for the current report. For these 17 participants, gender was 9M/8F, and age was 22.1 ± 3.0 (mean ± SD). In addition, EEG-Test 1 data were discarded for one participant due to substantial muscle artifact.

Motor skill performance across participants increased significantly from Test 1 to Test 3 (Figure 2.1E, repeated measures ANOVA, factor: Test, $p < 0.0001$), with % Improvement increasing from 24% time on target to 41%.

BASELINE BEHAVIORAL PERFORMANCE AND DEMOGRAPHIC DATA DO NOT CORRELATE WITH SUBSEQUENT MOTOR SKILL ACQUISITION

Baseline behavioral performance (*% on Target* at Test 1), age, and handedness by Edinburgh Handedness Inventory were each examined as correlates of subsequent motor skill acquisition (% Improvement), and none was significant ($p > 0.05$). Participants also completed a motor skills inventory that probed time spent typing, playing video games, playing a musical instrument, playing sports, driving, and other skilled activities of the hands (i.e., sewing, sign language). Although participants showed some range (1-4, max = 6, min = 0), motor skills inventory score also did not predict % Improvement ($p > 0.05$).

EEG COHERENCE AT REST PREDICTS SUBSEQUENT LEARNING IN A PLS MODEL

A fitted PLS model of beta coherence with left M1 using the EEG-Rest data found a pattern that strongly correlated with % Improvement ($R^2 = 0.93$, Figure 2.2A). This was not true in a control analysis of the EEG-Rest data that examined a PLS model of beta coherence with *right* M1 where no significant prediction of % Improvement was found. A second control analysis was also negative, whereby PLS analysis of EEG beta *power* also did not significantly predict % Improvement.

The primary method for assessing the predictive strength of the PLS model was a leave-one-out cross-validation approach using the EEG-Rest data acquired prior to training. With this approach, the cross-validated R^2 for predicting % Improvement was

0.81. As a secondary method for assessing strength of the PLS model, data from 17-*i* participants were randomly selected to serve as a training group to generate a PLS model, and data from the remaining *i* participants were then used as a test group to independently assess prediction. Stepping up from *i* = 2, *i* was then increased until the prediction error in the test group exceeded total variance in the training group, and the model was said to have failed validation. The PLS model failed validation at *i* = 6. At *i* = 5, cross-validated R^2 was 0.75 ± 0.19 across 500 random partitions.

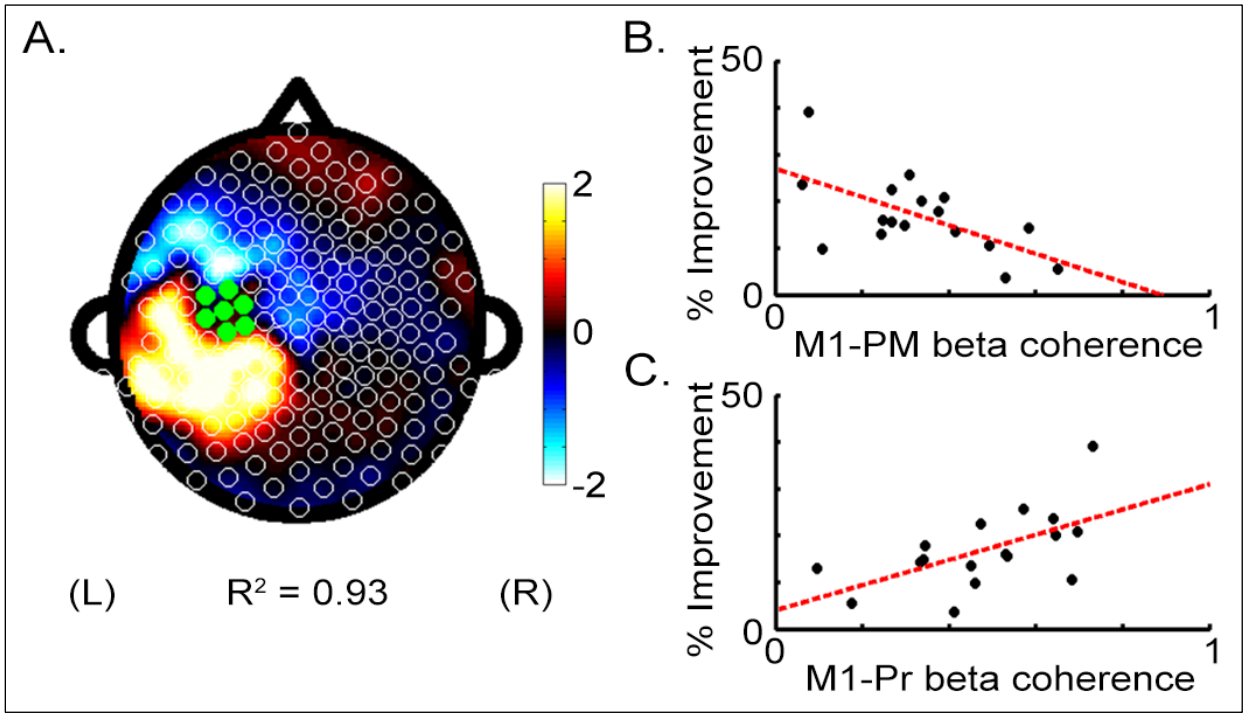

FIGURE 2.2. Coherence with left M1 during EEG-Rest predicts % Improvement on the motor task. **A.** Topographic plot of regression coefficients from the PLS model using M1 beta band (20-30 Hz) coherence. **B.** Mean beta coherence between left M1 and left frontal-premotor regions (M1-PM) is negatively correlated with improvement. **C.** Mean beta coherence between left M1 and left parietal regions (M1-Pr) is positively correlated with improvement.

Separate PLS models using coherence in theta (4-6 Hz), mu (11-14 Hz), lower beta (15-19 Hz), and gamma (31-50 Hz) frequency bands also predicted % Improvement, but with reduced prediction strength as compared to the beta (20-30 Hz) frequency band. Fitted R^2 was 0.82, 0.87, 0.80, and 0.90 for theta, mu, lower beta, and gamma coherences, respectively, and cross-validated R^2 was 0.71, 0.76, 0.68, and 0.79.

VARIATION IN PREMOTOR AND PARIETAL CONNECTIVITY AT REST DEMONSTRATE DIFFERENT EFFECTS ON LEARNING

From the PLS model of EEG-Rest using beta coherence with left M1, the subset of electrodes accounting for >90% of the regression weights on EEG coherence were identified. All were located in left Pr and left frontal-premotor (PM) regions. Focusing on these electrodes, bivariate analysis found that *greater* % Improvement was associated with *higher* M1-Pr coherence (Figure 2.2C, $r = 0.58$, $p < 0.05$) and with *lower* M1-PM coherence (Figure 2.2B, $r = -0.61$, $p < 0.01$). These two effects were independent, as M1-PM coherence and M1-Pr coherence were not significantly related ($p > 0.05$). Note that PM-Pr coherence also was not significantly related to % Improvement ($p > 0.05$).

POWER AND COHERENCE AT REST IN PREDEFINED M1, PREMOTOR, AND PARIETAL REGIONS ARE NOT STRONG PREDICTORS OF LEARNING

Mean beta power and coherence were calculated for predefined regions of interest at left M1 (C3), left PM (F3), and left Pr (P3) regions. When data from individual electrodes were used as correlates of % Improvement, mean power and coherence during EEG-Rest 1 did not correlate with subsequent % Improvement ($p > 0.05$). When data from

groups of electrodes were used for each ROI, mean coherence during EEG-Rest 1 for left M1-left PM, left M1-left Pr, and left PM-left Pr were not significantly related to subsequent % Improvement on the motor skill task ($p > 0.05$). Mean power during EEG-Rest 1 from left M1, left PM, and left Pr also did not relate significantly with % Improvement ($p > 0.05$).

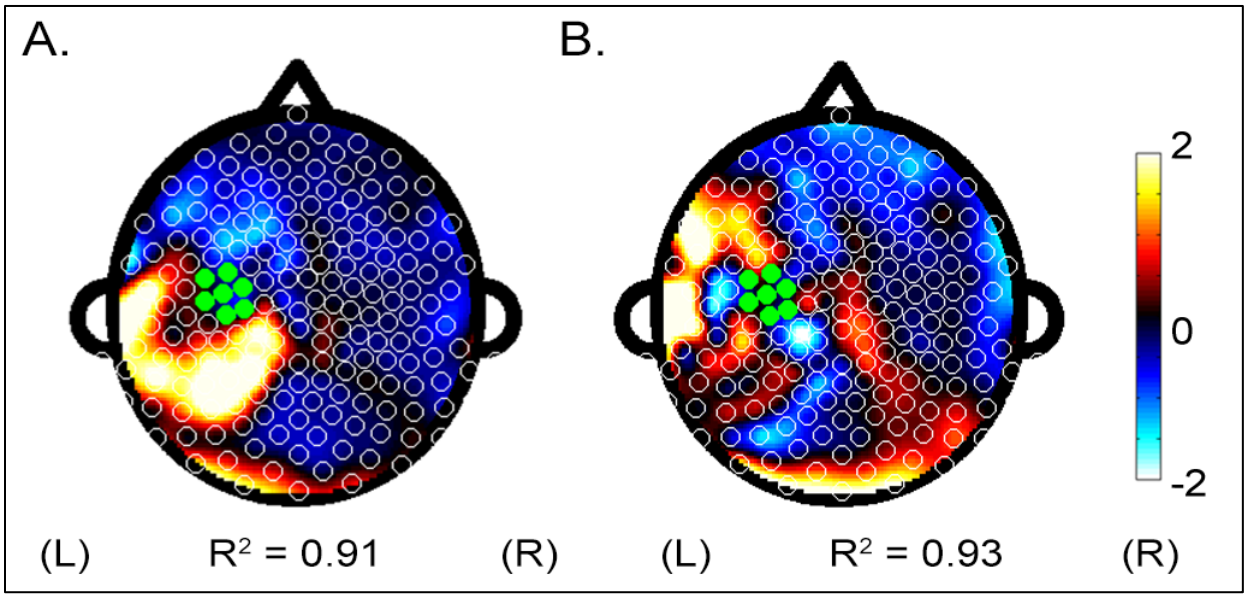

FIGURE 2.3. Topographic representation of regression coefficients derived from PLS models using M1 beta coherence during EEG-Test 1.

EEG COHERENCE DURING START OF PRACTICE (EEG-TEST 1) ALSO PREDICTS LEARNING

A secondary hypothesis was that M1 connectivity during the initial phase of motor skill practice (EEG-Test 1) would also predict skill acquisition. Coherence with left M1 was again a significant predictor of % Improvement. The PLS model of coherence with left M1 during EEG-Test 1 significantly predicted % Improvement (Figure 2.3, fitted model

R^2 = 0.91, cross-validated R^2 = 0.74), although this relationship was weaker compared to analyses using EEG-Rest.

As above, electrodes of interest were derived from the EEG-Test 1 PLS model with the subset of electrodes accounting for >90% of the regression weights all located in a left Pr cluster. Mean coherence for left M1-left Pr was significantly related to subsequent % Improvement (p = 0.006, r = 0.65). Using the left PM cluster from EEG-Rest 1, left M1-left PM and left PM-left Pr did not correlate with % Improvement. Mean power during EEG-Rest 1 from left M1, left PM, and left Pr also did not have a significant relationship with % Improvement (p > 0.05).

Separate PLS models using left M1 beta coherence during EEG-Test 2 and EEG-Test 3 showed weaker strength at predicting % Improvement compared to what was seen using EEG-Rest or using EEG-Test 1. The fitted R^2 was 0.81 and 0.86 for EEG-Test 2 and EEG-Test 3, respectively, and cross-validated R^2 was 0.66 and 0.45.

DISCUSSION

Measures of brain function using fMRI activity level or EEG power have been found to predict motor learning better than measures of baseline behavior, but the precision of prediction is modest. The current study examined the ability of a dense-array EEG measure of M1 cortical connectivity to predict individual differences in motor skill acquisition. Motor network connectivity measured during rest, prior to practice, was found to predict a remarkably high fraction of the variance in motor skill acquisition over

20 min of subsequent practice (R^2 = 0.81), while pre-practice behavior and demographic data had no predictive value. In comparison, an ROI-based approach showed much reduced predictive value (R^2 = 0.43). Current results emphasize the importance of activity in M1, parietal, and frontal-premotor cortical areas to motor learning, and furthermore reveal that M1-premotor connectivity and M1-parietal connectivity predict opposite effects on behavioral improvement.

Measures of resting-state network connectivity are proving highly useful for probing the functional potential of the brain[147]. This approach was used in the current study and predicted learning in human subjects with greater precision (R^2 = 0.81) than in any prior report of which we are aware. The strength of these findings may be due to several factors. First, use of EEG may offer some advantages for measuring synchronized activity across neural ensembles[174], as EEG provides higher temporal resolution than many other functional neuroimaging techniques. This might account for differences in prediction strength between the current study and studies using fMRI-based connectivity measures for prediction, e.g., of math skill acquisition (R^2 = 0.61[175]), performance on an associative memory task (R^2 = 0.35[145]), or a visual discrimination task (R^2 = 0.66[146]), although these are indirect comparisons and these studies differed from the current report in a number of key ways. The high temporal resolution may have been particularly advantageous in the current study as it permits measurement of brain function in high beta frequencies, a range closely associated with function of the cortical motor system[153,163]. In the current study, high beta frequencies were shown to be the best biological correlate of motor system function as prediction strength was weaker in

theta, mu, lower beta, and gamma frequency ranges. Second, connectivity-based measures, as compared to focal measures of brain activity, have an improved ability to provide insight into cortical processing underlying complex behaviors[59]. This is directly supported by the observation in the current study that connectivity but not regional spectral power measures predicted learning, and indirectly by comparing the strength of prediction in the current report with that found in a prior EEG study that used regional measures of spectral power to predict learning of a complex motor task ($R^2 = 0.53$[144]). Third, PLS modeling is useful for defining relationships between brain function and behavior[167,176], for example, decoding behavioral output with high accuracy using fewer variables than with other approaches[177]. Furthermore, a PLS approach has been found useful for understanding behavioral correlates of EEG in populations with a range of brain-related diagnoses, such as major depression[178] and Parkinson's disease[179].

To facilitate a closer comparison with previous studies, an ROI-based approach, in which regions of interest in frontal-premotor, primary motor, and parietal areas were defined a priori, was also examined. When single electrode ROIs were used, no significant relationships were found between brain data and behavior. This might be due in part to variability in brain morphology and in site of electrode placement across individuals. When regions were defined across several electrodes, some relationships between dEEG metrics and % Improvement were found. However, compared to the PLS approach, the ROI approach still showed reduced predictive value in establishing a brain-behavior relationship between brain function at rest and subsequent motor skill acquisition (R^2 range: PLS approach = 0.60 to 0.81, ROI approach = 0.26 to 0.43). The

predictive value of the ROI approach in the current study is similar to previous studies that also used an ROI-based approach in previous fMRI and EEG studies[144,145]. When comparing the same metric across approaches, such as M1-PM beta coherence to predict % Improvement, the PLS approach (R^2 = 0.37) also demonstrates improved prediction strength compared with the ROI approach (R^2 = 0.09). The favorable comparison of a PLS approach suggests whole-brain approaches, including graph-theoretical network analysis[180] and Independent Component Analysis[181], may be more sensitive to inter-individual variations that provide insight into differences in behavior.

The current approach not only predicts learning, but also provides insight into the neural circuits underlying this learning[175]. As in previous studies of motor learning[165], the current results show motor skill acquisition is linked to activity in primary motor cortex, parietal cortex, and frontal-premotor areas. Furthermore, the current results extend previous findings by demonstrating how inter-individual differences in resting-state cortical networks may relate to differences in capacity for skilled motor learning. M1-Pr connectivity was found to have an opposite relationship with predicting skill learning as compared to M1-PM connectivity. Thus, within the model, increased M1-Pr connectivity predicted *greater* skill acquisition. This may reflect greater capacity for visuomotor integration, as suggested by a recent study that reported that increased functional connectivity between sensorimotor and parietal regions during early motor learning coincided with significant behavioral improvement[182]. The model also found that increased M1-PM connectivity at rest predicted *reduced* skill acquisition. This may reflect basal differences in motor system efficiency, as premotor cortex activation has

been associated with increased task complexity[183] and cognitive effort[97]. It may be that increased M1-PM connectivity at rest is a marker of a inefficient motor system, similar to the aging motor system, which exhibits over-activity in premotor cortex during simple motor tasks[184]. Opposite findings regarding M1-Pr vs. M1-PM connectivity may therefore reflect individual differences in specific processing components that contribute to variability in early motor learning[185].

The current study has a number of limitations. Regarding localization of coherence effects, we acknowledge the use of scalp EEG has limitations in spatial localization. As such, the anatomical relationship between EEG electrodes and specific brain structures is imperfect. However, 256-electrodes systems, as used in the current study, are shown to provide significantly improved spatial resolution compared to traditional 10-20 systems[111,186]. A surface Laplacian could be used to further improve spatial resolution[187]. However, there is evidence that such a transform could erroneously distort coherence across distances in the range of left M1 to left PM and Pr regions[188]. Although not a focus of the current study, future work on the evolution of connectivity profiles in parallel with behavioral gains might provide additional insights into the mechanisms underying motor learning.

Predicting biological behavior remains a major challenge for understanding variation in healthy subjects and diseased populations. The current results show that a measure of connectivity obtained from three minutes of resting-state dEEG captures individual differences in brain state that are highly related to subsequent behavioral learning. The

current dEEG method has high potential clinical utility, as these data can be acquired easily, inexpensively, rapidly, safely, and in complex medical settings. Although it is known that patients demonstrate significant heterogeneity in motor learning, the current methods may be useful in clinical settings related to cortical plasticity, such as acute stroke or traumatic brain injury, where a high need exists for accurate methods of patient stratification[39].

CHAPTER 3

Connectivity predictors of short-term motor learning demonstrate specificity for training content

ABSTRACT

Humans demonstrate wide-ranging variability in each individual's ability to acquire a new motor skill. Although there is a significant literature documenting the neurophysiological processes that underlie acquisition of motor skills, the basal differences in brain state that underlie differences in response to motor training are less well understood. Recent studies suggest resting-state measures of brain function may provide key insights into inter-individual differences across a spectrum of behaviors, including motor skill learning. While several functional and structural measures of brain state have been identified that predict response to motor learning, it is unclear whether neuroimaging predictors of motor learning generalize across tasks or demonstrate specificity with respect to the task being trained. The current study examined the specificity of EEG connectivity predictors of motor skill acquisition across two motor skills known to engage different motor regions during task performance. Thirty-two healthy, young participants underwent resting EEG prior to a single training session on a wrist targeting (WT) task. Twenty-four hours later, participants underwent a second resting EEG prior to a single training session on a digital rotor pursuit (RP) task. Behaviorally, the group demonstrated improvement across a single training session for both tasks. Resting connectivity measures were then correlated with behavioral measures using partial least squares regression (PLS). Separate PLS models found

resting connectivity between left primary motor cortex (M1) and left frontal-premotor (PM) predicted subsequent skill acquisition of same-day training on WT and RP tasks. However, the direction of correlation was not the same. In WT, greater improvement was predicted by increased left M1-left PM coherence at rest, while greater RP improvement was predicted by decreased left M1-left PM coherence. The current results demonstrate EEG connectivity predictors of motor skill acquisition are specific to the trained task.

INTRODUCTION

The rate and extent to which an individual responds to motor training is highly variable [142,189–192]. In settings of average life, these differences differentiate the All Star little leaguer from the team bat boy or a hunt-and-peck typist from a stenographer. However, in clinical settings (motor recovery after stroke) or highly specialized motor training (prediction of pilot performance or selection of army recruits for sharpshooting training) these differences can have significant social and economic consequences. Improved methods for predicting individual response to motor training may be highly useful, particularly in clinical settings, in which innovative methods for patient stratification are a pressing concern[25].

Recent studies suggest connectivity measures, which capture the complex, dynamic interactions between distant brain areas, demonstrate improved correlation with behavior when compared to focal measures, like regional activation[59,164,193,194]. Indeed, resting-state functional connectivity has shown promise as a biomarker of perceptual,

arithmetic, and speech learning[146,175,195,196]. While fMRI-based measures of functional connectivity are useful neural predictors of individual response to training[146,148,196,197], expense and the cumbersome nature of data acquisition may limit broad applications.

Electroencephalography (EEG) is a relatively easy, inexpensive, and rapid method of acquiring functional brain data. In addition, the high temporal resolution of EEG permits the calculation of connectivity measures at higher frequencies, including the high-beta (20-30 Hz) band, a range associated with function of the cortical motor system[163,198,199]. In a previous study, resting-state high beta EEG connectivity was a strong predictor of subsequent motor skill acquisition[200]. Specifically, increased connectivity between contralateral primary motor cortex (M1) and contralateral parietal cortex predicted greater improvement with rotor pursuit (RP) training, and increased M1 connectivity with contralateral premotor cortex (PM) predicting less improvement. It was postulated in the previous study that the specific brain-behavior relationships observed reflect motor training content, as the RP task relies more heavily on parietal cortex-driven visuomotor integration than PM-driven motor planning[156].

The current study examined whether topography of the predictive model is influenced by the content of the motor task being trained, particularly when training two different motor tasks that are known to engage different cognitive and neural mechanisms. Specifically, we hypothesized that increased resting-state M1-PM connectivity would predict greater improvement with motor sequence training, a task known to engage the PM motor planning node[201]. Conversely, in-line with the previous study, we

hypothesized increased M1-PM connectivity would not be associated with greater improvement on the RP task. The current study also examined baseline resting-state connectivity as a predictor short-term motor learning assessed by a 24 hour retention test. EEG connectivity was expected to outperform baseline performance, baseline clinical measures, and EEG power, a regional measure of brain function, as a predictor of motor learning.

METHODS

PARTICIPANTS

Healthy young adults, aged 18-30 years, were recruited. Participants had no history of neurological or psychiatric conditions, and were right-handed according to the Edinburgh Handedness Scale[202]. Although it was not a specific exclusion criteria, no participants had a skull defect that could result in an EEG breach rhythm. The study was approved by the University of California, Irvine Institutional Review Board.

EXPERIMENTAL DESIGN

The experiment took place across two sessions, 24 hours apart (Fig. 1*A*). Participants sat in a chair facing a computer screen on a tabletop. At both Sessions, three minutes of awake, resting-state EEG was acquired before any description or practice of either motor task was provided. Session 1 included assessment of wrist range of motion followed by 4 Test with 3 interleaved Practice blocks on the wrist targeting (WT) task. Session 2 included the WT retention test, assessment of maximum arm movement speed, and 3 Test with 2 interleaved Practice blocks on the rotor pursuit (RP) task.

For all experiment procedures, participants sat in a standard chair with both feet flat on the floor, were instructed to stare straight ahead at the computer screen and to minimize body movements outside of the right arm.

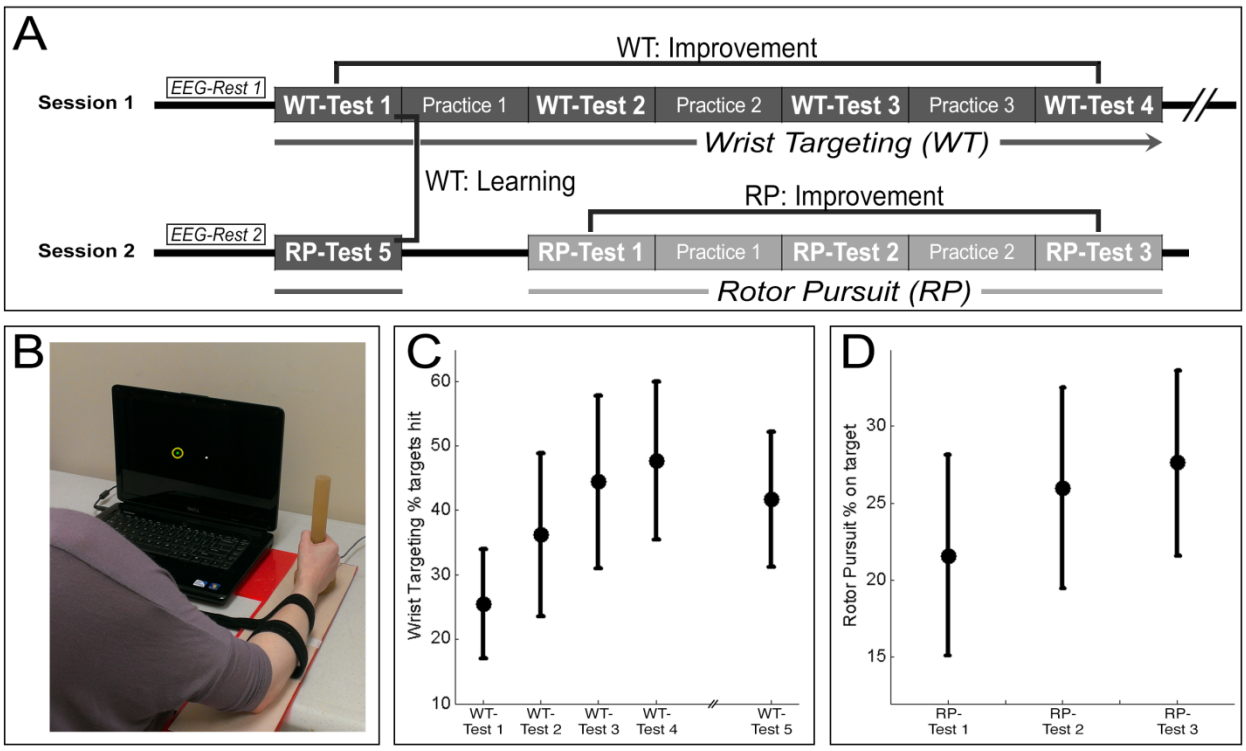

FIGURE 3.1. Experimental setup. **A**. Experiment timeline. **B**. Rotary joystick with presentation laptop. **C**. Motor learning (WT: Test 5 – WT: Test 1) was significant across the 24 hour retention test. WT skill acquisition (WT: Test 4 – WT: Test 1) was also significant across Session 1. **D**. RP skill acquisition (RP: Test 3 – RP: Test 1) was significant across Session 2.

WRIST TARGETING TASK

The WT task, which was used to assess single-session motor skill acquisition and motor learning across a 24 hour retention test, assessed an participant's ability to learn a of precision wrist extension and flexion movements. In the WT task, participants controlled

a white circle onscreen using a custom rotational joystick (single-turn potentiometer, Vishay Intertechnology, Inc., Malvern, PA). As all participants performed the task using the right hand, wrist flexion caused the cursor to move left and wrist extension resulted in a rightward cursor movement. For each target, a single green target circle (20-pixels) appeared in one of seven positions lying along a horizontal plane (Fig. 1*B*). Upon target onset, participants were instructed to make wrist movements to move the cursor to the target position as rapidly as possible. In order to account for target overshooting errors, a trial was scored successful only if the cursor was held at the target position for at least 500 ms; each trial was 1425 ms in duration. At the end of each trial, targets flashed green to indicate successful trials and red to indicate unsuccessful trials to provide real-time feedback to participants during task performance. To ensure arm movements were standardized across participants, two soft straps were applied to the participants' right forearm to limit elbow movement during wrist movements.

Each Test and Practice block consisted of 84 targets, which were separated into three sub-blocks with 10 second breaks between sub-blocks. The embedded target sequence consisted of 19 targets and was pseudo-randomly inserted into each sub-block. Pseudo-random targets were included before and after the sequence to minimize explicit awareness of the target sequence. The length of the target sequence was designed to ensure all participants remained in the same phase of learning, and to minimize potentially confounding contributions from right premotor and parietal regions, which have been associated with explicit motor sequence learning[203]. Across the 4 Test and 3 Practice blocks, the sequence was presented 21 times. Participants' awareness

of the target sequence was assessed at the end of Session 2. Motor learning of WT training at Session 1 was assessed at a retention test administered at Session 2 (Test 5). The retention test always occurred 24 hours following Session 1 and consisted of a single Test block which presented an identical target sequence as Test 1 at Session 1.

Performance was quantified as the percentage of successful trials of the embedded sequence trials (% targets hit). Skill acquisition was calculated from absolute change in % targets hit from Test 1 to Test 4 (Improvement). Motor learning was defined as the absolute change in % targets hit from Test 1 to Test 5 (Learning).

To standardize task difficulty, cursor movements were normalized to each participants' active range of motion. Therefore, the physical location of each target position on the screen and percent of total flexion or extension in either direction to reach each target was standardized across participants.

ROTOR PURSUIT TASK

The RP task was a continuous target tracking task in which participants used a pen tablet to follow a cursor along a fixed arc. The specifics of motor skill assessment and training were detailed previously[200]. In sum, each participants' maximum arm movement speed was measured and used to standardize task difficulty, standardized instructions were provided, and participants completed 3 Test and 2 Practice blocks. As previously, skill acquisition was calculated from absolute change in % on Target from Test 1 to Test 3 (Improvement).

EEG ACQUISITION

Resting-state EEG was collected with a 256-lead Hydrocel net (Electrical Geodesics, Inc., Eugene, OR) for 3 minutes. Participants were instructed to sit still and direct their gaze at a fixation cross displayed on the computer screen. The data were acquired with a Net Amp 300 amplifier (EGI) and Net Station 4.5.3 software (EGI). During recording, EEG signals were referenced to Cz with no bandpass filter applied. In post-processing, EEG data were re-referenced to the average of all channels, an approach that minimizes common reference effects[72].

EEG PREPROCESSING

EEG data were exported to Matlab (7.8.0, Mathworks, Inc., Natick, MA) for preprocessing. Given high muscle artifact content in EEG electrodes recording from cheek and neck areas, 62 electrodes were excluded from further analysis across all participants. In line with previously described methods[200], the data then underwent filtering, visual inspection, and Infomax Independent Component Analysis decomposition (EEGLAB[157]) to remove extra-brain artifacts, such as eye blinks, eye movements, muscle activity, and heart rhythm signals.

POWER AND COHERENCE

Spectral analysis was performed by submitting the EEG time series to a discrete Fast Fourier transform, and normalizing by epoch length. The frequency resolution was 1 Hz. In the frequency domain, frequency-specific measures of regional relative energy and inter-regional functional connectivity were assessed with EEG power and EEG

coherence, respectively. Specifically, spectral power was calculated from the square of the Fourier coefficients, and coherence was calculated from the cross-correlation of the Fourier coefficients. Coherence is a unit-less value that ranges from 0 to 1. For a given pair of signals, coherence values near 1 represent signals in which the difference in phase and amplitude are highly related for a given frequency. In contrast, coherence value near 0 represent two signals in which the difference in phase and amplitude are not related for a given frequency.

For the present study, the primary frequency band of interest was high-beta (20-30 Hz), as it is a range associated with function of the cortical motor system[163,204]. Furthermore, given the central role of primary motor cortex (M1) in motor learning[205,206], the primary coherence measure of interest was mean beta coherence with a seed region approximately overlying left M1; the left M1 seed was defined as C3 and the 6 electrodes that immediately surround C3[207]. Conversely, the right M1 seed was defined as C4 and the 6 electrodes that immediately surround C4.

PLS ANALYSIS

Brain-behavior relationships were established using partial least squares (PLS) regression analyses (N-way toolbox[208]). PLS is particularly suited for neuroimaging studies, in which multiple comparisons can reduce statistical power[167,176,209]. To permit comparison of prediction strength across models, all PLS models in the current study included the first two components. In addition, cross-validation of each model was performed using a leave-one-out and predict approach, which is an established method

for assessing generalization of a prediction model to independent data[210,211]. An arbitrary threshold was used to identify regions where coherence was most strongly related to behavioral status. For each PLS model, correlation coefficients were thresholded at $|r_i| > 0.7 * r_{max}$, where r_i is the correlation coefficients at the *i*th electrode and r_{max} is the largest $|r_i|$ value across all electrodes.

STATISTICAL ANALYSES

Motor skill retention (WT: Test 1 to Test 5) was assessed by a two-tailed paired t-test. Motor skill acquisition (WT: Test 1 to Test 4; RP: Test 1 to Test 3) was assessed by repeated measures ANOVA. Bivariate brain-behavior linear regression analyses were two-tailed. An interactive analysis of covariance (ANCOVA) was used to compare the effect of task (WT vs. RP) on brain-behavior relationships. Parametric statistical testing was used for normally distributed variables, and nonparametric for non-normally distributed variables. Statistical significance was set at $p < 0.05$, uncorrected for all statistical analyses.

RESULTS

Thirty-four healthy, right-handed participants were recruited and completed all study protocols. Data from two participants were excluded from analyses due to excessive muscle artifact in the EEG recording. For the remaining 32 participants, gender was 14M/18F, and age was 19.4 ± 1.6 years (mean ± SD).

BEHAVIORAL DATA

Skill acquisition was statistically significant across the single training session for both tasks. In the WT task, % targets hit increased from 25.4 ± 8.5% to 47.4 ± 11.8% (mean ± SD) from Test 1 to Test 4 (Figure 3.1*C*, $F(3, 93) = 93.7$, $p < 0.0001$, repeated measures ANOVA). In the RP task, % time on target increased from 21.6 ± 6.5% to 27.3 ± 5.9% (mean ± SD) from Test 1 to Test 3 (Figure 3.1*D*, $F(2,30) = 14.3$, $p < 0.0001$, repeated measures ANOVA).

With training, % targets hit in the WT task increased from 25.4 ± 8.5% to 41.7 ± 10.5% (mean ± SD) from Test 1 to Test 5 (Figure 3.1*C*, $t(31) = -9.57$, $p < 0.0001$, two-tailed paired t-test). In the questionnaire following the retention test at Session 2, 19 of 32 participants reported awareness of a sequence in target presentation. However, none of the participants were able to reproduce more than four sequential targets correctly. Thus, it was concluded that sequence learning remained implicit for all participants[212].

RESTING-STATE EEG COHERENCE PREDICTS SAME-DAY MOTOR SKILL ACQUISITION

Resting-state brain connectivity measured prior to training was used to predict subsequent skill acquisition in both tasks. At Session 1, beta coherence between left M1 and the rest of the scalp predicted WT improvement (WT: Test 4 - Test 1) with training in a PLS model with good prediction strength (Figure 3.2*A*, fitted $R^2 = 0.58$, validated $R^2 = 0.55$). At Session 2, beta coherence between left M1 and the rest of the scalp predicted RP improvement (RP: Test 3 - Test 1) with training in a PLS model with

reduced prediction strength in comparison to the results in Chapter 2 (Figure 3.2*B*, fitted R^2 = 0.60, validated R^2 = 0.22). Comparing the two tasks, all participants demonstrated improvement with training on the WT task, but several showed minimal or negative motor skill improvement with training on the RP task. Of the 32 participants, 11 demonstrated RP skill acquisition (RP: Test 3 – RP: Test 1) below the lowest performer from Chapter 2. When repeating the Session 2 PLS model using the remaining 21 participants that demonstrated RP improvement (RP: Test 3 - Test 1 > 2.67), prediction strength was greater (fitted R^2 = 0.63, validated R^2 = 0.53).

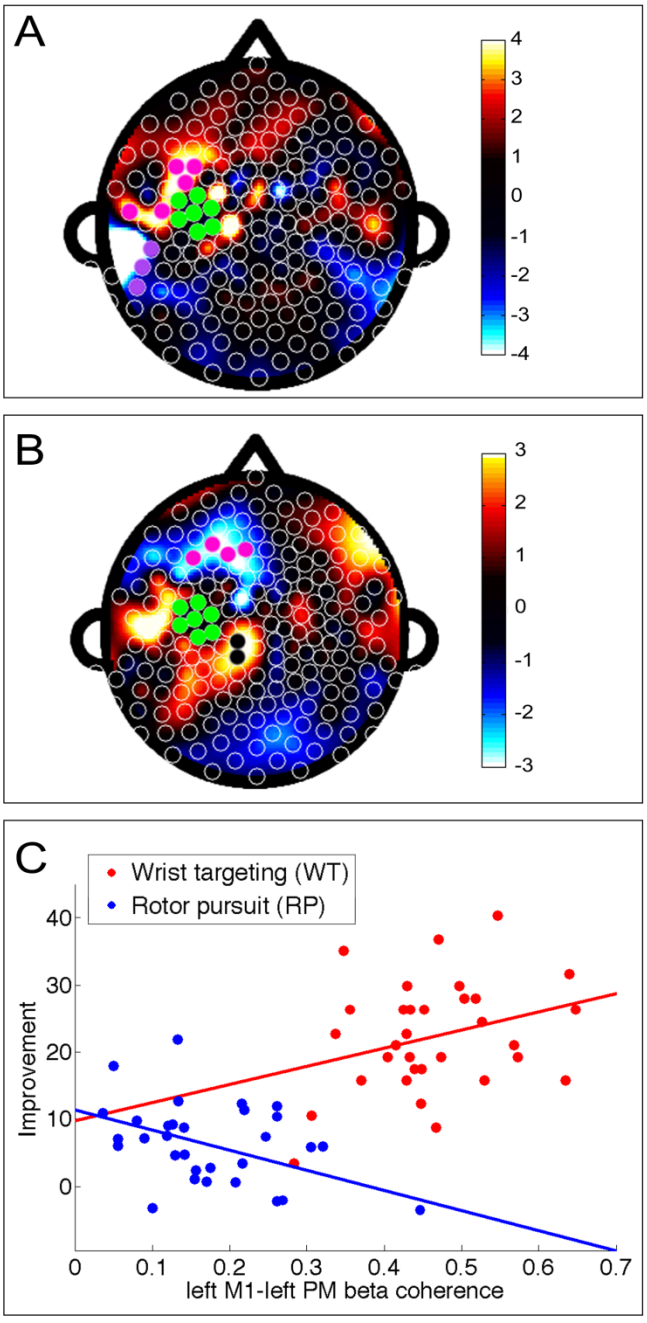

FIGURE 3.2. Resting-state coherence with left M1 predicts motor skill improvement on WT and RP tasks. Topographic plots of regression coefficients from the PLS model using beta (20-30 Hz) band coherence with left M1 to predict **A**. WT improvement (fitted R^2 = 0.58, validated R^2 = 0.55), and **B**. RP improvement (fitted R^2 = 0.63, validated R^2 = 0.53). **C**. Overlayed scatterplots demonstrate increased coherence between left M1 and left frontal-premotor (M1-PM) regions is positively correlated with WT improvement (red, r = 0.30, p = 0.09) and negatively correlated with RP improvement (blue, r = -0.43, p = 0.01).

CONTENT OF MOTOR TRAINING INFLUENCES EEG PREDICTION OF SUBSEQUENT IMPROVEMENT

In both PLS models, in which beta coherence with M1 was used to predict subsequent motor improvement (WT at Session 1 or RP at Session 2), electrodes where variance in coherence were most strongly related to training-induced improvement were clustered in regions approximately overlying left frontal-premotor (PM) as indicated in Figures 3.2A and 3.2B. As significant electrodes are dictated by specific beta coefficients from each PLS model, there was a spatial difference in PM electrode clusters for each PLS model (predicting improvement in WT and RP, respectively). Regardless, task condition did demonstrate a significant interaction on the correlation between left M1-left PM beta coherence and subsequent training-induced motor skill improvement on each task (ANCOVA results, Table 3.1). This interaction was attributable to opposite bivariate relationships between left M1-left PM coherence and training-induced improvement on each task. In separate bivariate correlations, greater WT skill acquisition was related to greater left M1-left PM coherence at Session 1 (Figure 3.2*C*, red points, $r = 0.30$, $p = 0.09$), while greater RP skill acquisition was predicted by decreased left M1-left PM coherence at Session 2 (Figure 3.2*C*, blue points, $r = -0.43$, $p = 0.01$).

TABLE 3.1. ANCOVA results

Source	d.f.	Sum Sq	Mean Sq	F	p > F
Task	1	1334.34	1334.34	29.98	0
left M1-left PM beta coherence	1	2.47	2.47	0.05	0.824
Task*left M1-left PM beta coherence	1	429.4	429.4	8.68	0.0046
Error	60	2967.36	49.46		

RESTING-STATE EEG COHERENCE AT BASELINE PREDICTS SHORT-TERM MOTOR LEARNING

Session 1 beta coherence between left M1 and the rest of the scalp correlated strongly with learning scores (WT: Test 5 - Test 1) in a PLS regression model (Figure 3.3*A*, fitted $R^2 = 0.89$). Cross-validation with the leave-one-out approach found the model generalized with good prediction strength (validated $R^2 = 0.68$). Session 1 beta coherence between left M1 and the rest of the scalp did not predict baseline WT performance (WT: Test 1). In addition, Session 1 beta coherence between *right* M1 and the rest of the scalp also did not predict learning. Beta coherence between left M1 and the rest of the scalp also outperformed beta power (validated $R^2 = 0.43$) as a predictor of short-term motor learning.

In the PLS model of Session 1 beta coherence predicting learning scores (WT: Test 5 – Test 1), significant electrodes were clustered in three primary locations, overlying the left frontal-premotor region (PM), overlying the left parietal operculum (PAR), and

overlying the left medial sensory region (S1). Bivariate linear regression found that greater motor learning was predicted by higher left M1-left PM coherence (Figure 3.3*B*, r = 0.52, p = 0.002) and lower left M1-left PAR coherence (Figure 3.3*C*, r = -0.40, p = 0.03). Bivariate correlation between learning and M1-S1 coherence did not achieve significance (r = 0.09, p = 0.6). Note that the two significant effects were independent, as left M1-left PM coherence and left M1-left PAR coherence were not significantly correlated (r = -0.2, p = 0.2).

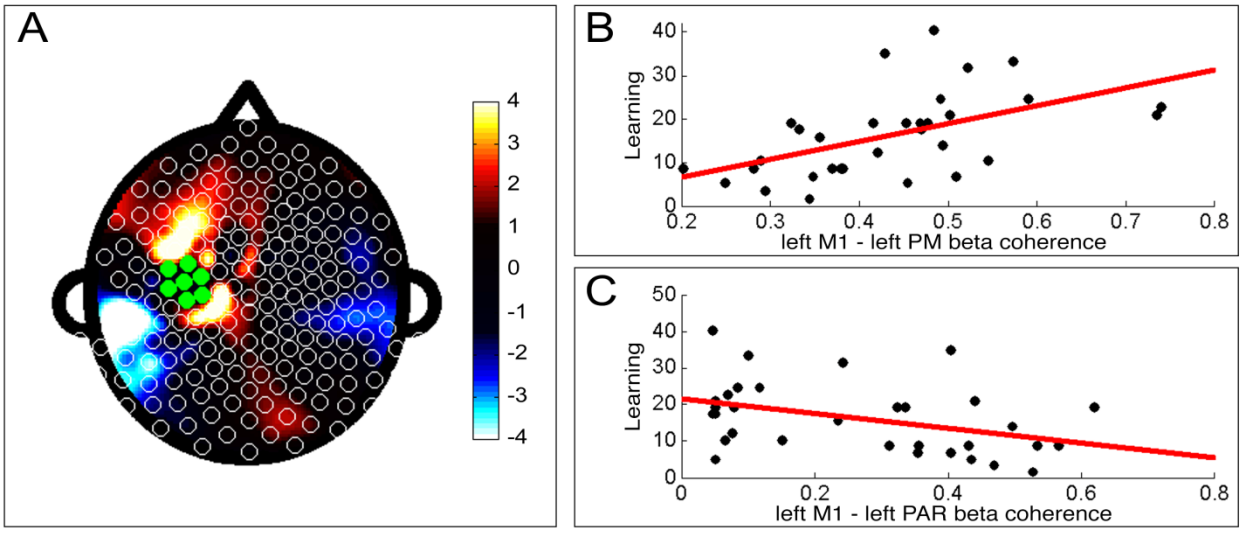

FIGURE 3.3. Resting-state coherence with left M1 predicts motor learning on the WT task. **A**. Topographic plot of regression coefficients from the PLS model using beta (20-30 Hz) band coherence with left M1 to predict subsequent learning (fitted R^2 = 0.89, validated R^2 = 0.68). **B**. Mean beta coherence between left M1 and left frontal-premotor (M1-PM) regions is positively correlated with learning (r = 0.52, p = 0.002). **C**. Mean beta coherence between left M1 and left parietal (M1-PAR) regions is negatively correlated with learning (r = -0.40, p = 0.03).

BEHAVIORAL PARAMETERES DID NOT PREDICT SHORT-TERM MOTOR LEARNING

Several behavioral parameters assessed at baseline did not perform as well as EEG parameters when predicting motor learning. Baseline performance (% targets hit at Test 1, r = -0.3, p = 0.09), age (r = -0.05, p = 0.8), and handedness (r = -0.3, p = 0.07) did not predict subsequent training-induced motor learning. Scores on a motor skills inventory that probed total time spent performing skilled activities of the hands also did not predict motor learning (r = 0.1, p = 0.5). Furthermore, wrist range of motion of the right hand in flexion (r = 0.05, p = 0.8) and extension (r = -0.05, p = 0.8) directions and an average of the two values did not predict subsequent motor learning (r = 0.007, p = 1.0).

DISCUSSION

The current study found that resting-state EEG connectivity predictors of subsequent training-induced motor skill acquisition demonstrate specificity with respect to task. The current results also show resting-state EEG connectivity is a robust predictor of short-term motor learning (R^2 = 0.68), outperforming EEG power and several clinical measures, including baseline performance.

The current results demonstrate resting-state EEG coherence in the beta band between electrodes overlying left M1 and the rest of the scalp, when combined with a partial least squares regression analysis, can be used to predict subsequent improvement with training on a novel motor skill. Furthermore, this resting-state predictor of motor learning showed specificity with respect to the content of the trained motor task. Specifically,

increased left M1-left PM coherence at baseline was positively related to greater subsequent WT skill improvement with training, while increased left M1-left PM coherence was negatively related to subsequent RP skill improvement with training. This dichotomy likely reflects the divergent neural mechanisms that underlie performance of the two tasks. In the WT task, activation of left premotor cortex has an established role in motor sequence encoding[213], and thus, increased coherence between left M1 and left PM at baseline represents a brain state that is primed to acquire and perform the WT task with greater efficiency. Conversely, in the RP task, where increased parietal activity is a more efficient pathway for performing visuomotor integration[200], increased left M1-left PM coherence at baseline represents a less effective brain state for performing the RP task. This finding has important clinical implications, as the present results demonstrate an EEG measure of brain state could be used to individualize motor training and rehabilitation programs in order to optimize training effects[25].

Baseline resting-state EEG coherence was also a robust predictor of subsequent short term motor learning, as assessed by a 24 hour retention test (validated $R^2 = 0.68$). This result is an important extension of the previous study[200], as a 24 hour retention test is a more robust measure of motor learning compared to motor skill acquisition across a single training session[214]. Furthermore, a measure of motor learning across a retention test has greater implications for translation to clinical settings in which motor training-based therapies generally span many days and weeks[8,215].

In the PLS model of baseline coherence between electrodes overlying left M1 and the rest of the scalp predicting subsequent short-term motor learning, greater motor learning was associated with higher left M1 coherence with left PM and reduced left M1 coherence with left PAR. The model reflects previous work that highlights a cortical network that includes left M1, PM, and PAR regions underlying motor sequence learning[201,203,216]. Furthermore, longitudinal studies of motor sequence learning demonstrate a transition in activity from parietal areas in early learning to premotor areas in later stages of learning[217]. This shift may reflect differential roles of PM and PAR regions across the stages of motor sequence learning. In early learning, activation of parietal regions are thought to play a role in visuomotor transformation processes[218], and as learning progresses, parietal activity attenuates[219], while increased premotor activity develops in parallel with the transition to sequence encoding[213]. Therefore, in the context of the present model, individuals with greater M1-PM connectivity at baseline are primed to make a rapid transition towards sequence encoding earlier during training.

There are several limitations associated with the current study. The first, the relatively poor spatial resolution of EEG, is inherent in all EEG studies. However, dense array systems, like the 256-electrode system used in the current study, have demonstrated significantly better spatial resolution compared to traditional 10-20 systems[111,186]. Next, for unclear reasons, participants demonstrated inconsistent improvement with training on the RP task at Session 2, resulting in poorer cross-validated prediction strength in the PLS model of resting-state beta coherence predicting subsequent training-induced

motor skill acquisition on the RP task. Further examination is needed to determine whether the reduced training effects were related to participant fatigue or if the 24 hour interval between training sessions was insufficient to prevent interference from contaminating acquisition of the RP task at Session 2[220]. Finally, all participants underwent the same training schedule, with WT training occurring at Session 1 and RP training occurring at Session 2. Therefore, we were unable to determine whether an ordering effect existed. Regardless, the current results provide support for the concept that inter-individual differences in brain state can be measured and exploited to stratify patients for motor training-based therapies and can be used to predict subsequent motor skill learning. Subsequent studies are needed to determine how the prediction model is affected by intra-individual differences in resting brain state across days.

Understanding variability in capacity to acquire motor skills in healthy individuals and neural injured populations remains a major challenge. The current results show that inter-individual differences in resting-state connectivity are a promising method for stratifying individuals based on brain state and individualizing motor training-based interventions, including rehabilitation practice, to improve outcome. In conclusion, as an inexpensive, rapid, and safe method of acquiring functional brain data, EEG coherence may be useful in a multitude of settings in which prediction of response to motor training have significant social and economic repercussions.

CHAPTER 4

Connectivity measures are robust biomarkers of cortical function and plasticity after stroke

ABSTRACT

Valid biomarkers of motor system function after stroke could improve clinical decision-making. EEG-based measures are safe, inexpensive, and accessible in complex medical settings and so are attractive candidates. This study examined specific EEG cortical connectivity measures as biomarkers by assessing their relationship with motor deficits across 28 days of intensive therapy. Resting-state connectivity measures were acquired 4 times using dense array (256 leads) EEG in 12 hemiparetic patients (7.3 ± 4.0 months post-stroke, age 26 - 75 years, 6M/6F) across 28-days of intensive therapy targeting arm motor deficits. Structural MRI measured corticospinal tract (CST) injury and infarct volume. At baseline, connectivity with leads overlying ipsilesional primary motor cortex (M1) was a robust and specific marker of motor status, accounting for 78% of variance in impairment; ipsilesional M1 connectivity with leads overlying ipsilesional frontal-premotor (PM) regions accounted for most of this (R^2 = 0.51) and remained significant after controlling for injury. Baseline impairment also correlated with CST injury (R^2 = 0.52), though not infarct volume. A model that combined a functional measure of connectivity with a structural measure of injury (CST injury) performed better than either measure alone (R^2 = 0.93). Across the 28-days of therapy, change in connectivity with ipsilesional M1 was a good biomarker of motor gains (R^2 = 0.61). Ipsilesional M1-PM connectivity increased in parallel with motor gains, with *greater*

gains associated with *larger increases* in ipsilesional M1-PM connectivity (R^2 = 0.34); *greater* gains were also associated with *larger decreases* in M1-parietal connectivity (R^2 = 0.36). In sum, EEG measures of motor cortical connectivity--particularly between ipsilesional M1 and ipsilesional PM--are strongly related to motor deficits and their improvement with therapy after stroke and so may be useful biomarkers of cortical function and plasticity. Such measures might provide a biological approach to distinguishing patient subgroups after stroke.

INTRODUCTION

Motor deficits are the most common impairments after stroke, present in 85 percent of patients acutely and persisting in approximately 50 percent of stroke survivors[221]. Many different brain states can produce the same pattern of motor deficits; however, it is likely that a subset of these are more likely to respond favorably to restorative therapies[222]. Identifying accurate neural markers of motor impairment could maximize therapeutic effects by informing individualization of therapy selection, timing, and duration[39]. Furthermore, an examination of how neural markers differ across therapies could provide insight into differences in the neurobiology that underlie specific therapeutic approaches.

In the search for neuroimaging markers of motor status after stroke, prior studies have generally emphasized measures of injury or regional brain function. For example, measures of white matter integrity or of lesion load within descending motor tracts have been found to correlate with degree of motor impairment in patients with chronic

hemiparetic stroke[116,223]. In addition, gains in motor status resulting from experimental therapies have been associated with increased activity in secondary sensorimotor regions[224,225]. However, such approaches do not directly evaluate network interactions, which can provide key insights on heterogeneity in stroke recovery[226] and are the focus of the current report.

Convergent evidence supports the value of a network-based approach for understanding the relationship between dysfunctional neural activity and behavioral deficit after stroke[227]. This has been well demonstrated in connectivity studies using functional MRI (fMRI), where greater motor deficits were associated with reduced connectivity across cortical motor regions[62,228]. Thus, reduced connectivity between key nodes of the cortical motor system could serve as a marker of reduced efficiency in processing sensorimotor signals in the stroke-injured brain[229]. Consistent with this, rat models report motor dysfunction after experimental stroke is paralleled by reduced connectivity between cortical motor regions, and behavioral recovery is related to restoration of functional connectivity between cortical motor areas[230]. Similarly, human fMRI studies report that individuals with persistent motor deficits demonstrate significantly reduced connectivity across ipsilesional cortical motor regions during movement[228,231], and that behavioral recovery occurs in concert with increased connectivity among cortical motor regions[232]. Together, these findings suggest that measures of cortical motor connectivity may be good biomarkers of post-stroke sensorimotor signal processing.

The current study approached these issues using dense array EEG, which has advantages such as low cost, high safety, and high accessibility in complex medical settings. In addition, the high temporal resolution of EEG may be particularly salient in studies of the motor system, as it permits measurement of connectivity in the beta (20-30 Hz) range, a frequency range that is associated with motor system function[153,154,163]. The current study examined a resting-state EEG measure of functional connectivity, coherence with ipsilesional primary motor cortex in the beta band, as a neural marker of motor impairment and a biomarker of change in motor status across a period of intensive therapy in patients with chronic stroke. The study hypothesized that this motor system measure of resting-state EEG functional connectivity would: (1) perform better than MRI measures of structural injury such as total infarct volume and corticospinal tract lesion load as a neural marker of baseline motor impairment, (2) demonstrate specificity, i.e., correlate with motor behavior but not non-motor behaviors, and (3) change in parallel with motor gains over 28-days of intensive therapy.

Additional hypotheses were focused on neurobiological insights based on the spatial distribution of this EEG connectivity measure. Studies using PET and functional MRI in patients with stroke have found that greater activation within ipsilesional premotor areas is associated with better motor outcomes[233,234], and that larger increases in ipsilesional premotor activation parallel better motor recovery[224,235]. Conversely, greater activation within contralesional primary motor areas is associated with poorer motor outcomes[52,236], and larger increases in contralesional primary motor area activation parallel worse motor recovery[237,238]. Therefore, the current study further hypothesized

that: (1) greater connectivity between ipsilesional M1 and ipsilesional PM would be associated with better baseline motor status, and furthermore that increases in connectivity between ipsilesional M1 and ipsilesional PM would parallel greater gains with therapy, and (2) greater connectivity between ipsilesional M1 and contralesional M1 would be associated with poorer baseline motor status, and furthermore that increases in connectivity between ipsilesional M1 and contralesional M1 would parallel reduced motor gains with therapy. Additional analyses explored EEG coherence as a predictor of motor gains across therapy.

METHODS

STUDY DESIGN

Subjects with hemiparesis and chronic stroke were recruited. All subjects signed informed consent in accordance with the University of California, Irvine Institutional Review Board.

Inclusion criteria included age >18 years, stroke that occurred 3-24 months prior to first behavioral assessment, FM score of 22-55 (normal = 66), and English speaking. Exclusion criteria included deficits in communication or attention that would interfere with reasonable study participation, contraindication to MRI scanning, active major neurological or psychiatric disease, or another diagnosis substantially affecting the arm. A skull defect that could result in an EEG breach rhythm was not a specific exclusion criterion but was not present in any subject.

Approximately one week following the initial screening visit, subjects returned for structural MRI and EEG assessments. As previously described [8], after the initial screening, subjects underwent two baseline assessments of upper extremity motor status to insure behavioral recovery was at a stable plateau, i.e., any difference between Baseline 1 and Baseline 2 FM scores was <3 points, smaller than the minimal detectable change[239].

Treatment protocol

The protocol included 28 days of intensive home-based rehabilitation targeting the upper extremity[24] (Figure 4.1A). In sum, each day, subjects completed a 2-hour session focused on arm motor rehabilitation therapy. The daily therapy sessions included standard physical therapy and occupational therapy exercises guided by slide show diagrams, as well as virtual reality computer games designed to emphasize control of range, speed, timing, and accuracy of hand movements. Content of therapy was adjusted according to individual deficits.

EEG RECORDING AND SIGNAL PROCESSING

Three minutes of awake, eyes-open, resting-state brain activity was acquired by dense array surface EEG using the 256-lead Hydrocel net (Electrical Geodesics, Inc, Eugene, OR). The netted design of the Hydrocel system allows for rapid application of the 256 leads. For the typical subject, net preparation (including head measurement, net preparation in saline solution, net placement, and net adjustments) was < 10 minutes, recording time was 3 minutes, and net removal was < 5 minutes. As a result, average

start-to-finish time for a complete EEG Exam was 15-20 minutes, with no EEG Exam exceeding 30 minutes.

Participants were seated upright with feet flat on the floor. During recording, lights were dimmed, and participants were requested to minimize movements/speaking and to focus their gaze at the center of a fixation cross displayed on a laptop. An investigator in the room visually confirmed subject compliance with these instructions. Data were collected with a high input impedance amplifier (Net Amp 300, EGI) using Net Station 4.5.3 (EGI) at 1000 Hz sampling rate.

Pre-processing

EEG data were exported to MATLAB 7.8.0 (MathWorks, Inc., Natick, MA) for subsequent pre-processing and analysis steps. For three minutes of recording time, 180 one-second epochs of EEG data were collected. Data were re-referenced offline to the mean signal across all electrodes. Pre-processing steps to remove extra-brain artifacts were applied, as described previously[200]. In sum, continuous EEG data were low-pass filtered at 50 Hz, segmented into non-overlapping 1-second epochs, and then mean detrended. Next, visual inspection removed epochs contaminated by muscle activity, including neck and face movements. EEG data then underwent ICA decomposition, in which components representing eye blinks, eye movements, and cardiac rhythms were removed[157,158]. The remaining components were transformed back to channel space before undergoing an additional round of visual inspection to ensure absence of all extra-brain artifacts in the remaining data. Across all EEG recordings (12 subjects x 4

EEG Exams/ subject), 171.4 ± 12.0 (mean ± s.d.) of the 180 epochs per EEG exam (93.6%), were retained for subsequent analyses.

Coherence

Functional connectivity between brain regions was estimated from EEG coherence between electrodes overlying the corresponding regions[72]. Coherence ranges from zero to one, with a coherence value near one indicating EEG signals have similar phase and amplitude difference at all time points, and a coherence value near zero indicating signals have a random difference in phase and amplitude. Although coherence has been widely adopted in EEG studies as a surrogate marker of communication between cortical neural sources[72], there is potential that an observed increased in coherence may result from increased input from a tertiary common neural source[161].

The high beta (20-30 Hz) frequencies are associated with function of the motor system[154,163]. Therefore, the primary metric in the present study was mean coherence in the high beta frequency range using a seed region over ipsilesional M1, a central motor execution node of the cortical motor system[165]. For the 256-lead system used, the M1 seed was defined as either C3 or C4 (left or right M1, respectively), which some studies have suggested largely reflects activity from the precentral gyrus[207], and its six immediately surrounding leads. Coherence matrices from individuals with infarcts in the right hemisphere were flipped across the midline for subsequent analyses.

PLS modeling

PLS analyses are particularly well suited for analyzing very large data sets that contain many predictors, for which multiple comparisons would reduce statistical power, as is common in neuroimaging data[167], and for analyzing data sets that have multicollinearity among predictors. Similar to previous studies from our group[171,200], the current study used the N-way Toolbox for MATLAB[168] to implement PLS analyses. The resultant PLS model from each analysis was then used to identify electrodes of interest for characterizing brain function-behavior relationships.

The mathematics of PLS can be conceptualized as a variant of ICA. With both PLS and ICA, a multivariate signal such as EEG is reduced to a series of additive subcomponents. In ICA, the objective is to maximize representation of variance in the independent variable in as few components as possible. Conversely, in PLS, the objective is to maximize representation of variance in the dependent variable in as few components as possible. This is accomplished by optimizing a least squares fit for a partial correlation matrix between the independent and dependent variables. For the present analyses, the independent variable was EEG coherence and the dependent variable was FM score. As preprocessing steps, data were first mean detrended and then underwent a direct orthogonal signal correction to allow for more efficient PLS models with fewer components[169]. From the PLS regression, a series of models with successively more components were generated that maximally accounted for variance in the dependent variable. The fitted PLS model included as many components as were required to achieve 80% of variance in the dependent variable explained.

To test predictive strength of each PLS connectivity model, cross-validation was performed using a leave-one-out and predict approach. With this validation method, data from each subject are iteratively removed from the PLS model, and the removed subject's behavioral data are predicted from his/her EEG coherence data using the PLS model generated from the remaining *n-1* subjects. This method of cross-validation was selected because a leave-one-out and predict validation scheme has established utility for accurately assessing generalization of results to an independent data set, particularly with smaller sample sizes[210,211].

Leads where coherence with ipsilesional M1 was most strongly related to behavioral status were identified by setting an arbitrary threshold for each model using the approach described by Menzies et al[240]: correlation coefficients were thresholded at $|r_i| > 0.8 * r_{max}$, where r_i is the correlation coefficient at the *i*th lead and r_{max} is the largest $|r_i|$ value across all 249 leads (256 total electrodes minus the 7 seed leads overlying M1).

MAGNETIC RESONANCE IMAGING

High resolution T1-weighted images were acquired with a Philips Achieva 3T MRI scanner using a 3D MPRAGE sequence (TR = 8.5 ms; TE = 3.9 ms; slices = 150; voxel size = 1x1x1 mm^3). Infarct volume and the percent of the CST affected by stroke (*CST injury*) were calculated using previously described methods[241]. Infarct volume was outlined by hand on a T1-weighted MRI image. CST injury was quantified by overlapping each subject's infarct in MNI stereotaxic space with a normal M1 corticospinal tract generated from healthy controls[47,223,242].

STATISTICAL ANALYSES

Change in motor impairment score was analyzed by a two-tailed paired t-test, with statistical significance set at $p < 0.05$. Simple bivariate analyses between a clinical measure (behavior or demographic) and brain state (MRI injury or EEG coherence) were performed using two-tailed linear regression models with statistical significance set at $p < 0.05$. Parametric statistical methods were used, as all measures were normally distributed or could be transformed to a normal distribution. Statistical tests were performed using the MATLAB 7.8.0 statistical package.

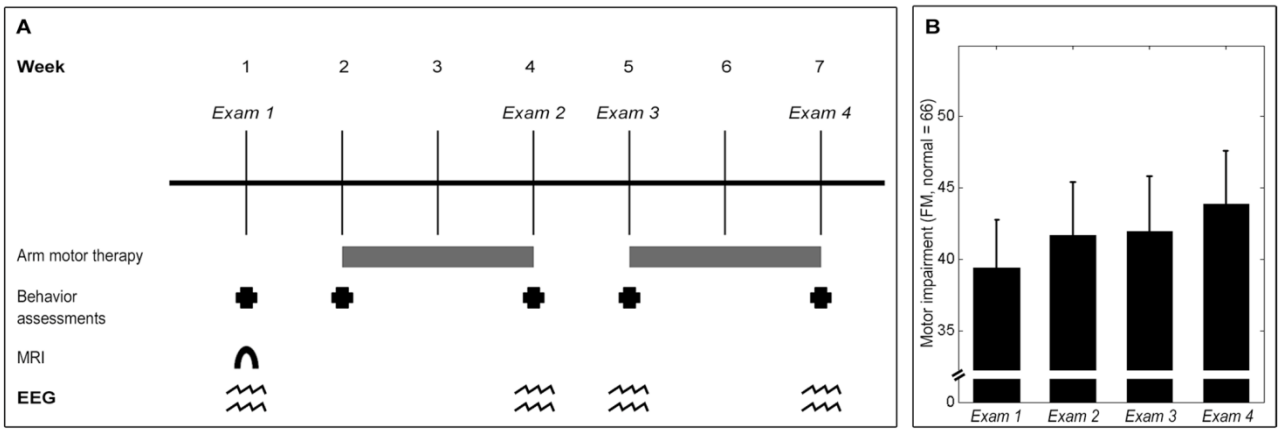

FIGURE 4.1. Experimental setup. **A**. Experiment timeline. Behavioral and EEG assessments were performed at baseline, then after 2 weeks of therapy, following the 1 week break, and at end of 28 days of therapy. A baseline structural MRI scan was also acquired. **B**. The group showed statistically and clinically significant gains in upper-extremity motor status, as measured by the Fugl-Meyer Arm Motor Assessment (mean ± s.e.), across therapy ($t_{11} = 5.89$, $p = 0.0001$).

RESULTS

SUBJECTS

Twelve subjects, age 26-75 (mean = 54.0 ± 16.6 years), 6M/6F, in the chronic phase of stroke recovery (mean time post-stroke = 7.3 ± 4.0 months) with persistent hemiparesis were recruited. All 48 EEG Exams (four Exams/subject x 12 subjects, Figure 4.1A) were completed successfully, with no EEG Exam excluded for reasons such as excessive movement or muscle artifact during data acquisition or hardware malfunction.

The patient group showed heterogeneity in both size and location of brain infarcts (Table 4.1). Overall, the group showed mild-moderate arm motor impairment at Exam 1 (mean FM = 39 ± 12, range 23-56, normal = 66). At baseline, motor deficits were stable, as the group did not show a significant change in FM score across the two baseline behavioral assessments (t_{11} = -0.20, p = 0.85). Across therapy, motor deficits improved significantly, as FM scores increased by 4.5 ± 2.7 points (Figure 4.1B), achieving statistical significance (t_{11} = 5.89, p = 0.0001) and exceeding the minimal clinically important difference[239].

TABLE 4.1. Subject Characteristics

Patient No.	Age (years)	Gender	Affected arm	Infarct volume (cc)	Infarct site	Months post-stroke	Baseline FM score
1	66	M	R	3	Left pontine	8.4	55
2	39	M	L	21.5	Right cingulate	5.4	42
3	75	F	R	5	Left frontal	5.5	51
4	68	M	L	100.6	Right frontal	6.3	39
5	39	M	R	0.4	Left internal capsule/temporal	4.8	56
6	47	M	R	10.3	Left temporal	8.5	49
7	43	F	L	59.1	Right frontal	10.2	25
8	65	F	R	1.2	Left internal capsule	3.6	38
9	70	F	L	32.2	Right parietal	5.6	23
10	26	F	R	30.1	Left parietal	18.4	36
11	70	F	L	25.7	Right parietal	4.7	23
12	40	M	L	0.8	Right pontine	5.6	36

CONNECTIVITY IS A ROBUST AND SPECIFIC CROSS-SECTIONAL MARKER OF MOTOR STATUS

The PLS connectivity model at Exam 1 ("*Exam 1 PLS model*") identified a pattern of beta coherence with M1 that correlated strongly with Exam 1 FM score (fitted R^2 = 0.96). Cross-validation using the leave-one-out approach found that the *Exam 1 PLS model* remained highly accurate (validated R^2 = 0.78, Figure 4.2A), i.e., connectivity between ipsilesional M1 and the rest of the scalp accounted for 78% of the variance in Exam 1 FM score across the 12 subjects.

To better understand the *Exam 1 PLS model*, those leads where variance in connectivity with M1 was most strongly related to Exam 1 FM score were identified. These were clustered in ipsilesional PM (indicated by black dots in Figure 4.2A). Focusing on these ipsilesional PM leads, bivariate linear regression found that individuals with higher ipsilesional M1-PM connectivity at Exam 1 had higher Exam 1 FM scores. Furthermore, variance in ipsilesional M1-PM connectivity accounted for a majority of the variance in Exam 1 FM scores (R^2 = 0.51, p = 0.009, Figure 4.2B). This relationship between M1-PM connectivity and FM score measured at the same Exam remained robust across each of the four EEG Exams (Exam 2: R^2 = 0.67, p = 0.001; Exam 3: R^2 = 0.37, p = 0.036; and Exam 4: R^2 = 0.46, p = 0.014).

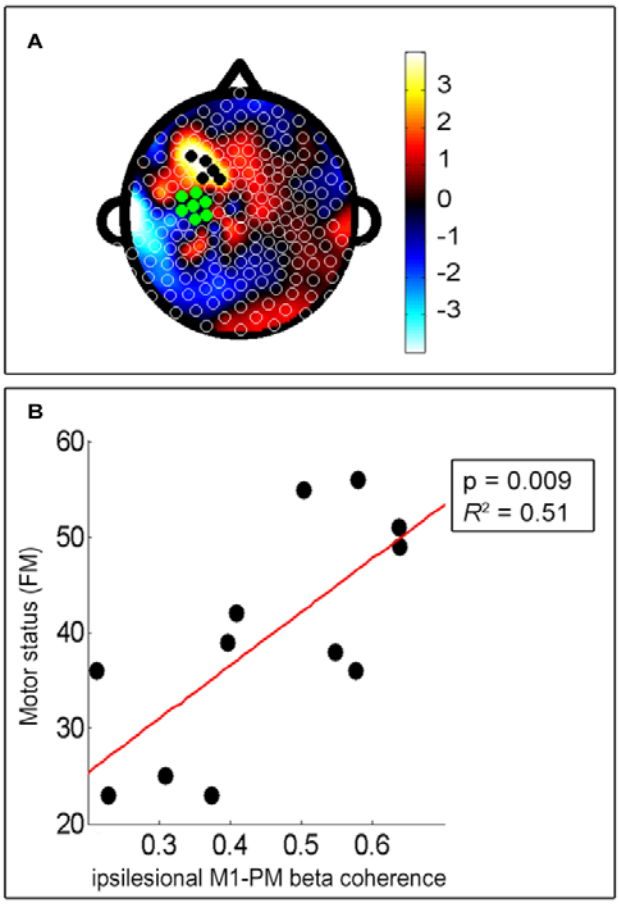

FIGURE 4.2. Cortical connectivity with ipsilesional M1 was a good marker of FM score at baseline. **A**. Topographic map of correlation coefficients of PLS model correlating baseline ipsilesional M1 connectivity across whole scalp and baseline FM score (fitted R^2 = 0.96, cross-validated R^2 = 0.78). The left side of the figure is ipsilesional, the right side is contralesional, green electrodes indicate the ipsilesional M1 seed, and the black dots indicate leads overlying the ipsilesional frontal-premotor cortical region (PM). **B**. Greater degree of ipsilesional M1-PM connectivity was correlated with higher FM score (R^2 = 0.51, p = 0.009).

To examine the specificity of the relationship between motor deficits and ipsilesional M1-PM connectivity in the *Exam 1 PLS model*, this connectivity measure was also examined in relation to two non-motor assessments, the Geriatric Depression Scale score (GDS) and the Mini Mental Status Exam score (MMSE). Neither correlated

significantly (GDS: $p = 0.85$; MMSE: $p = 0.25$), indicating that ipsilesional M1-PM connectivity at Exam 1 demonstrates specificity as a neural marker of motor status. In addition, a new PLS model was generated examining ipsilesional M1 connectivity in relation to GDS. This too did not reach significance, further supporting that whole scalp connectivity with ipsilesional M1 demonstrates specificity for function of the motor system.

An additional analysis examined connectivity between ipsilesional M1 and contralesional M1 (defined as the homologous leads over the contralesional hemisphere) in relation to motor status. Connectivity between ipsilesional M1 and contralesional M1 at Exam 1 was not significantly related to Exam 1 FM score ($p = 0.87$). A secondary analysis examined connectivity between ipsilesional M1 and contralesional PM at Exam 1, and this was also not related to Exam 1 FM score ($p = 0.41$).

MRI measures of injury as cross-sectional markers of motor status

Infarct volume, a global measure of injury, did not correlate with Exam 1 FM score ($p > 0.05$), but percent CST injury, a measure more related to motor system injury, did ($R^2 = 0.52$, $p = 0.008$). The strength of this brain injury-behavior relationship was similar to the strength of the brain function-behavior relationship (i.e., ipsilesional M1-PM connectivity, $R^2 = 0.51$, above).

Clinical measures were poor predictors of baseline motor impairment. Time post-stroke (p = 0.85), age (p = 0.81), mood (GDS, p = 0.55), and cognitive status (MMSE, p = 0.30) did not correlate significantly with Exam 1 FM score.

Neural structure and function in combination contribute to motor status

Neural structure (injury) and functional factors each had an independent role in explaining motor status. A partial correlation was performed to determine the degree of association that EEG connectivity and CST injury each had with Exam 1 FM score. Both CST injury (R^2 = 0.58, p = 0.007) and ipsilesional M1-PM connectivity (R^2 = 0.42, p = 0.03) remained significant; note that CST injury and baseline ipsilesional M1-PM connectivity were not significantly correlated (p = 0.12).

Furthermore, the combination of CST injury and EEG connectivity was found to be a better marker of motor status than either measure alone. CST injury and EEG connectivity were combined through two methods. When CST injury was added as an additional predictor in the *Exam 1 PLS model* of EEG connectivity, prediction was improved significantly (R^2 = 0.93, $F_{0.05,1,10}$ = 21.04, p = 0.0001). CST injury and M1-PM connectivity were also combined in a multivariate least squares regression model, which also significantly improved prediction (R^2 = 0.86, $F_{0.05,1,10}$ = 6.70, p = 0.03).

CHANGES IN CONNECTIVITY ARE A GOOD BIOMARKER OF MOTOR GAINS WITH THERAPY

A separate analysis examined how change in EEG connectivity performed as a biomarker of change in motor status over the 28 days of therapy. The PLS model examining change in connectivity and change in FM score from Exam 1 to Exam 4 ("*Change PLS model*") had a fitted R^2 = 0.92 and cross-validated R^2 = 0.61. The leads from the *Change PLS model* most strongly related to change in FM score over this period were clustered in regions overlying ipsilesional parietal (PAR) and ipsilesional PM cortex (indicated by black dots in Figure 4.3A). *Greater gains* in FM from Exam 1 to Exam 4 were related to *larger increases* in ipsilesional M1-PM connectivity (Figure 4.3B, R^2 = 0.34, p = 0.04) and to *larger decreases* in ipsilesional M1-PAR connectivity (Figure 4.3C, R^2 = 0.36, p = 0.04); note that change in ipsilesional M1-PM connectivity and change in ipsilesional M1-PAR connectivity from Exam 1 to Exam 4 were not significantly correlated (p = 0.96). Change in connectivity between ipsilesional M1 and contralesional M1 regions did not correlate with change in FM score (p = 0.65).

FIGURE 4.3. Change in ipsilesional M1 connectivity was a significant biomarker of motor gains across therapy. **A**. Topographic map of correlation coefficients in the PLS model correlating change in ipsilesional M1 connectivity across whole scalp and change in FM score across the 28 days of therapy (fitted R^2 = 0.92, cross-validated R^2 = 0.61). **B**. Greater degree of ipsilesional M1 connectivity with ipsilesional frontal-premotor cortical regions (PM) was correlated with higher FM gains (R^2 = 0.34, p = 0.04); compared to the ipsilesional PM electrodes identified in the *Exam 1 PLS model*, PM electrodes in this *change PLS model* were more ventrally located. **C**. Greater degree of ipsilesional M1 connectivity with ipsilesional parietal (PAR) cortical regions was correlated with smaller FM gains (R^2 = 0.36, p = 0.04).

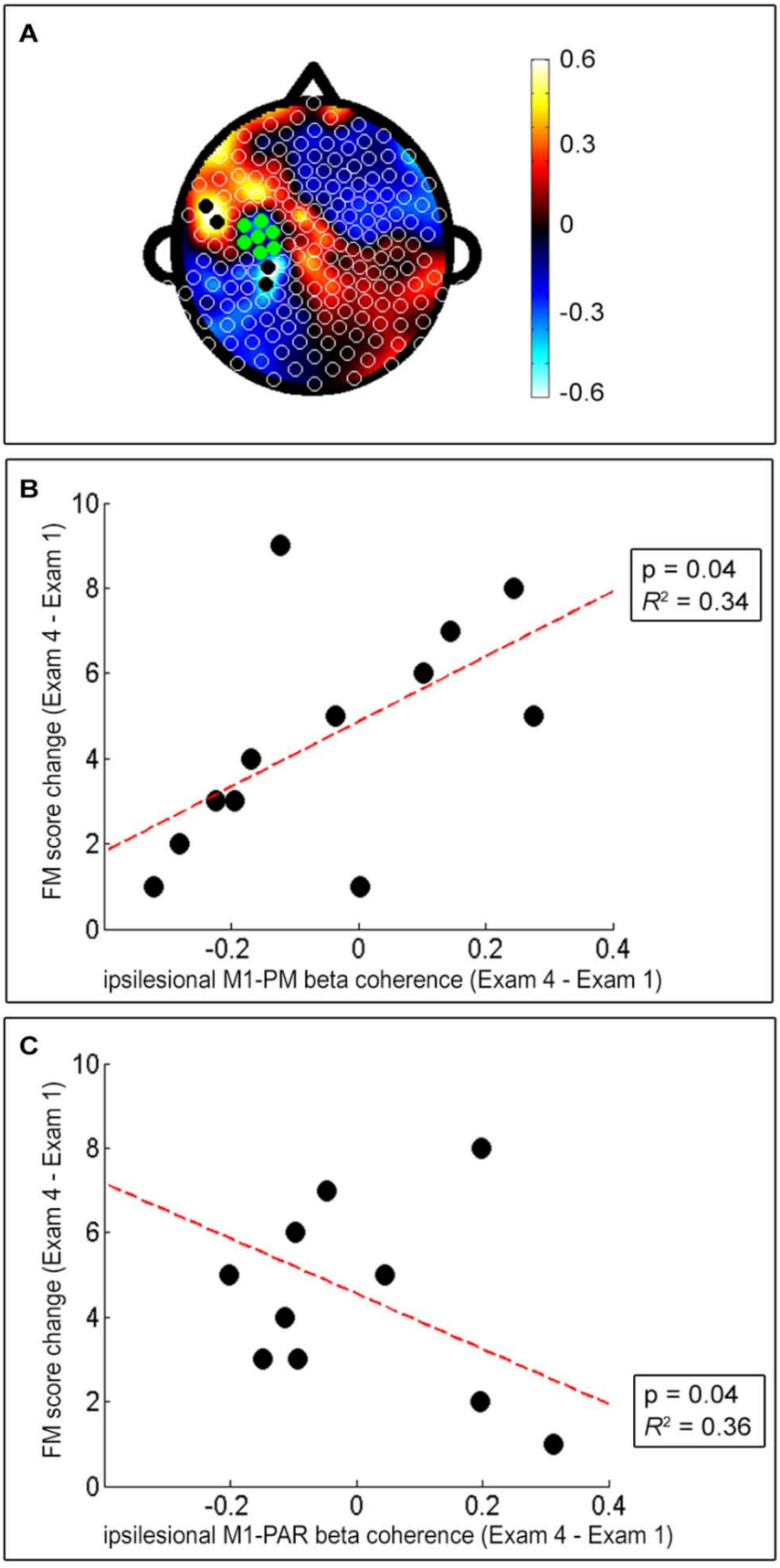
A
0.6
0.3
0
-0.3
-0.6
B
FM score change (Exam 4 - Exam 1)
10
8
6
4
2
0
-0.2
0
0.2
0.4
ipsilesional M1-PM beta coherence (Exam 4 - Exam 1)
p = 0.04
R² = 0.34
C
FM score change (Exam 4 - Exam 1)
10
8
6
4
2
0
-0.2
0
0.2
0.4
ipsilesional M1-PAR beta coherence (Exam 4 - Exam 1)
p = 0.04
R² = 0.36

BASELINE CONNECTIVITY PREDICTS GAINS FROM THERAPY

The PLS model of connectivity with ipsilesional M1 at Exam 1 predicting change in FM score across therapy (from Exam 1 to Exam 4) had a fitted R^2 of 0.97 and a cross-validated R^2 of 0.79 (Figure 4.4A). The leads from this Exam 1 predictive model that most strongly related to change in FM score were clustered in a region overlying ipsilesional parietal operculum (PAROperc). *Greater gains* in FM from Exam 1 to Exam 4 were predicted by lower M1-PAROperc connectivity at Exam 1 (Figure 4.4B, R^2 = 0.60, p = 0.003).

Clinical and MRI measures at Exam 1 do not predict motor gains from therapy

None of the clinical measures (age, time post-stroke, Exam 1 FM score, GDS score, Edinburgh handedness score, and MMSE score) predicted change in FM score from Exam 1 to Exam 4. In addition, neither of the MRI-based measures of injury (infarct volume and percent CST injury) predicted change in FM score across therapy.

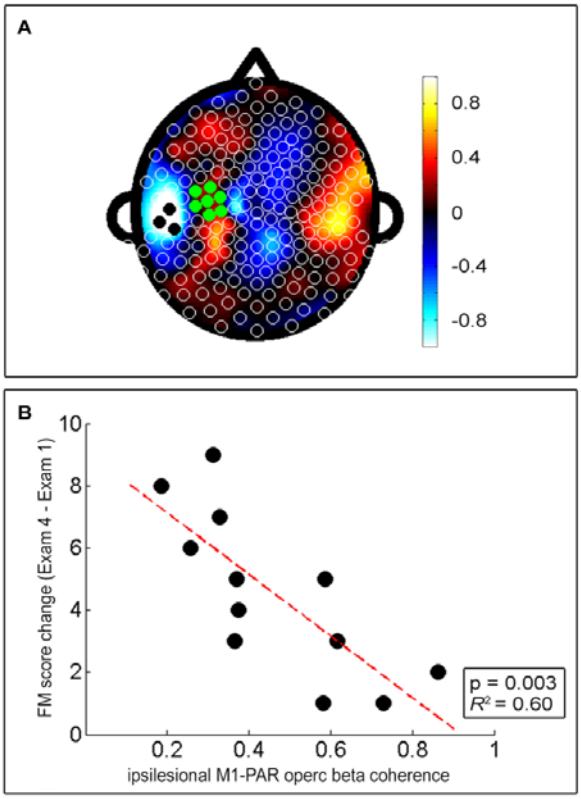

FIGURE 4.4. Cortical connectivity with ipsilesional M1 at baseline predicted motor gains across therapy. **A**. Topographic map of correlation coefficients in the PLS model correlating ipsilesional M1 connectivity across whole scalp at baseline with change in FM score across the 28 days of therapy (fitted R^2 = 0.97, cross-validated R^2 = 0.79). **B**. Greater degree of ipsilesional M1 connectivity with ipsilesional parietal operculum (PAROperc) predicted smaller FM gains (R^2 = 0.60, p = 0.003).

DISCUSSION

Patient care and clinical trials often rely on bedside assessments for decision-making after stroke. Biomarkers may be able to inform such decisions, e.g., to define therapy content[243], to stratify patients in a trial[25], or to assess changes in brain function across a period of therapy[131] based on a patient's specific biological state. Evidence suggests that measures of cortical connectivity have the potential to serve as such biomarkers[62,228–230]. However, cortical connectivity has generally been measured using

MRI, which may have limitations in clinical application. A previous report found an EEG-based measure of connectivity was useful for predicting motor skill acquisition in healthy subjects[200]. The current study extended this approach and found the same EEG-based measure (resting coherence between ipsilesional M1 and the rest of the cortex, in the high beta band) was a robust marker of baseline motor status, biomarker of change in motor status across 28 days of intensive therapy, and predictor of gains from therapy. Ipsilesional M1 connectivity with ipsilesional PM regions was consistently associated with favorable motor status, while measures of ipsilesional M1 connectivity with contralesional M1 were not significant. These findings support the potential of EEG-based measures of cortical connectivity as biomarkers after stroke.

The current study found that, among 12 patients with hemiparetic chronic stroke, functional connectivity with ipsilesional M1 across the brain had a robust relationship with baseline impairment, with a cross-validated R^2 of 0.78, and furthermore was a powerful predictor of motor gains across the period of therapy, with an R^2 of 0.79. By comparison, an MRI-based measure of motor system injury (percent CST injury) had a comparable relationship with baseline motor status at baseline (R^2 = 0.52) but did not significantly predict treatment gains. The strength of the current results speak to clinical applications of the current methods as reliable biomarkers of brain state that can be serially measured in patients with stroke. EEG has poorer spatial resolution as compared to neuroimaging modalities such as MRI. In addition, localization is limited by the fact that recordings are obtained at the scalp, and so current results are presented as occurring in the leads overlying a brain area rather than strictly within cortical regions

per se. Nonetheless, EEG-based methods may have substantial clinical utility given their established safety record, low expense per exam, and relative ease and rapidity of data acquisition across complex medical settings.

Increasingly, multimodal approaches that consider both brain function and brain structure have been found to have advantages for explaining variance across patients with stroke[15,16]. Consistent with these reports, the current study found that a combination of a brain functional assessment (motor network connectivity derived from dense array EEG) and a brain structural assessment (of motor system injury, CST injury based on MRI) demonstrated improved prediction of motor impairment status as compared to either measure alone. While motor system injury and a measure of motor system function (M1-PM beta coherence) each explained about 50% of variance in motor impairment, prediction was improved (R^2 = 0.86) when structural and functional measures were combined in a multivariate model. Prediction was also improved when CST injury was included with connectivity measures in a PLS model of baseline impairment (validated R^2 = 0.93). Thus, the current results represent a progression from previous studies that separately demonstrated EEG measures of connectivity and MRI measures of motor system damage to each be a good marker of motor status after stroke[81,223]. The current results are also in line with previous studies demonstrating that both brain structure (injury) and brain function (connectivity via fMRI) contribute to motor status after stroke[13,14].

Current methods also provide some insights into the neural events underlying the EEG findings. At baseline, larger ipsilesional M1-PM connectivity correlated with better motor status, accounting for much of the *Exam 1 PLS model* (Figure 4.2B) and explained a majority of the variance in Exam 1 FM scores. Ipsilesional M1-PM connectivity remained informative across the 28 days of therapy, increasing in parallel with motor gains (Figure 4.3B). These results are consistent with abundant data describing an association between good motor recovery after stroke and increased activation of ipsilesional PM during motor tasks[52,97,127]. Although much of the previous work regarding the role of ipsilesional PM in motor recovery after stroke was derived from task-related data, several recent studies suggest brain activity acquired at rest is representative of engagement of brain networks during a task[147,244]. Furthermore, several recent studies demonstrate that individual differences in brain function at rest are predictive of subsequent performance[149,150,200]. Additionally, studies that examine connectivity measures derived from both resting and task-related data have produced similar results with respect to ipsilesional M1-PM connectivity and its relationship with behavioral status after stroke[61,231,245]. The similarities across these reports are consistent with the parallels between current resting-state results and previously reported findings from task-related studies.

An additional hypothesis in the current study was that increased ipsilesional M1-contralesional M1 connectivity would be associated with lower baseline FM scores and with smaller motor gains across therapy[228]. However, ipsilesional M1-contralesional M1 connectivity was not significantly related to baseline motor status or to its change with

therapy. The reasons for this finding are uncertain but may be multifactorial. First, clinical characteristics of subjects enrolled in the current study, including time post-stroke and stroke severity, might have influenced the M1-M1 connectivity results. Indeed, longitudinal studies[246,247] report that it is at earlier, and not later, points in stroke recovery that contralesional regions, including contralesional M1, are most prominent, and that M1-M1 connectivity is most asymmetric. Thus, the chronicity of patients enrolled in the current study compared to previous studies that report significant associations between M1-M1 connectivity and motor status after stroke[62,245] may partially account for the negative M1-M1 connectivity findings in the current study. Additionally, increased activation of contralesional M1 after stroke has been implicated as a compensatory mechanism in individuals with more severe stroke deficits[248,249] and thus might be expected to be a less robust marker of motor status in the mild-moderately impaired subjects enrolled in the current study. Second, the contribution of contralesional M1 to motor network processes after stroke may be less apparent when brain function is probed at rest, in contrast with the contribution of ipsilesional PM (see above). Indeed, in subjects with chronic stroke, interhemispheric inhibition measured between bilateral M1 showed greater correlation with behavioral parameters when assessed during motor preparation compared to during the resting state[250]. Further, in healthy subjects, M1-M1 connectivity is more apparent during movement compared to at rest[251], and is further enhanced by increasing task complexity[252]. The current findings are concordant with a prior fMRI-based study that found ipsilesional M1-contralesional M1 connectivity to be a less robust marker of motor status after stroke compared to ipsilesional M1-PM connectivity[61]. Overall, results suggest that M1-M1

connectivity, particularly when measured at rest, may have limitations as a marker of motor system function in patients with mild-to-moderate impairment in the chronic phase of stroke.

The current study presents a novel application of PLS regression for analysis of EEG data in a stroke population, resulting in robust correlations between neural measures of connectivity and motor impairment. Such an approach is similar to graph theoretical approaches that examine stroke-related changes in cortical motor network centrality[245,253]. While graph theory analysis requires *a priori* definition of network nodes, PLS is a whole brain approach for identifying regions of interest, and may be less likely to overlook contributions from brain regions that were not considered at the outset, such as the contribution of larger M1-PAR connectivity across therapy as a biomarker of smaller motor gains; increased M1-PAR connectivity may reflect greater reliance on regions posterior to ipsilesional M1, a compensatory mechanism associated with greater damage to the motor system[222,254]. Notably, the structure of the models is defined by brain states of the specific patients enrolled in the study and are likely also influenced by therapy content. These caveats underscore the need to further evaluate the current model more broadly, e.g., in separate and different stroke populations, with a different class of therapeutic intervention, or in relation to non-motor deficits after stroke.

High inter-subject variability in response to treatment is common after stroke and is an important concern in clinical stroke research[244,255,256]. Serial measurement of brain

functional connectivity over a course of rehabilitation therapy has the potential to provide biological insights into this variability and thereby improve the precision with which post-acute care is prescribed. Since the current methods demonstrate a consistent relationship between ipsilesional M1-PM coherence and FM score at each of the four Exams spanning the 28 days of therapy, the EEG-derived measure of connectivity therefore appears to be a reliable neural marker of motor system status after stroke. Parallels between previous reports and the current results with respect to ipsilesional M1-PM connectivity and post-stroke motor status suggest validity of the current EEG-based methods as a neural probe of motor system function after stroke. In addition, as data could be obtained at all 48 EEG sessions, with no EEG Exam excluded due to reasons such as hardware malfunction or excessive movement artifact during data acquisition, the present EEG-based methods may be less restrictive as compared to fMRI-based methods, which exclude some individuals such as those with certain metal implants. EEG is a safe and relatively inexpensive neuroimaging method that can be rapidly performed at the bedside and so may be useful in complex clinical settings such as acute stroke[111], where measuring brain function has historically been challenging. In addition, targeted engagement of a specific brain network[257] such as the ipsilesional PM circuit[243] is a strategy that might be useful for maximizing rehabilitation gains, and that would benefit from availability of a brain state biomarker at the bedside. Together, the current results suggest that EEG measures of cortical connectivity may have value as biomarkers of cortical function and plasticity after stroke.

CHAPTER 5

Brain function and neural injury predict early post-stroke impairment

ABSTRACT

Bedside measures of brain function could significantly improve clinical decision-making. EEG-based measures are attractive candidates because they are safe, inexpensive, and readily accessible, and because of recent hardware and software advances. In 24 patients, resting-state dense-array (256-electrode) EEG was acquired at bedside during acute stroke admission (3 hours - 12 days post-onset), in the ER, ICU, and acute stroke ward. Traditional quantitative EEG measures were weak predictors of admission NIHSS score. However, a partial least squares (PLS) model of beta (13 - 19 Hz) power across the whole brain was highly correlated with NIHSS (R^2 = 0.90) and remained a robust predictor of NIHSS in model cross-validation (R^2 = 0.73). Similar results were found using delta (1 - 3 Hz) power. In contrast, measures of neural injury demonstrated only modest correlation with NIHSS score (infarct volume, R^2 = 0.17; corticospinal tract injury, R^2 = 0.19), and neither survived as a predictor in model cross-validation. Nevertheless, prediction of admission NIHSS was significantly improved (from R^2 = 0.73 to R^2 = 0.81) when a measure of neural injury (infarct volume) was added to the PLS model of beta power. Functional markers of impairment differed according to infarct volume. With large strokes (n = 9), NIHSS correlated with beta power in leads overlying both ipsilesional and contralesional sensorimotor cortex (SMC), while with small strokes (n = 15), NIHSS correlated with beta power in leads overlying only ipsilesional SMC. Dense array EEG analyzed with PLS modeling performed well as a bedside measure of

brain function in patients with acute stroke. Predictive models were improved by including measures of both neural function and neural injury.

INTRODUCTION

Stroke is a very heterogeneous condition. Measurement of inter-subject differences in neural function and neural injury can individualize treatment decision-making in clinical practice and patient selection and stratification in clinical trials[39]. In the days after acute stroke, measures of neural injury such as infarct volume have a significant, though incomplete, relationship with clinical status and outcomes[258,259,41]. Measures of neural function provide additional insights[260]. The strongest evidence for this comes from animal[261] and human[13] studies in chronic stroke. Studies in acute stroke using functional MRI (fMRI), transcranial magnetic stimulation, and positron emission tomography (PET) are also supportive[262,249,263,264]. However, implementation of these techniques in the acute stroke setting can be challenging, underscoring the need for additional approaches for measuring brain function early after stroke.

EEG is useful for studying brain function safely and rapidly in complex medical settings, and has been used to evaluate acute stroke for many decades[128,64,63]. EEG measures have high temporal resolution and are directly linked with neuronal metabolism, and as a result reflect ischemic injury very rapidly[265,130,75]. A number of EEG changes have been described after stroke such as increased slow EEG rhythms and reduced fast EEG rhythms. However, broad adoption of EEG into acute stroke clinical practice remains limited due to a number of factors such as optimal choice of quantitative EEG

metric[106,107,125] and uncertainty regarding the significance of contralesional EEG changes[63,130,92]. In addition, some authors average EEG signals across many or all scalp leads, informing some analyses but sacrificing spatial resolution[134]. Perhaps most important has been the difficulty of mounting traditional 10-20 EEG electrode systems with the speed and ready availability needed in the acute stroke setting[106].

Advances in EEG hardware and software analysis may be able to overcome many of these barriers. New EEG systems substantially reduce preparation time by using dry leads, or embedding electrodes in a cap or saline-based geodesic net[266]. Dense-array systems with up to 256 electrodes demonstrate improved spatial resolution compared to standard 20 lead systems[111,267]. Newer computational methods are better equipped to handle high dimensional neuroimaging data as compared to prior linear regression methods, and provide improved resolution of task-related brain function, thus achieving improved correlation with behavioral state[268]. For example, recent studies using partial least squares (PLS) regression, which retains the high dimensionality of EEG available with dense-array recordings, found this method outperformed bivariate correlations for predicting behavioral variation[200,269].

The current study builds on these findings, using a 256-electrode saline net EEG system and PLS analyses to study patients admitted for acute stroke. Hypotheses were that: (1) dense-array EEG analyzed with PLS models of whole brain function significantly predict impairment level (NIHSS score) hours-days after stroke onset; (2) these PLS models predict impairment better than traditional quantitative EEG metrics

do; and (3) measures of neural function from dense-array EEG recordings add significantly to the predictive power of neural injury measures, in line with preclinical[261] and human[13,270] stroke studies. An additional study aim examined whether dense-array EEG and PLS modeling provide insights into differences in stroke effects according to infarct volume.

METHODS

STUDY DESIGN

Inpatients with a radiologically confirmed ischemic stroke were recruited from the University of California, Irvine Medical Center. All subjects signed informed consent in accordance with the University of California, Irvine Institutional Review Board. Inclusion criteria included age >18 years and English speaking. Exclusion criteria included active substance abuse; inability to comply with study procedures; pregnancy; significant disability prior to stroke; significant problems with attention, alertness, or cognitive function; a major psychiatric or neurologic diagnosis apart from the index stroke; and inability to communicate. As part of standard stroke center procedure[271], all subjects had NIHSS scored on admission. After consent, each subject underwent EEG assessment, and clinical data were recorded.

EEG ACQUISITION AND ANALYSIS

A dense-array surface EEG (256-electrode Hydrocel net, Electrical Geodesics, Inc., Eugene, OR) was used to acquire three minutes of awake, eyes-open, resting-state brain activity. Due to the netted design of the Hydrocel system, all 256 electrodes are

mounted onto the scalp at the same time. As a result, start-to-finish time for EEG preparation (including head measurement, net preparation in the saline conducting solution, net placement, and net adjustments), three minutes of EEG recording, EEG removal, and cleanup was typically 20 minutes.

Participants who were ambulatory were seated upright in a chair with feet flat on the floor. Otherwise, the head of the hospital bed was raised to 30 degrees and the participant's arms were set onto pillows to prevent contact with any hospital bed metal. During recording, overhead lights were dimmed, and participants were instructed to minimize movements and speaking during recording and to focus their gaze at a fixation point. An examiner observed the subject to ensure compliance. Data were collected with a high input impedance amplifier (Net Amp 300, EGI) using Net Station 4.5.3 (EGI) at 1000 Hz sampling rate, with no digital filters applied to the raw recorded signal.

Pre-processing

EEG data were exported to MATLAB 7.8.0. (MathWorks, Inc., Natick, MA) for pre-processing and analyses. In-line with previously described methods[200,269], preprocessing steps included applying a second-order 50 Hz low-pass Butterworth filter, mean de-trending, and re-referencing to the average signal across all channels. Continuous EEG data were then epochized into 180 sequential, non-overlapping, one-second trials. Following a visual inspection to remove trials contaminated by overt movement and speaking, the time series was subjected to an Infomax Independent Component Analysis (EEGLAB[157]), in which components containing characteristic extra-

brain artifacts (including eye blinks, eye movements, and cardiac rhythms) were identified and removed[158]. The remaining components were then transformed back to channel space before undergoing a subsequent visual inspection to ensure absence of all extra-brain artifacts in the remaining data. Across the 24 EEG recordings, 167.9±20.4 (mean±SD) of the 180 epochs per EEG exam (88.2%) were retained for subsequent analysis.

Quantitative EEG (QEEG): spectral power and coherence

Regional activation was approximated using spectral power. Power measures were extracted by submitting the time series in each channel to a discrete Fast Fourier transform, and then normalizing by epoch length. Average absolute power at each electrode was calculated for a 1 - 30 Hz frequency band in 1 Hz bins, then in all cases expressed as relative power, i.e., divided by total power across 1 - 30 Hz at each electrode. Based on prior studies of EEG in acute brain injury, relative delta (1 - 3 Hz) power was selected as the primary measure of spectral power; relative power in theta (4 - 6 Hz), alpha (7 - 12 Hz), beta (13 - 19 Hz), and high beta (20 - 30 Hz) bands were also examined.

Recent findings suggest connectivity measures better represent complexity in human cortical processing and thus may demonstrate a stronger relationship with behavior[59]. In the current study, functional connectivity between brain regions was estimated using EEG coherence between electrodes overlying corresponding brain regions[72]. Coherence is a dimensionless quantity that ranges from zero to one and describes the

degree of frequency and amplitude correspondence between signals. Specifically, a coherence value near zero for a given pair of electrodes indicates a random difference in phase and amplitude, while a coherence value equal to one indicates no difference in phase and amplitude across all time points. Similar to spectral power, coherence is a frequency specific measure, and so mean coherence was calculated for each of the five frequency bands of interest. For individuals with infarcts in the right hemisphere, power arrays and coherence matrices were flipped across the midline for subsequent analyses. Since the NIHSS scale is weighted towards motor impairments[272], the current study focused on mean coherence with a seed cluster of seven electrodes overlying ipsilesional sensorimotor cortex (SMC); the SMC seed was defined as the C3 lead, which largely reflects activity from precentral gyrus[207], and its six immediately surrounding leads.

PLS modeling

Partial least squares (PLS) analyses have advantages for analyzing large data sets, such as those acquired with neuroimaging, that have multicollinearity across a large number of predictors, which can reduce statistical power[167]. The current study used a previously described implementation of PLS regression to correlate behavioral measures and whole brain EEG measures[200,269]. To allow for more efficient PLS models with fewer components, the data first underwent a direct-orthogonal signal correction[169]. From the PLS decomposition, a series of models, each with successively more components, was generated that maximally account for variance in the dependent variable. The resultant models each represent a complex linear regression where each

electrode is associated with a correlation coefficient. The magnitude and direction of the correlation coefficient represent the degree and direction of correlation between variance in the EEG measure and variance in the dependent measure, here the NIHSS score. As previously[200,269], the fitted PLS model included as many components as were required for 80% of variance in the dependent variable to be explained, generally two components.

In order to identify specific clusters of leads where variance in the EEG measure of interest was most strongly correlated with variance in the dependent measure, an arbitrary threshold was predefined and applied to the correlation coefficients in each PLS model. Thus, using a previously detailed approach[269], regression coefficients were thresholded at $|r_i| > 0.75 * r_{max}$ where r_i is the correlation coefficient at the ith electrode and r_{max} is the largest $|r_i|$ value across all electrodes. Clusters were required to have a minimum of two contiguous electrodes exceeding the threshold. EEG measures were then averaged across clusters of leads and regressed against the dependent measure, using bivariate correlations.

MAGNETIC RESONANCE IMAGING

Acute stroke imaging protocols at UC Irvine Medical Center included diffusion-weighted imaging (DWI), which was performed using a Siemens Avanto 1.5T MRI scanner (TR = 3700 ms; TE = 109 ms; b = 1000). Using previously described methods[13], infarct volume was outlined by hand on the DWI image, and corticospinal tract (CST) injury

was quantified by overlapping each subject's infarct in MNI stereotaxic space with a normal corticospinal tract generated from healthy controls[47].

STASTICAL ANALYSES

Parametric statistical testing was used throughout, as all measures were normally distributed or could be transformed to a normal distribution. Statistical significance was two-tailed and set at $p < 0.05$. Statistical tests were performed with the MATLAB 7.8.0 statistical package.

PLS model results were compared to the bivariate linear regression analyses commonly employed in prior quantitative EEG studies in subjects with acute stroke. Thus 10 quantitative EEG measures (relative power in each of the five frequency bands, and coherence with ipsilesional SMC in each of the five frequency bands) were each regressed against the dependent measure, NIHSS score, at each electrode, without correction for multiple comparisons.

To test the ability of a given model to extrapolate to a test case, a leave-one-out and predict cross-validation was performed for each linear regression model and for each fitted PLS model. In this validation method, data from a single subject is iteratively removed from the model set. Then, the behavioral data from the removed subject (test case) is predicted from his/her EEG data using either the linear regression model or the PLS model generated from the remaining *n-1* subjects. The reported validated R^2 was calculated from the sum of errors across all *n* iterations of the leave-one-out and predict

sequence. This cross-validation method was selected because a leave-one-out and predict validation has established utility for accurately assessing the potential of a model to generalize to an independent data set, especially with smaller sample sizes[211].

RESULTS

SUBJECTS

Twenty-five stroke patients were recruited and signed informed consent. One patient (S17) was excluded from subsequent analyses due to hardware malfunction during data acquisition. The remaining 24 patients were age 35 - 88 years old (60.9 ± 13.1, mean ± SD), and were studied early after stroke (time post-stroke = 3.5 ± 2.9 days, range = 3 hours - 12 days). Twenty patients were right-handed and four were ambidextrous. There was substantial heterogeneity (Table 5.1): infarcts were 22.6 ± 43.6 cc (range 0.14 - 166.1), with 15 in the left and 9 in the right hemisphere, and total NIHSS scores ranged 1-19 (median [IQR] = 5.5 [3 - 7]).

TABLE 5.1. Subject characteristics

ID	Age (yrs)	Gender	Handedness	Time post-stroke (days)	Lesion side	Lesion location	Lesion size (cc)	% CST injury	NIHSS (normal = 0)
1	88	F	R	0.25	L	cortical	0.24	0	6
2	49	M	A	3	L	subcortical	2.24	0.063	5
3	62	M	R	3	R	cortical/subcortical	50.9	0.88	14
4	52	M	R	2	R	cortical/subcortical	32.1	0.19	2
5	76	F	R	1	L	subcortical	0.97	0	4
6	49	M	R	3	R	subcortical	2.7	0.56	1
7	57	M	R	1	L	cortical/subcortical	77.9	0	7
8	50	M	A	2	R	cortical	11.1	0.38	7
9	63	F	R	12	L	subcortical	0.54	0.38	6
10	83	M	R	5	R	cortical/subcortical	17.8	0	9
11	53	M	R	6	L	subcortical	1.13	0.13	3
12	64	F	R	0.125	L	cortical/subcortical	3.14	0.063	1
13	46	M	A	2	L	cortical/subcortical	130.9	0.88	19
14	48	M	R	3	R	subcortical	2.33	0	4
15	62	F	R	2	L	cortical/subcortical	5.7	0.13	1
16	43	M	R	4	R	cortical	0.14	0	2
18	71	M	R	1	R	cortical/subcortical	166.1	0.88	18
19	71	M	A	1	L	subcortical	1.31	0	4
20	68	M	R	3	L	subcortical	0.18	0	3
21	61	M	R	2	L	subcortical	2.08	0.13	7
22	68	F	R	4	L	subcortical	0.36	0	9
23	66	F	R	7	L	subcortical	0.37	0.13	4
24	35	F	R	3	L	cortical/subcortical	31.5	0	6
25	76	M	R	11	R	subcortical	1.05	0.31	6

IMPROVED PREDICTION OF IMPAIRMENT EARLY AFTER STROKE USING PLS MODELING AS COMPARED TO BIVARIATE LINEAR REGRESSION

Across the 10 EEG measures examined (power in five frequency bands and coherence with ipsilesional SMC in five frequency bands), significant correlations were identified between NIHSS score and spectral power in the high beta band, within a cluster of electrodes overlying a contralesional SMC region (maximum $R^2 = 0.65$, $p < 0.0001$). However, this bivariate correlation did not survive leave-one-out and predict validation.

TABLE 5.2. Fitted and validated R^2 for PLS models of EEG measures predicting NIHSS total across all subjects

EEG predictor	# components in fitted model	Fitted model R^2	Validated model R^2
Delta power	2	0.85	0.72
Mean delta coherence with ipsilesional M1	3	0.84	0.47
Theta power	3	0.88	0.36
Mean theta coherence with ipsilesional M1	3	0.88	0.48
Alpha power	3	0.84	0.69
Mean alpha coherence with ipsilesional M1	2	0.81	NA†
Beta-1 power	1	0.90	0.73
Mean beta-1 coherence with ipsilesional M1	2	0.87	NA†
Beta-2 power	1	0.81	0.70
Mean beta-2 coherence with ipsilesional M1	2	0.90	0.35

† NA indicates a PLS model that did not survive the leave-one-out and predict validation

Prediction of acute stroke impairment from EEG measures of brain function was significantly improved using PLS regression. Table 5.2 presents results for each of the 10 EEG measures, with the fitted model R^2 representing the best fit correlation between EEG across all electrodes and NIHSS score, and the validated model R^2 representing the prediction strength of each PLS model obtained using the leave-one-out and predict cross-validation. As demonstrated by consistently higher validated R^2 values, power outperformed coherence with ipsilesional SMC for all five frequency bands examined. Beta power was the strongest predictor of NIHSS score (Figure 5.1D, fitted $R^2 = 0.90$, validated $R^2 = 0.73$). In this PLS model, electrodes having the strongest correlation with NIHSS score were clustered in a region overlying ipsilesional SMC, with higher beta power correlating with less impairment (Figure 5.1E, $r = -0.67$, $p = 0.0004$ in this cluster of leads). Delta power was also a robust predictor of NIHSS score (Figure 5.1A, fitted $R^2 = 0.85$ validated $R^2 = 0.72$). Electrodes where variance in delta power mostly strongly correlated with NIHSS score were in two clusters, one overlying ipsilesional SMC, where higher delta power correlated with larger impairment (Figure 5.1B, $r = 0.59$, $p = 0.002$ in this cluster of leads), and the other overlying contralesional SMC, where higher delta power again correlated with larger impairment (Figure 5.1C, $r = 0.53$, $p = 0.008$ in this cluster of leads).

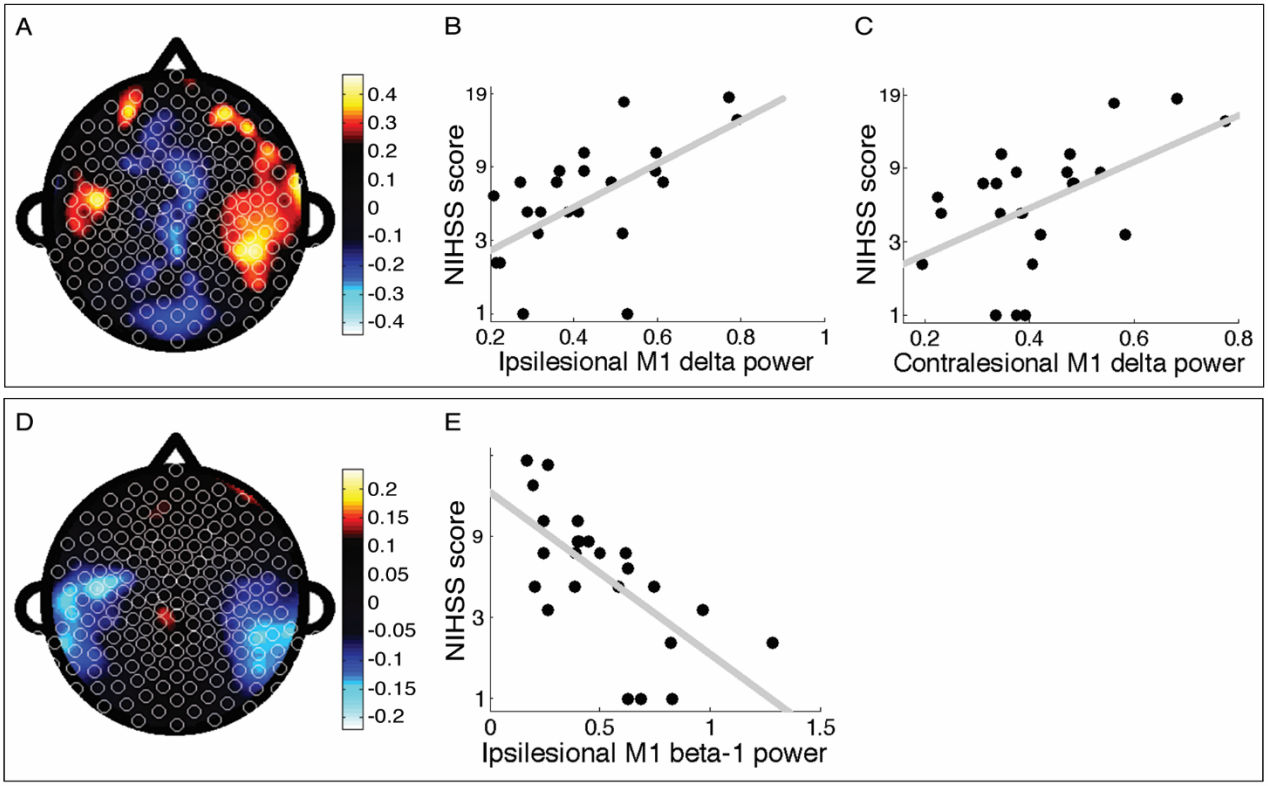

FIGURE 5.1. EEG measurement of brain function was a good predictor of admission NIHSS score. **A**. Topographic map of correlation coefficients in PLS model correlating delta (1 - 3 Hz) power across whole brain with admission NIHSS score (fitted $R^2 = 0.85$, validated $R^2 = 0.72$). **B**. Increased ipsilesional SMC delta power correlated with higher NIHSS score ($r = 0.59$, $p = 0.002$ in this cluster of leads). **C**. Increased contralesional SMC delta power also correlated with higher NIHSS score ($r = 0.53$, $p = 0.008$ in this cluster of leads). **D**. Topographic map of correlation coefficients in PLS model correlating beta (13 - 19 Hz) power across whole brain with admission NIHSS score (fitted $R^2 = 0.90$, validated $R^2 = 0.73$). **E**. Increased ipsilesional SMC beta power correlated with lower NIHSS score ($r = -0.67$, $p = 0.0004$ in this cluster of leads). I: ipsilesional, C: contralesional, SMC: sensorimotor cortex

MRI ASSESSMENT OF NEURAL INJURY AND IMPAIRMENT EARLY AFTER STROKE

Injury measures outperformed clinical variables as markers of impairment status in simple linear regression analyses. Thus, time from stroke onset to EEG acquisition ($p > 0.7$) and age ($p > 0.4$) did not correlate significantly with NIHSS total, while both injury measures did (infarct volume, $r = 0.41$, $p = 0.046$; CST injury, $r = 0.59$, $p = 0.03$). However, the injury measures did not demonstrate predictive value, as neither survived (infarct volume: $p > 0.2$, CST injury: $p > 0.9$) leave-one-out and predict cross-validation.

MEASURES OF NEURAL INJURY AND FUNCTION IN COMBINATION BEST PREDICT EARLY IMPAIRMENT EARLY AFTER STROKE

Combining an MRI-based measure of neural injury with an EEG-based measure of neural function provided better prediction of impairment early after stroke as compared to either measure alone. Structural and functional measures were combined using two methods. First, infarct volume was added as a predictor in the PLS models of delta power and of beta power predicting NIHSS score. Second, EEG measures were added to the injury measure in a forward stepwise multivariate linear regression model.

The addition of an MRI measure of neural injury to EEG measures of neural function in PLS models significantly improved prediction of impairment early after stroke. When infarct volume was added as a predictor to the PLS model of beta power, validated prediction improved (from $R^2 = 0.73$ to $R^2 = 0.81$), to an extent that was statistically significant ($F_{0.05,1,22} = 10.7$, $p = 0.004$). Similarly, when infarct volume was added as a

predictor in the PLS model of delta power, validated prediction improved (from $R^2 = 0.72$ to $R^2 = 0.77$) to a significant extent ($F_{0.05,1,22} = 4.35$, $p < 0.05$).

TABLE 5.3. Multivariate predictor model

Variable	Estimate	Standard Error	*p*
Intercept	2.32	0.28	< 0.0001
Lesion volume	0.12	0.06	0.06
Ipsilesional M1 beta-1 power	-1.83	0.45	0.0005

Conversely, addition of EEG measures of neural function to the MRI measure of neural injury also improved the linear model. Injury and region-specific functional measures were combined using a forward stepwise multivariate linear regression approach (0.1 to enter, 0.15 to leave the model). The EEG measures examined for the forward stepwise model included ipsilesional SMC delta power, contralesional SMC delta power, and ipsilesional SMC beta power, as defined by the preceding PLS models. The resultant model ($R^2 = 0.54$, $p = 0.0003$, Table 5.3) was less robust than the PLS models, emphasizing that the higher EEG dimensionality representation in PLS provides improved brain-behavior relationships. The brain injury measure (infarct volume) and a measure of regional brain function (ipsilesional SMC beta power) remained significant in this model. Note that infarct volume and ipsilesional SMC beta power were not significantly correlated ($p > 0.4$).

TABLE 5.4. Fitted and validated R^2 for PLS models of EEG prediction of NIHSS score in large infarct and small infarct subgroups

	Large infarcts subgroup (≥ 4 cc, n = 9)			Small infarcts subgroup (< 4 cc, n = 15)		
EEG predictor	# components in fitted model	Fitted model R^2	Validated model R^2	# components in fitted model	Fitted model R^2	Validated model R^2
Delta power	1	0.91	0.8	2	0.98	0.83
Mean delta coherence with ipsilesional M1	2	0.95	0.41	2	0.82	0.47
Theta power	2	0.99	0.59	3	0.92	0.34
Mean theta coherence with ipsilesional M1	1	0.84	0.52	2	0.88	0.42
Alpha power	2	0.82	0.77	2	0.92	0.84
Mean alpha coherence with ipsilesional M1	2	0.85	NA†	2	0.98	0.57
Beta-1 power	1	0.96	0.77	1	0.91	0.85
Mean beta-1 coherence with ipsilesional M1	2	0.84	0.37	1	0.82	0.63

EEG MARKERS OF EARLY STROKE IMPAIRMENTS DIFFER BY INFARCT VOLUME SUBGROUP

An additional analysis examined whether EEG markers of impairment varied by infarct volume. PLS models were repeated separately for the 15 subjects with small infarcts (≤4cc[112]) and the 9 subjects with large infarcts (>4cc). Lesion volume for the small infarct subgroup ranged from 0.14 - 3.13 cc (1.25 ± 1.0, mean ± SD, n = 15) and lesion volume for the large infarct subgroup ranged from 5.70 - 166.1 cc (58.2 ± 56.3, n = 9). These two subgroups did not show differences in age, gender, time of EEG exam post-stroke, or side of infarct. The NIHSS score differed significantly ($p < 0.05$) between the large stroke subgroup (median = 7) and the small stroke subgroup (median = 4).

When comparing prediction of early post-stroke impairment between the large stroke and small stroke subgroups, PLS models of beta power and delta power remained the most robust (Table 5.4). However, in the current analysis, the key differences between stroke subgroups lay in the topography of the PLS models. In the PLS model of beta power predicting NIHSS score in the subgroup with large strokes (Figure 5.2*A*, validated $R^2 = 0.77$), higher NIHSS score most strongly correlated with decreased beta power in *contralesional* SMC ($r = -0.84$, $p = 0.005$ in this cluster of leads) as well as in *ipsilesional* SMC ($r = -0.82$, $p = 0.007$ in this cluster of leads), while in the PLS model of beta power predicting NIHSS score in the subgroup with small strokes (Figure 2*B*, validated $R^2 = 0.85$), higher NIHSS score most strongly correlated with decreased beta power in *ipsilesional* SMC ($r = -0.63$, $p = 0.01$ in this cluster of leads) but not contralesional SMC ($p = 0.7$ in this cluster of leads). Similar results were found in the PLS model of delta

power, where in the subgroup with large strokes (Figure 2*C*, validated $R^2 = 0.80$), higher NIHSS score most strongly correlated with increased *contralesional* SMC delta power ($r = 0.81$, $p = 0.008$ in this cluster of leads) but in the PLS model of delta power predicting NIHSS score in the subgroup with small strokes (Figure 2*D*, validated $R^2 = 0.83$), higher NIHSS score most strongly correlated with increased *ipsilesional* SMC delta power although this correlation did not achieve significance in this cluster of leads. Thus in both frequency bands, *contralesional* SMC EEG measures were informative for *large strokes* but not small strokes.

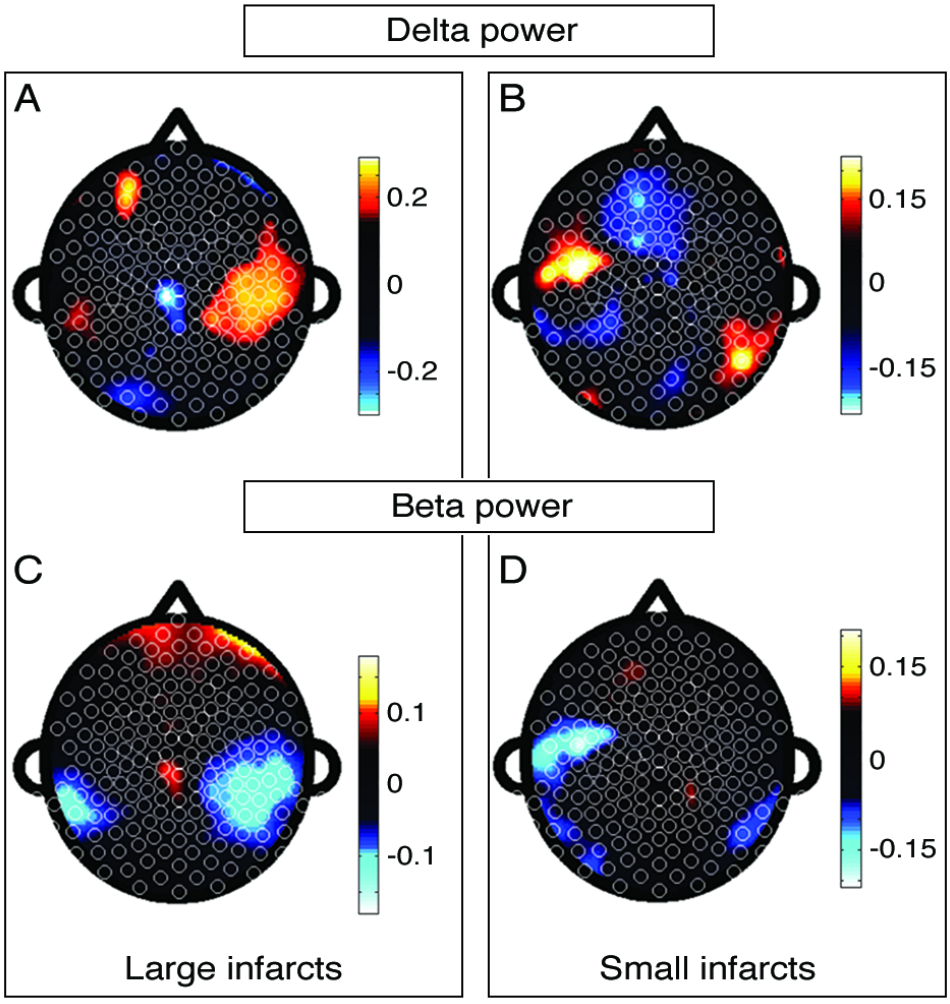

FIGURE 5.2. Topographic maps of correlation coefficients in PLS models correlating admission NIHSS score with whole brain. **A**. beta (13-19 Hz) power, in large (>4cc) infarcts (fitted R^2=0.96, validated R^2=0.77); **B**. beta power, in small (≤4cc) infarcts (fitted R^2=0.91, validated R^2=0.85); **C**. delta (1-3 Hz) power, in large infarcts (fitted R^2=0.91, validated R^2=0.80); and **D**. delta power, in small infarcts (fitted R^2=0.98, validated R^2=0.83). I: ipsilesional, C: contralesional, SMC: sensorimotor cortex

Contralesional correlations during acute stroke are independent of mass effect

Additional analyses were performed to better interpret the relationship between contralesional SMC EEG measures and impairment in patients with large strokes. First, there was not a significant difference between the two stroke subgroups for delta power

($p > 0.05$) or for beta power ($p = 0.2$) when examining all contralesional electrodes. The same was true when examining only those electrodes identified by PLS analyses and overlying contralesional SMC, for delta power ($p = 0.06$) and for beta power ($p > 0.3$). Next, infarct volume was evaluated in relation to EEG power measures in these nine subjects, and was found not to correlate significantly with delta power across all contralesional electrodes ($p = 0.3$) or within contralesional SMC electrodes ($p = 0.2$), or with beta power across all contralesional electrodes ($p = 0.2$) or within contralesional SMC electrodes ($p = 0.1$).

Finally, brain imaging was reviewed (by SCC), including any head CT scans acquired closer to the time of EEG acquisition than the brain MRI. For the nine subjects in the large stroke subgroup, EEG was acquired 2.3±1.2 days (range 1 - 5) after stroke onset, and the shortest time between EEG and any brain imaging was 2.8 ± 4.7 days (range = -1.1 to +13.0 days). On review, 8 of these subjects had no mass effect or edema in the contralesional hemisphere, while a single subject (S13) had mild mass effect (Figure 5.3).

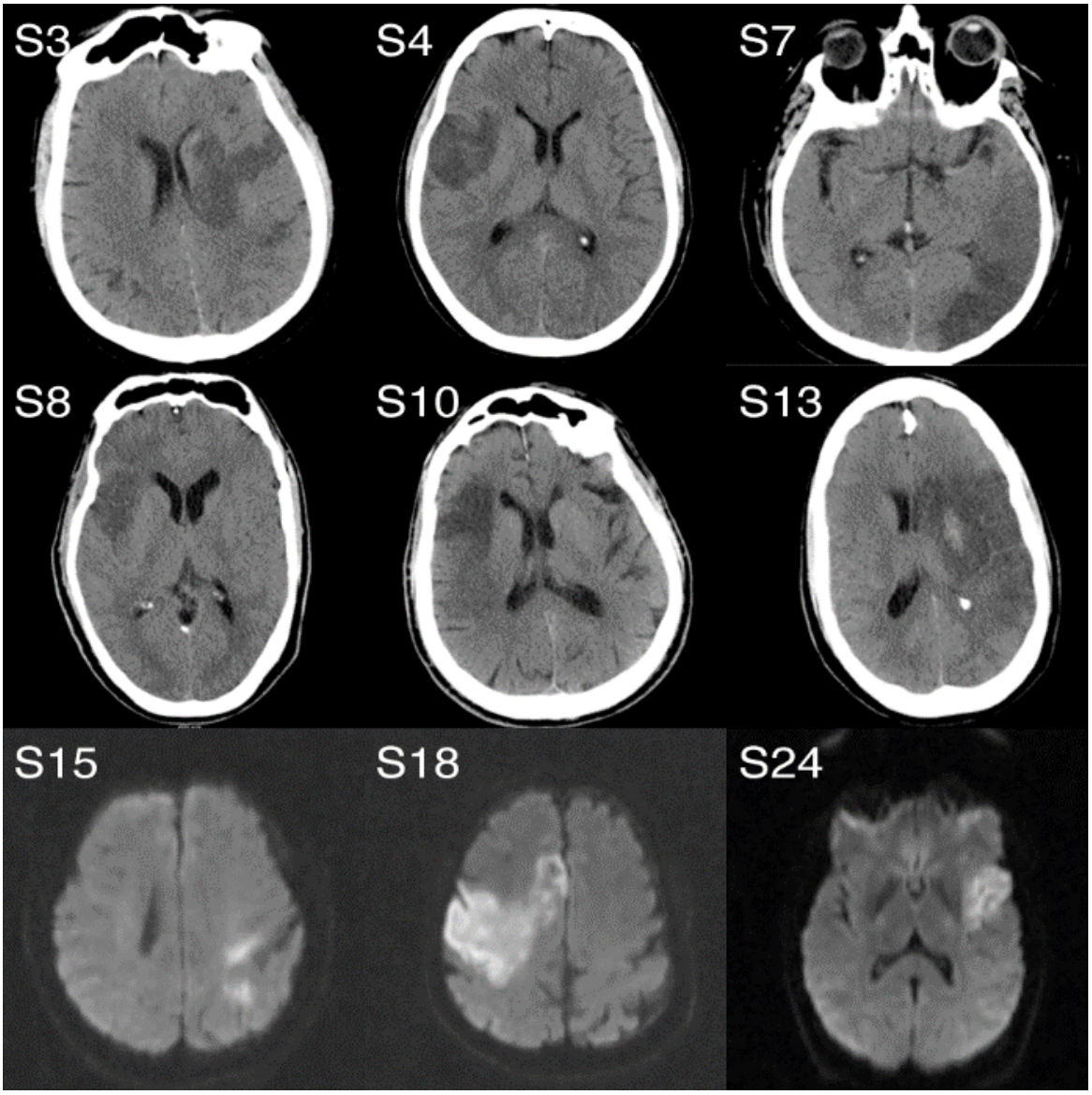

FIGURE 5.3. Representative images from the DWI MRI or CT taken at the closest time to EEG for the nine subjects with large (>4cc) infarcts indicate no important mass effect from the infarct onto the contralesional hemisphere, with the exception of S13.

DISCUSSION

Evidence suggests that a measure of brain function provides useful insights in the setting of stroke[13,249,261–263,273,274], however candidate techniques such as fMRI and PET are challenging to implement in the acute care setting, e.g., due to accessibility and cost. EEG has established value for measuring altered brain function in the acute stroke setting[63,64,75,128,130,265] and overcomes many of these challenges, but has not been widely adopted. Building on advances in EEG hardware and software, the current study found that dense-array EEG analyzed using PLS modeling was a powerful predictor of behavioral status, performing better than quantitative EEG metrics or measures of brain injury in the current cohort of 24 patients admitted for stroke. In addition, the current EEG methods provide insights into differences in brain function in relation to infarct volume, as contralesional events were associated with impairment status with large but not small infarcts. Patients could be studied in wide-ranging clinical settings including ER and ICU. Together these findings suggest that dense-array EEG studies provide an accessible measure of brain function that is complementary to injury measures for understanding behavioral status early after stroke.

Previous studies of patients with acute stroke have found that EEG changes correlate with behavioral status[106,107,125] and improve upon outcome prediction afforded by neuroimaging alone[270]. The current study builds upon these efforts, addressing issues that have limited adoption of EEG in the acute stroke setting. First, use of a single saline net, rather than traditional application of 20 separate leads with paste, shortens the time to begin acquiring EEG signals[266]. Second, use of a dense-array (256 electrodes) cap

increases spatial resolution as compared to 10-20 lead montages[111,267]. Third, use of PLS analyses maximizes statistical power by maintaining dimensionality and spatial resolution of the data[167,200,269]. As such, several PLS models were powerful predictors of behavioral status (Table 5.2), for example, the PLS model of delta power was a robust predictor of impairment in the leave-one-out model validation ($R^2 = 0.72$). In contrast, across the 10 quantitative EEG measures examined, although several correlated with behavioral status using linear regression, none survived leave-one-out and predict model validation.

Prediction of post-stroke impairment was significantly improved when a measure of neural injury was added to the EEG predictive PLS model. This is consistent with prior studies that found a multimodal approach incorporating both neural function and neural injury best explained post-stroke behavior[13,261,270]. Thus in the present study, adding a measure of neural injury (infarct volume) to the PLS model of beta power significantly increased strength of validated prediction, from $R^2 = 0.73$ to $R^2 = 0.81$. Similarly, adding an EEG measure of brain function to infarct volume in a forward stepwise model significantly increased prediction ($R^2 = 0.17$ to $R^2 = 0.54$). These results indicate that both neural function and neural injury are related to impairment early after stroke, and confirm that an approach combining the two is significantly better than either measure alone for predicting behavior. In addition, the more robust prediction using PLS compared with forward stepwise modeling further emphasizes advantages of models using PLS as compared to linear regression.

The current approach also provides neurobiological insights into the functional anatomy of acute impairment in large vs. small strokes. In both the delta and beta frequency bands, contralesional SMC EEG measures were significantly related to behavioral state for large strokes but not for small strokes. These differences in EEG map topography (Figure 5.2) could potentially identify therapeutic targets or serve as biomarkers in a pathophysiologically specific manner. Prior studies have reached mixed results regarding the presence and significance of contralesional changes in relation to behavioral state early after stroke[63,102,112,123,275], and some have suggested that EEG measures of contralesional dysfunction in acute stroke strictly reflect mass effect[63,129]. Current analyses suggest a broader interpretation. Contralesional SMC delta power and beta power were not correlated with total lesion volume, and neither differed between large stroke and small stroke subgroups. Furthermore, review of brain images acquired within the shortest interval to EEG study found that only one of the nine large strokes showed mass effect (Figure 5.3). Such behaviorally relevant contralesional SMC EEG changes seen early after a large stroke that are not due to mass effect may be a marker of diaschisis[123].

There are a number of strengths and weaknesses associated with the current study. As with all scalp EEG studies, limited spatial localization provides an imperfect anatomical relationship between EEG electrodes and specific brain structures. However, this concern is mitigated in part by use of dense array (256 electrodes) EEG[111,267], and by the fact that for the C3 and C4, a particularly strong relationship exists between underlying cortical brain function and the signals measured at the scalp[207]. Given the

highly heterogeneous nature of stroke, a subsequent study enrolling a larger patient cohort is needed to confirm the current results and determine broad applicability. This is particularly true for the infarct volume subgroup analyses, as cohort partitioning resulted in relatively small numbers of subjects in each PLS model.

Rapid, non-invasive methods for measuring brain function that are accessible across the various settings of acute stroke care could provide useful insights for understanding inter-patient differences and thus for driving therapeutic decision-making. The current study presents a novel application of dense-array EEG combined with PLS analyses in an acute stroke population, and was found to outperform traditional imaging measures, including infarct volume and quantitative EEG measures of brain function, as a predictor of behavioral deficits early after stroke. In line with studies suggesting that both neural function and neural injury are important to understanding impairment level, prediction was significantly improved when neural injury was included in the PLS model of EEG measured brain function. EEG findings related to impairment differed according to infarct volume and suggested a potential marker for stroke-induced transhemispheric diaschisis. EEG is safe, relatively inexpensive, and can be performed rapidly in complex clinical settings and may have utility for measuring brain function early after stroke.

CHAPTER 6

Summary and conclusions

Stroke is highly heterogeneous, with individuals demonstrating variation in initial clinical presentation, degree of spontaneous recovery, and response to intervention and treatment. Biomarkers and predictors of stroke recovery have the potential to significantly improve stroke care and management by guiding clinical decision making, maximizing degree of recovery, and optimizing allocation of rehabilitation and financial resources. Although bedside examination is the gold standard for determining severity of stroke injury, neuroimaging measures of brain function are likely to provide an improved characterization of an individual's potential for neural reorganization compared to behavioral assessments.

Electroencephalography (EEG), as a safe, non-invasive, easy, and inexpensive neuroimaging modality is well-suited for rapid, bedside assessment of brain function, particularly in traditionally difficult clinical settings, like acute stroke. In addition, EEG provides excellent temporal resolution which enables the evaluation of brain function at a time scale nearing that of neuronal activity. Furthermore, the temporal resolution of EEG permits frequency resolution in both regional and inter-regional assessments of connectivity. The present dissertation aimed to determine utility of EEG measures for measuring inter-individual differences in brain function, with an emphasis on predicting response to motor training in both healthy, control and stroke populations.

The first aim of this dissertation was to establish methodology for acquiring and analyzing dense-array EEG data. Using a 3 minute EEG scan acquired at rest, the first study found (Chapter 2) baseline coherence in the beta (20-30 Hz) frequency range between a seed region overlying primary motor cortex (M1) and the rest of the scalp was found to predict subsequent improvement with training on a visuomotor integration task with 81% accuracy. In the second study (Chapter 3), prediction of motor improvement with training was found to demonstrate specificity for motor task content. Specifically, individuals with higher beta coherence between M1 and leads overlying left premotor cortex (PM) at rest showed greater improvement with motor sequence training but reduced improvement with the visuomotor integration task. Conversely, individuals with relatively lower M1-PM coherence at rest showed greater improvement with the visuomotor integration task, but reduced improvement with motor sequence training. Therefore, these first two studies demonstrate that resting-state EEG measures of inter-regional connectivity not only predict individual response to training, but also demonstrate promise as a method for stratifying individuals to maximize response to motor training.

In Chapter 4, EEG coherence was examined as a biomarker and predictor of arm motor impairment in patients with chronic stroke enrolled in an arm rehabilitation therapy. At baseline, coherence between leads overlying ipsilesional M1 and the rest of the scalp was a robust and specific marker of motor status (R^2 = 0.78). Furthermore, a multimodal model that included both the EEG measure of function connectivity with a structural measure of injury (CST injury) was found to outperform either measure alone (R^2 =

0.93). Next, across the 28 day period of therapy, change in M1 coherence demonstrated a good correlation with change in arm impairment status (R^2 = 0.61), with both improved baseline impairment status and greater decreases in arm impairment across therapy related to greater M1 coherence with ipsilesional PM. Finally, M1 coherence also demonstrated strong prediction of total improvement in arm impairment across therapy (R^2 = 0.79). Thus, this third study found EEG measures of brain function demonstrate promise as a biomarker and predictor of motor impairment status and response to arm motor training in individuals with chronic stroke.

The finally study of this dissertation examined EEG correlates of impairment in hospitalized patients during early recovery after stroke (Chapter 5). Across the patient group, relative delta power was a robust predictor of impairment state, as it accounted for 72% of variation in NIHSS score, outperforming both infarct volume and CST injury. In addition, EEG markers of impairment were also found to differ according to infarct volume subgroup, with larger strokes showing a significant correlation between contralesional delta power and impairment (r = 0.81), while smaller strokes did not show a similar relationship. In sum, the study in Chapter 5 is an important proof-of-concept demonstrating the beside EEG assessment measures inter-individual differences in brain function that are related to behavioral measures of post-stroke impairment.

The studies that comprise this dissertation include both corroborative and novel data towards the utility of EEG measures of brain function to assessing an individual's potential for neural reorganization. In the context of stroke, these data provide strong

evidence for the need to include EEG measures of brain function as part of clinical decision making at all points of the recovery process. The current EEG methodology demonstrates promise for both individualizing clinical decision making and stratifying patients in order to maximize recovery in individuals and improve allocation of resources across patients. Moreover, considering that many novel stroke therapeutics result in disappointing outcomes in translation[276–278], an EEG assessment may be instrumental in reducing patient variance and maximizing power in clinical trials. The present results also have important scientific implications for elucidating the neurobiology that underlies heterogeneity in potential for neural reorganization both in individuals without neural injury and in individuals with stroke.

The strength of the current results, especially when compared with ROI-based analyses, lies in the use of partial least squares regression (PLS) in the primary analyses across all four studies. PLS was originally developed in the field of chemometrics, and was first introduced to neuroimaging analyses by McIntosh in 1996[209]. Since its introduction, PLS methods have been used to identify the neural circuits that underlie differences in affective measures[279], to discriminate brain states across varying severity of cognitive decline[280], and to determine the neurobiological changes associated with various neuropsychiatric disorders[167]. Multivariate analysis methods that collapse very large neuroimaging data sets into a reduced series of components, including independent components analysis and graph theory analysis in addition to PLS, have been found to reliably resolve functional brain networks associated with specific cortical processes[151,281]. As a result, these multivariate methods

demonstrate improved capabilities to characterize brain networks compared to classic ROI-based methods. In addition, these component-based analyses reduce the decreases in statistical power associated with large neuroimaging data sets that include a large number of independent variables. Finally, by building components with the intent to extract commonalities between brain function and behavioral measures, PLS methods optimize the identification of brain states that underlie complex behaviors.

Future studies are needed to truly appreciate some of the current results. For example, in Chapter 3, it was found that resting coherence predicted subsequent improvement with motor training performed at the same session. However, this effect did not generalize across sessions. Further study is needed to determine whether individuals demonstrate significant differences in resting coherence across days and whether these intra-individuals differences relate to capacity to acquire a specific motor task. In addition, it would be informative to test whether increased M1-PM coherence at baseline also predicted better outcomes on a different PM task, like the action selection[97,282], or if this effect was specific to a motor sequencing task. For the stroke studies in particular, future studies should enroll a larger number of patients. While the study in Chapter 5 included 24 patients, larger samples are much needed in order to maintain sufficient power to generate robust patient subgroups. Multimodal studies that include TMS and fMRI measures of functional and structural connectivity are also needed to provide insight into the neurobiological correlates of EEG coherence, particularly in the context of stroke injury.

CONCLUSIONS

In summary, EEG measures of brain function are robust predictors of potential for reorganization, both in the context of motor learning in healthy individuals, and in motor recovery after stroke. Overall, the EEG measure of connectivity showed particular utility in this respect, outperforming baseline behavioral status and several other clinical and demographic measures in multiple studies. Hopefully, the strength of the present results will reinvigorate enthusiasm for EEG as a legitimate candidate method for rapid, bedside assessment of brain function after stroke.

REFERENCES

1. Prevention, C. for D. C. and. Prevalence and most common causes of disability among adults: United States. *MMWR Morb Mortal Wkly Rep* **58,** 421–6 (2009).

2. Mozaffarian, D. *et al.* Heart Disease and Stroke Statistics--2015 Update: A Report From the American Heart Association. *Circulation* **131,** e29–e322 (2015).

3. Go, A. S. *et al.* Heart disease and stroke statistics--2014 update: a report from the American Heart Association. *Circulation* **129,** e28–e292 (2014).

4. Duncan, P. W., Goldstein, L. B., Matchar, D., Divine, G. W. & Feussner, J. Measurement of motor recovery after stroke. *Stroke* **23,** 1084–1089 (1992).

5. The National Institute of Neurological Disorders and Stroke rt-PA Stroke Study Group. Tissue plasminogen activator for acute ischemic stroke. The National Institute of Neurological Disorders and Stroke rt-PA Stroke Study Group. *N Engl J Med* **333,** 1581–1587 (1995).

6. Bhatia, R. *et al.* Low rates of acute recanalization with intravenous recombinant tissue plasminogen activator in ischemic stroke: real-world experience and a call for action. *Stroke* **41,** 2254–2258 (2010).

7. Muchada, M. *et al.* Impact of Time to Treatment on Tissue-Type Plasminogen Activator-Induced Recanalization in Acute Ischemic Stroke. *Stroke* 1–5 (2014). doi:10.1161/STROKEAHA.114.006222

8. Takahashi, C. D., Der-Yeghiaian, L., Le, V., Motiwala, R. R. & Cramer, S. C. Robot-based hand motor therapy after stroke. *Brain* **131,** 425–37 (2008).

9. Gauthier, L. V, Taub, E., Mark, V. W., Perkins, C. & Uswatte, G. Improvement after constraint-induced movement therapy is independent of infarct location in chronic stroke patients. *Stroke* **40,** 2468–72 (2009).

10. Lo, A. *et al.* Robot-assisted therapy for long-term upper-limb impairment after stroke. *New Engl J Med* **362,** 1772–1783 (2010).

11. Langhorne, P., Coupar, F. & Pollock, A. Motor recovery after stroke: a systematic review. *Lancet Neurol* **8,** 741–754 (2009).

12. Weimar, C., Konig, I. R., Kraywinkel, K., Ziegler, A. & Diener, H. C. Age and National Institutes of Health Stroke Scale Score within 6 hours after onset are accurate predictors of outcome after cerebral ischemia: development and external validation of prognostic models. *Stroke* **35,** 158–162 (2004).

13. Burke Quinlan, E. *et al.* Neural function, injury, and stroke subtype predict treatment gains after stroke. *Ann. Neurol.* 1–14 (2015). doi:10.1002/ana.24309

14. Carter, A. R. *et al.* Upstream dysfunction of somatomotor functional connectivity after corticospinal damage in stroke. *Neurorehabil. Neural Repair* **26,** 7–19 (2012).

15. Stinear, C. *et al.* Functional potential in chronic stroke patients depends on corticospinal tract integrity. *Brain* **130,** 170–80 (2007).

16. Gerloff, C. *et al.* Multimodal imaging of brain reorganization in motor areas of the contralesional hemisphere of well recovered patients after capsular stroke. *Brain* **129,** 791–808 (2006).

17. Haley Jr., E. C. *et al.* Urgent therapy for stroke. Part II. Pilot study of tissue plasminogen activator administered 91-180 minutes from onset. *Stroke* **23,** 641–645 (1992).

18. Hacke, W. *et al.* Intravenous Thrombolysis With Recombinant Tissue Plasminogen Activator for Acute Hemispheric Stroke. *JAMA* **274,** 1017 (1995).

19. Ifejika-Jones, N. L., Harun, N., Mohammed-Rajput, N. A., Noser, E. A. & Grotta, J. C. Thrombolysis with intravenous tissue plasminogen activator predicts a favorable discharge disposition in patients with acute ischemic stroke. *Stroke* **42,** 700–704 (2011).

20. Kwiatkowski, T. G. *et al.* Effects of tissue plasminogen activator for acute ischemic stroke at one year. National Institute of Neurological Disorders and Stroke Recombinant Tissue Plasminogen Activator Stroke Study Group. *N Engl J Med* **340,** 1781–1787 (1999).

21. Chollet, F. *et al.* Fluoxetine for motor recovery after acute ischaemic stroke (FLAME): a randomised placebo-controlled trial. *Lancet Neurol.* **10,** 123–130 (2011).

22. Dromerick, A. W., Birkenmeier, R. L., Miller, J. P., Videen, T. O. & Edwards, D. F. Very Early Constraint-Induced Movement during Stroke Rehabilitation (VECTORS). *Neurology* **73,** 195–201 (2009).

23. Wolf, S. L. *et al.* The EXCITE stroke trial: comparing early and delayed constraint-induced movement therapy. *Stroke* **41,** 2309–2315 (2010).

24. Dodakian, L. *et al.* A Home-Based Telerehabilitation System for Patients With Stroke. in *Internaiontal Stroke Conf.* (2014).

25. Cramer, S. C. Stratifying patients with stroke in trials that target brain repair. *Stroke* **41,** S114–6 (2010).

26. Uchino, K., Billheimer, D. & Cramer, S. C. Entry criteria and baseline characteristics predict outcome in acute stroke trials. *Stroke* **32,** 909–16. (2001).

27. Veerbeek, J. M., Kwakkel, G., van Wegen, E. E., Ket, J. C. & Heymans, M. W. Early prediction of outcome of activities of daily living after stroke: a systematic review. *Stroke* **42,** 1482–1488 (2011).

28. Shelton, F. D., Volpe, B. T. & Reding, M. Motor impairment as a predictor of functional recovery and guide to rehabilitation treatment after stroke. *Neurorehabil Neural Repair* **15,** 229–237 (2001).

29. Ng, Y. S., Stein, J., Salles, S. S. & Black-Schaffer, R. M. Clinical characteristics and rehabilitation outcomes of patients with posterior cerebral artery stroke. *Arch. Phys. Med. Rehabil.* **86,** 2138–43 (2005).

30. Galski, T., Bruno, R. L., Zorowitz, R. & Walker, J. Predicting length of stay, functional outcome, and aftercare in the rehabilitation of stroke patients. The dominant role of higher-order cognition. *Stroke* **24,** 1794–800 (1993).

31. Alexander, M. P. Stroke rehabilitation outcome. A potential use of predictive variables to establish levels of care. *Stroke* **25,** 128–134 (1994).

32. Fong, K. N., Chan, C. C. & Au, D. K. Relationship of motor and cognitive abilities to functional performance in stroke rehabilitation. *Brain Inj.* **15,** 443–53 (2001).

33. Sato, S. *et al.* Baseline NIH Stroke Scale predicting outcome in anterior and posterior circulation strokes. *Neurology* **70,** 2371–77 (2008).

34. Adams, H. P. *et al.* Baseline NIH Stroke Scale score strongly predicts outcome after stroke: A report of the Trial of Org 10172 in Acute Stroke Treatment (TOAST). *Neurology* **53,** 126–131 (1999).

35. Acciarresi, M. *et al.* First-Ever Stroke and Outcome in Patients Admitted to Perugia Stroke Unit: Predictors for Death, Dependency, and Recurrence of Stroke within the First Three Months. *Clin. Exp. Hypertens.* **28,** 287–294 (2006).

36. Kelly, P. J. *et al.* Functional recovery following rehabilitation after hemorrhagic and ischemic stroke. *Arch. Phys. Med. Rehabil.* **84,** 968–972 (2003).

37. Gillen, R., Tennen, H., McKee, T. E., Gernert-Dott, P. & Affleck, G. Depressive symptoms and history of depression predict rehabilitation efficiency in stroke patients. *Arch Phys Med Rehabil* **82,** 1645–1649 (2001).

38. Luk, J. K. H., Cheung, R. T. F., Ho, S. L. & Li, L. Does age predict outcome in stroke rehabilitation? A study of 878 Chinese subjects. *Cerebrovasc. Dis.* **21,** 229–34 (2006).

39. Burke, E. & Cramer, S. C. Biomarkers and predictors of restorative therapy effects after stroke. *Curr. Neurol. Neurosci. Rep.* **13,** 329 (2013).

40. Toth, G. & Albers, G. W. Use of MRI to estimate the therapeutic window in acute stroke: is perfusion-weighted imaging/diffusion-weighted imaging mismatch an EPITHET for salvageable ischemic brain tissue? *Stroke* **40,** 333–5 (2009).

41. Davalos, A. *et al.* The clinical-DWI mismatch: a new diagnostic approach to the brain tissue at risk of infarction. *Neurology* **62,** 2187–92 (2004).

42. Campbell, B. C. V. *et al.* Endovascular Therapy for Ischemic Stroke with Perfusion-Imaging Selection. *N. Engl. J. Med.* 150211090353006 (2015). doi:10.1056/NEJMoa1414792

43. Johnston, K. C., Barrett, K. M., Ding, Y. H. & Wagner, D. P. Clinical and imaging data at 5 days as a surrogate for 90-day outcome in ischemic stroke. *Stroke* **40,** 1332–1333 (2009).

44. Vora, N. A. *et al.* A 5-item scale to predict stroke outcome after cortical middle cerebral artery territory infarction: validation from results of the Diffusion and Perfusion Imaging Evaluation for Understanding Stroke Evolution (DEFUSE) Study. *Stroke* **42,** 645–649 (2011).

45. Saunders, D. E., Clifton, A. G. & Brown, M. M. Measurement of infarct size using MRI predicts prognosis in middle cerebral artery infarction. *Stroke* **26,** 2272–2276 (1995).

46. Mark, V. W., Taub, E., Perkins, C., Gauthier, L. & Uswatte, G. MRI infarction load and CI therapy outcomes for chronic post-stroke hemiparesis. *Restor Neurol Neurosci* **26,** 13–33 (2008).

47. Riley, J. D. *et al.* Anatomy of stroke injury predicts gains from therapy. *Stroke* **42,** 421–426 (2011).

48. Lindenberg, R., Zhu, L. L., Ruber, T. & Schlaug, G. Predicting functional motor potential in chronic stroke patients using diffusion tensor imaging. *Hum. Brain Mapp.* **33,** 1040–1051 (2012).

49. Gauthier, L. V, Taub, E., Mark, V. W., Barghi, A. & Uswatte, G. Atrophy of spared gray matter tissue predicts poorer motor recovery and rehabilitation response in chronic stroke. *Stroke* **43,** 453–7 (2012).

50. Nouri, S. & Cramer, S. C. Anatomy and physiology predict response to motor cortex stimulation after stroke. *Neurology* **77,** 1076–83 (2011).

51. Cramer, S. C. Repairing the human brain after stroke: I. Mechanisms of spontaneous recovery. *Ann. Neurol.* **63,** 272–87 (2008).

52. Ward, N., Brown, M., Thompson, A. & Frackowiak, R. Neural correlates of outcome after stroke: a cross-sectional fMRI study. *Brain* **126,** 1430–1448 (2003).

53. Corbetta, M., Kincade, M. J., Lewis, C., Snyder, A. Z. & Sapir, A. Neural basis and recovery of spatial attention deficits in spatial neglect. *Nat. Neurosci.* **8,** 1603–10 (2005).

54. Pizzamiglio, L. *et al.* Recovery of neglect after right hemispheric damage: H2(15)O positron emission tomographic activation study. *Arch Neurol* **55,** 561–568 (1998).

55. Heiss, W. D., Kessler, J., Thiel, A., Ghaemi, M. & Karbe, H. Differential capacity of left and right hemispheric areas for compensation of poststroke aphasia. *Ann. Neurol.* **45,** 430–438 (1999).

56. Warburton, E., Price, C. J., Swinburn, K. & Wise, R. J. Mechanisms of recovery from aphasia: evidence from positron emission tomography studies. *J Neurol Neurosurg Psychiatry* **66,** 155–161 (1999).

57. Cramer, S. C. *et al.* Predicting functional gains in a stroke trial. *Stroke* **38,** 2108–14 (2007).

58. Laible, M. *et al.* Association of activity changes in the primary sensory cortex with successful motor rehabilitation of the hand following stroke. *Neurorehabil. Neural Repair* **26,** 881–8 (2012).

59. Bullmore, E. & Sporns, O. Complex brain networks: graph theoretical analysis of structural and functional systems. *Nat. Rev. Neurosci.* **10,** 186–98 (2009).

60. Westlake, K., Hinkley, L. & Bucci, M. Resting state alpha-band functional connectivity and recovery after stroke. *Exp. Neurol.* **237,** 160–169 (2012).

61. Rehme, A. K., Eickhoff, S. B., Wang, L. E., Fink, G. R. & Grefkes, C. Dynamic causal modeling of cortical activity from the acute to the chronic stage after stroke. *Neuroimage* **55,** 1147–1158 (2011).

62. Carter, A. R. *et al.* Resting interhemispheric functional magnetic resonance imaging connectivity predicts performance after stroke. *Ann. Neurol.* **67,** 365–75 (2010).

63. Macdonell, R., Donnan, G., Bladin, P., Berkovic, S. & Wriedt, C. The electroencephalogram and acute ischemic stroke: distinguishing cortical from lacunar infarction. *Arch. Neurol.* **47,** 520–524 (1988).

64. Marquardsen, J. & Harvald, B. The electroencephalogram in acute cerebrovascular lesions: A report of 50 cases verified at autopsy. *Neurology* **14,** 275–282 (1964).

65. Sharbrough, F. W., Messick, J. M. & Sundt, T. M. Correlation of continuous electroencephalograms with cerebral blood flow measurements during carotid endarterectomy. *Stroke* **4,** 674–683 (1973).

66. Murri, L. *et al.* Evaluation of acute ischemic stroke using quantitative EEG: a comparison with conventional EEG and CT scan. *Neurophysiol. Clin.* **28,** 249–257 (1998).

67. Van Putten, M. J. a M. & Tavy, D. L. J. Continuous quantitative EEG monitoring in hemispheric stroke patients using the brain symmetry index. *Stroke* **35,** 2489–2492 (2004).

68. Sheorajpanday, R. V. A., Nagels, G., Weeren, A. J. T. M. & De Deyn, P. P. Quantitative EEG in ischemic stroke: Correlation with infarct volume and functional status in posterior circulation and lacunar syndromes. *Clin. Neurophysiol.* **122,** 884–890 (2011).

69. Ramon, C. & Holmes, M. D. Noninvasive epileptic seizure localization from stochastic behavior of short duration interictal high density scalp EEG data. *Brain Topogr.* **25,** 106–15 (2012).

70. Van Putten, M. J. A. M. *et al.* A brain symmetry index (BSI) for online EEG monitoring in carotid endarterectomy. *Clin. Neurophysiol.* **115,** 1189–1194 (2004).

71. Petit, D., Gagnon, J. F., Fantini, M. L., Ferini-Strambi, L. & Montplaisir, J. Sleep and quantitative EEG in neurodegenerative disorders. *J. Psychosom. Res.* **56,** 487–496 (2004).

72. Nunez, P. L. & Srinivasan, R. *Electric Fields of the Brain*. (Oxford University Press, 2006).

73. Steriade, M., Gloor, P., Llinas, R., Lopes da silva, F. & Mesulam, M. M. Basic mechanisms of cerebral rhythmic activity. *Electroencephalogr Clin Neurophysiol* **76,** 481–508 (1990).

74. Steriade, M., McCormick, D. A. & Sejnowski, T. J. Thalamocortical oscillations in the sleeping and aroused brain. *Science (80-.).* **262,** 679–685 (1993).

75. Foreman, B. & Claasen, J. Quantitative EEG for the detection of brain ischemia. *Crit. Care* **16,** (2012).

76. Steriade, M. Grouping of brain rhythms in corticothalamic systems. *Neuroscience* **137,** 1087–1106 (2006).

77. Lakatos, P., Karmos, G., Mehta, A. D., Ulbert, I. & Schroeder, C. E. Entrainment of neuronal oscillations as a mechanism of attentional selection. *Science* **320,** 110–3 (2008).

78. Fries, P., Reynolds, J. H., Rorie, a E. & Desimone, R. Modulation of oscillatory neuronal synchronization by selective visual attention. *Science* **291,** 1560–3 (2001).

79. Perfetti, B. *et al.* Modulation of Gamma and Theta Spectral Amplitude and Phase Synchronization Is Associated with the Development of Visuo-Motor Learning. *J. Neurosci.* **31,** 14810–14819 (2011).

80. Gevins, a & Smith, M. E. Neurophysiological measures of working memory and individual differences in cognitive ability and cognitive style. *Cereb. Cortex* **10,** 829–39 (2000).

81. Dubovik, S. *et al.* The behavioral significance of coherent resting-state oscillations after stroke. *Neuroimage* **61,** 249–257 (2012).

82. Jensen, O., Gelfand, J., Kounios, J. & Lisman, J. E. Oscillations in the alpha band (9-12 Hz) increase with memory load during retention in a short-term memory task. *Cereb. cortex* **12,** 877–882 (2002).

83. Cooper, N. R., Croft, R. J., Dominey, S. J. J., Burgess, A. P. & Gruzelier, J. H. Paradox lost? Exploring the role of alpha oscillations during externally vs. internally directed attention and the implications for idling and inhibition hypotheses. *Int. J. Psychophysiol.* **47,** 65–74 (2003).

84. Del Percio, C. *et al.* Visuo-attentional and sensorimotor alpha rhythms are related to visuo-motor performance in athletes. *Hum. Brain Mapp.* **30,** 3527–40 (2009).

85. Mima, T., Oluwatimilehin, T., Hiraoka, T. & Hallett, M. Transient interhemispheric neuronal synchrony correlates with object recognition. *J. Neurosci.* **21,** 3942–3948 (2001).

86. Meeuwissen, E. B., Takashima, A., Fernández, G. & Jensen, O. Increase in posterior alpha activity during rehearsal predicts successful long-term memory formation of word sequences. *Hum. Brain Mapp.* **32,** 2045–2053 (2011).

87. Guggisberg, A. G. *et al.* Mapping functional connectivity in patients with brain lesions. *Ann Neurol* **63,** 193–203 (2008).

88. Martino, J. *et al.* Resting functional connectivity in patients with brain tumors in eloquent areas. *Ann Neurol* **69,** 521–532 (2011).

89. Ford, M. R., Goethe, J. W. & Dekker, D. K. EEG coherence and power in the discrimination of psychiatric disorders and medication effects. *Biol Psychiatry* **21,** 1175–1188 (1986).

90. Güntekin, B., Saatçi, E. & Yener, G. Decrease of evoked delta, theta and alpha coherences in Alzheimer patients during a visual oddball paradigm. *Brain Res.* **1235,** 109–16 (2008).

91. Jordan, K. G. Emergency EEG and continuous EEG monitoring in acute ischemic stroke. *J. Clin. Neurophysiol.* **21,** 341–52 (2004).

92. Faught, E. Current role of electroencephalography in cerebral ischemia. *Stroke* **24,** 609–613 (1993).

93. Miller, K. J. *et al.* Human Motor Cortical Activity Is Selectively Phase-Entrained on Underlying Rhythms. *PLoS Comput. Biol.* **8,** (2012).

94. Roopun, A. K. *et al.* A beta2-frequency (20-30 Hz) oscillation in nonsynaptic networks of somatosensory cortex. *Proc. Natl. Acad. Sci. U. S. A.* **103,** 15646–50 (2006).

95. Schroeder, C. & Lakatos, P. Low-frequency neuronal oscillations as instruments of sensory selection. *Trends Neurosci.* **32,** 1–16 (2009).

96. Rose, F. C. Cerebral localization in antiquity. *J. Hist. Neurosci.* **18,** 239–247 (2009).

97. Kantak, S. S., Stinear, J. W., Buch, E. R. & Cohen, L. G. Rewiring the brain: potential role of the premotor cortex in motor control, learning, and recovery of function following brain injury. *Neurorehabil. Neural Repair* **26,** 282–292 (2012).

98. Lotze, M. *et al.* Contralesional Motor Cortex Activation Depends on Ipsilesional Corticospinal Tract Integrity in Well-Recovered Subcortical Stroke Patients. *Neurorehabil. Neural Repair* (2011). doi:10.1177/1545968311427706

99. Ward, N. S. *et al.* Motor system activation after subcortical stroke depends on corticospinal system integrity. *Brain* **129,** 809–819 (2006).

100. Messick, J. *et al.* Correlation of regional cerebral blood flow (rCBF) with EEG changes during isoflurane anesthesia for carotid endarterectomy: critical rCBF. *Anesthesiology* **66,** 344–349 (1987).

101. Nagata, K., Tagawa, K., Hiroi, S., Shishido, F. & Uemura, K. Electroencephalographic correlates of blood flow and oxygen metabolism provided by positron emission tomography in patients with cerebral infarction. *Electroencephalogr. Clin. Neurophysiol.* **72,** 16–30 (1989).

102. Tecchio, F. *et al.* Rhythmic brain activity at rest from rolandic areas in acute mono-hemispheric stroke: A magnetoencephalographic study. *Neuroimage* **28,** 72–83 (2005).

103. Zappasodi, F., Tombini, M., Milazzo, D., Rossini, P. M. & Tecchio, F. Delta dipole density and strength in acute monohemispheric stroke. *Neurosci. Lett.* **416,** 310–314 (2007).

104. Nuwer, M., Jordan, S. & Anh, S. Evaluation of stroke using EEG frequency analysis and topographic mapping. *Neurology* **37,** (1987).

105. Assenza, G. *et al.* Neuronal functionality assessed by magnetoencephalography is related to oxidative stress system in acute ischemic stroke. *Neuroimage* **44,** 1267–1273 (2009).

106. Finnigan, S. P., Walsh, M., Rose, S. E. & Chalk, J. B. Quantitative EEG indices of sub-acute ischaemic stroke correlate with clinical outcomes. *Clin. Neurophysiol.* **118,** 2525–32 (2007).

107. Sheorajpanday, R. V. a, Nagels, G., Weeren, A. J. T. M., van Putten, M. J. a M. & De Deyn, P. P. Reproducibility and clinical relevance of quantitative EEG parameters in cerebral ischemia: A basic approach. *Clin. Neurophysiol.* **120,** 845–855 (2009).

108. Giaquinto, S., Cobianchi, A., Macera, F. & Nolfe, G. EEG recordings in the course of recovery from stroke. *Stroke* **25,** 2204–2209 (1994).

109. Finnigan, S. P., Rose, S. E. & Chalk, J. B. Rapid EEG changes indicate reperfusion after tissue plasminogen activator injection in acute ischaemic stroke. *Clin. Neurophysiol.* **117,** 2338–2339 (2006).

110. Butz, M. *et al.* Perilesional pathological oscillatory activity in the magnetoencephalogram of patients with cortical brain lesions. *Neurosci Lett* **355,** 93–96 (2004).

111. Luu, P. *et al.* Localizing acute stroke-related EEG changes: assessing the effects of spatial undersampling. *J. Clin. Neurophysiol.* **18,** 302–17 (2001).

112. Burghaus, L. *et al.* Early electroencephalography in acute ischemic stroke: Prediction of a malignant course? *Clin. Neurol. Neurosurg.* **109,** 45–49 (2007).

113. Burghaus, L. *et al.* Prognostic value of electroencephalography and evoked potentials in the early course of malignant middle cerebral artery infarction. *Neurol. Sci.* **34,** 671–678 (2012).

114. Schaul, N., Green, L., Peyster, R. & Gotman, J. Structural determinants of electroencephalographic findings in acute hemispheric lesions. *Ann. Neurol.* **20,** 703–711 (1986).

115. Goldman, R. I., Stern, J. M., Engel, J. & Cohen, M. S. Simultaneous EEG and fMRI of the alpha rhythm. *Neuroreport* **13,** 2487–92 (2002).

116. Lindenberg, R. *et al.* Structural integrity of corticospinal motor fibers predicts motor impairment in chronic stroke. *Neurology* **74,** 280–287 (2010).

117. Thickbroom, G. W., Byrnes, M. L., Archer, S. A. & Mastaglia, F. L. Motor outcome after subcortical stroke correlates with the degree of cortical reorganization. *Clin Neurophysiol* **115,** 2144–2150 (2004).

118. Zemke, A. C., Heagerty, P. J., Lee, C. & Cramer, S. C. Motor cortex organization after stroke is related to side of stroke and level of recovery. *Stroke* **34,** E23–8 (2003).

119. Kümmerer, D. *et al.* Damage to ventral and dorsal language pathways in acute aphasia. *Brain* **136,** 619–29 (2013).

120. Assenza, G., Zappasodi, F., Pasqualetti, P., Vernieri, F. & Tecchio, F. A contralesional EEG power increase mediated by interhemispheric disconnection provides negative prognosis in acute stroke. *Restor. Neurol. Neurosci.* **31,** 177–188 (2013).

121. Visser, G. H., Wieneke, G. H. & Van Huffelen, a. C. Carotid endarterectomy monitoring: Patterns of spectral EEG changes due to carotid artery clamping. *Clin. Neurophysiol.* **110,** 286–294 (1999).

122. Sheorajpanday, R. V. a, Nagels, G., Weeren, a. J. T. M., De Surgeloose, D. & De Deyn, P. P. Additional value of quantitative EEG in acute anterior circulation syndrome of presumed ischemic origin. *Clin. Neurophysiol.* **121,** 1719–1725 (2010).

123. Juhasz, C., Kamondi, A. & Szirmai, I. Spectral EEG analysis following hemispheric stroke: evidences of transhemispheric diaschisis. *Acta Neurol. Scand.* **96,** 397–400 (1997).

124. De Vos, C. C., van Maarseveen, S. M., Brouwers, P. J. a M. & van Putten, M. J. a M. Continuous EEG monitoring during thrombolysis in acute hemispheric stroke patients using the brain symmetry index. *J. Clin. Neurophysiol.* **25,** 77–82 (2008).

125. Xin, X., Gao, Y., Zhang, H., Cao, K. & Shi, Y. Correlation of continuous electroencephalogram with clinical assessment scores in acute stroke patients. *Neurosci. Bull.* **28,** 611–617 (2012).

126. Milot, M.-H. & Cramer, S. C. Biomarkers of recovery after stroke. *Curr. Opin. Neurol.* **21,** 654–9 (2008).

127. Carey, J. R. *et al.* Analysis of fMRI and finger tracking training in subjects with chronic stroke. *Brain* **125,** 773–88 (2002).

128. De Weerd, A. W., Veldhuizen, R. J., Veering, M. M., Poortvliet, D. C. & Jonkman, E. J. Recovery from cerebral ischaemia. EEG, cerebral blood flow and clinical symptomatology in the first three years after a stroke. *Electroencephalogr. Clin. Neurophysiol.* **70,** 197–204 (1988).

129. Newey, C. R., Sarwal, a. & Hantus, S. Continuous electroencephalography (cEEG) changes precede clinical changes in a case of progressive cerebral edema. *Neurocrit. Care* **18,** 261–265 (2013).

130. Finnigan, S. P., Rose, S. E. & Chalk, J. B. Contralateral hemisphere delta EEG in acute stroke precedes worsening of symptoms and death. *Clin. Neurophysiol.* **119,** 1690–1694 (2008).

131. Burke, E., Dobkin, B., Noser, E., Enney, L. & Cramer, S. Predictors and Biomarkers of Treatment Gains in a Clinical Stroke Trial Targeting the Lower Extremity. *Stroke* **45,** 2379–84 (2014).

132. Sainio, K., Stenberg, D., Keskimaki, I., Muuronen, A. & Kaste, M. Visual and spectral EEG analysis in the evaluation of the outcome in patients with ischemic brain infarction. *Electroencephalogr. Clin. Neurophysiol.* **56,** 117–124 (1983).

133. Sheorajpanday, R. V. A., Nagels, G., Weeren, A. J. T. M., van Putten, M. J. A. M. & De Deyn, P. P. Quantitative EEG in ischemic stroke: correlation with functional status after 6 months. *Clin. Neurophysiol.* **122,** 874–83 (2011).

134. Cuspineda, E. *et al.* QEEG prognostic value in acute stroke. *Clin. EEG Neurosci.* **38,** 155–160 (2007).

135. Chen, Y. *et al.* Soft , Comfortable Polymer Dry Electrodes for High Quality ECG and EEG Recording. *Sensors* **14,** 23758–80 (2014).

136. Jakab, A. *et al.* Novel wireless electroencephalography system with a minimal preparation time for use in emergencies and prehospital care. *Biomed. Eng. Online* **13,** 60 (2014).

137. Do Valle, B., Cash, S. & Sodini, C. Wireless behind-the-ear EEG recording device with wireless interface to a mobile device (iPhone/iPod touch). in *IEEE Eng Med Biol Mag* 5952–5 (2014).

138. Wu, J. *et al.* Cortical connectivity is a powerful predictor of motor recovery in chronic stroke. in *Int. Stroke Conf.* (2014).

139. Ackerman, P. L. Individual differences in skill learning: An integration of psychometric and information processing perspectives. *Psychol. Bull.* **102,** 3–27 (1987).

140. King, A., Ranganathan, R. & Newell, K. Individual differences in the exploration of a redundant space-time motor task. *Neurosci. Lett.* **529,** 144–149 (2012).

141. Stinear, C. Prediction of recovery of motor function after stroke. *Lancet Neurol.* **9,** 1228–32 (2010).

142. Tomassini, V. *et al.* Structural and functional bases for individual differences in motor learning. *Hum. Brain Mapp.* **32,** 494–508 (2011).

143. Vo, L. *et al.* Predicting individuals' learning success from patterns of pre-learning MRI activity. *PLoS One* **6,** (2011).

144. Mathewson, K. *et al.* Different slopes for different folks: Alpha and delta EEG power predict subsequent video game learning rate and improvements in cognitive control tasks. *Psychophysiology* **49,** 1558–1570 (2012).

145. Wang, L. *et al.* Intrinsic connectivity between the hippocampus and posteromedial cortex predicts memory performance in cognitively intact older individuals. *Neuroimage* **51,** 910–7 (2010).

146. Baldassarre, A. *et al.* Individual variability in functional connectivity predicts performance of a perceptual task. *Proc. Natl. Acad. Sci.* **109,** 3516–3521 (2012).

147. Deco, G., Jirsa, V. K. & McIntosh, A. R. Emerging concepts for the dynamical organization of resting-state activity in the brain. *Nat. Rev. Neurosci.* **12,** 43–56 (2011).

148. Lewis, C., Baldassarre, A., Committeri, G., Romani, G. & Corbetta, M. Learning sculpts the spontaneous activity of the resting human brain. *Proc. Natl. Acad. Sci.* **106,** 17558–17563 (2009).

149. Hampson, M., Driesen, N., Skudlarski, P., Gore, J. & Constable, R. Brain connectivity related to working memory performance. *J. Neurosci.* **26,** 13338–13343 (2006).

150. Tambini, A., Ketz, N. & Davachi, L. Enhanced brain correlations during rest are related to memory for recent experiences. *Neuron* **65,** 280–290 (2010).

151. Mantini, D., Perrucci, M. G., Del Gratta, C., Romani, G. L. & Corbetta, M. Electrophysiological signatures of resting state networks in the human brain. *Proc. Natl. Acad. Sci. U. S. A.* **104,** 13170–5 (2007).

152. Tropini, G., Chiang, J., Wang, Z. J., Ty, E. & McKeown, M. J. Altered directional connectivity in Parkinson's disease during performance of a visually guided task. *Neuroimage* **56,** 2144–56 (2011).

153. Deeny, S. P., Haufler, A. J., Saffer, M. & Hatfield, B. D. Electroencephalographic Coherence During Visuomotor Performance: A Comparison of Cortico-Cortical Communication in Experts and Novices. *J. Mot. Behav.* **41,** 106–116 (2009).

154. Pfurtscheller, G., Stancák, a & Neuper, C. Post-movement beta synchronization. A correlate of an idling motor area? *Electroencephalogr. Clin. Neurophysiol.* **98,** 281–93 (1996).

155. Adams, J. Warm-up decrement in performance on the pursuit-rotor. *Am. J. Psychol.* **65,** 404–414 (1952).

156. Grafton, S. T., Woods, R. P. & Tyszka, M. Functional imaging of procedural motor learning: Relating cerebral blood flow with individual subject performance. *Hum. Brain Mapp.* **1,** 221–234 (1994).

157. Delorme, A. & Makeig, S. EEGLAB: an open source toolbox for analysis of single-trial EEG dynamics including independent component analysis. *J. Neurosci. Methods* **134,** 9–21 (2004).

158. Delorme, A., Sejnowski, T. & Makeig, S. Enhanced detection of artifacts in EEG data using higher-order statistics and independent component analysis. *Neuroimage* **34,** 1443–1449 (2007).

159. Murias, M., Swanson, J. M. & Srinivasan, R. Functional connectivity of frontal cortex in healthy and ADHD children reflected in EEG coherence. *Cereb. cortex* **17,** 1788–1799 (2007).

160. Srinivasan, R., Winter, W. R., Ding, J. & Nunez, P. L. EEG and MEG coherence: measures of functional connectivity at distinct spatial scales of neocortical dynamics. *J. Neurosci. Methods* **166,** 41–52 (2007).

161. Saltzberg, B., Burton, W. D., Burch, N. R., Fletcher, J. & Michaels, R. Electrophysiological measures of regional neural interactive coupling. Linear and non-linear dependence relationships among multiple channel electroencephalographic recordings. *Int. J. Biomed. Comput.* **18,** 77–87 (1986).

162. Mima, T., Matsuoka, T. & Hallett, M. Functional coupling of human right and left cortical motor areas demonstrated with partial coherence analysis. *Neurosci. Lett.* **287,** 93–6 (2000).

163. Roopun, A. K. *et al.* A beta2-frequency (20-30 Hz) oscillation in nonsynaptic networks of somatosensory cortex. *Proc. Natl. Acad. Sci. U. S. A.* **103,** 15646–50 (2006).

164. Halsband, U. & Lange, R. K. Motor learning in man: a review of functional and clinical studies. *J. Physiol. Paris* **99,** 414–24 (2006).

165. Hardwick, R., Rottschy, C., Miall, R. & Eickhoff, S. A quantitative meta-analysis and review of motor learning in the human brain. *Neuroimage* **67,** 283–97 (2013).

166. McIntosh, A., Chau, W. & Protzner, A. Spatiotemporal analysis of event-related fMRI data using partial least squares. *Neuroimage* **23,** 764–75 (2004).

167. Krishnan, A., Williams, L. J., McIntosh, A. R. & Abdi, H. Partial Least Squares (PLS) methods for neuroimaging: a tutorial and review. *Neuroimage* **56,** 455–75 (2011).

168. Andersson, C. A. & Bro, R. The N-way Toolbox for MATLAB. *Chemom. Intell. Lab. Syst.* **52,** 1–4 (2000).

169. Westerhuis, J. A., de Jong, S. & Smilde, A. K. Direct orthogonal signal correction. *Chemom. Intell. Lab. Syst.* **56,** 13–25 (2001).

170. Svensson, O., Kourti, T. & MacGregor, J. An investigation of orthogonal signal correction algorithms and their characteristics. *J. Chemom.* **16,** 176–188 (2002).

171. Krishnan, L., Kang, A., Sperling, G. & Srinivasan, R. Neural strategies for selective attention distinguish fast-action video game players. *Brain Topogr.* **26,** 83–97 (2013).

172. Esteban-Diez, I., Gonzalez-Saiz, J. & Pizarro, C. An evaluation of orthogonal signal correction methods for the characterisation of arabica and robusta coffee varieties by NIRS. *Anal. Chim. Acta* **514,** 57–67 (2004).

173. Williams, H. *et al.* Characterization of Inflammatory Bowel Disease With Urinary Metabolic Profiling. *Am. J. Gastroenterol.* **104,** 1435–1444 (2009).

174. Ganguly, K. *et al.* Cortical representation of ipsilateral arm movements in monkey and man. *J. Neurosci.* **29,** 12948–56 (2009).

175. Supekar, K. *et al.* Neural predictors of individual differences in response to math tutoring in primary-grade school children. *Proc. Natl. Acad. Sci.* **110,** 8230–8235 (2013).

176. McIntosh, A. & Lobaugh, N. Partial least squares analysis of neuroimaging data: applications and advances. *Neuroimage* **23 Suppl 1,** S250–63 (2004).

177. Chao, Z. C., Nagasaka, Y. & Fujii, N. Long-term asynchronous decoding of arm motion using electrocorticographic signals in monkeys. *Front. Neuroeng.* **3,** 3 (2010).

178. Khodayari-Rostamabad, A., Hasey, G., MacCrimmon, D., Reilly, J. & de Bruin, H. A pilot study to determine whether machine learning methodologies using pre-treatment electroencephalography can predict the symptomatic response to clozapine therapy. *Clin. Neurophysiol.* **121,** 1998–2006 (2010).

179. Chiang, J., Wang, Z. & McKeown, M. A multiblock PLS model of cortico-cortical and corticomuscular interactions in Parkinson's disease. *Neuroimage* **63,** 1498–1509 (2012).

180. Langer, N. *et al.* Functional brain network efficiency predicts intelligence. *Hum. Brain Mapp.* **33,** 1393–406 (2011).

181. Lin, C.-L., Shaw, F.-Z., Young, K.-Y., Lin, C.-T. & Jung, T.-P. EEG correlates of haptic feedback in a visuomotor tracking task. *Neuroimage* **60,** 2258–73 (2012).

182. Ma, L., Narayana, S., DA, R., Fox, P. & Xiong, J. Changes occur in resting state network of motor system during 4 weeks of motor skill learning. *Neuroimage* **58,** 226–233 (2010).

183. O'Shea, J., Sebastian, C., Boorman, E. D., Johansen-Berg, H. & Rushworth, M. F. S. Functional specificity of human premotor-motor cortical interactions during action selection. *Eur. J. Neurosci.* **26,** 2085–95 (2007).

184. Ward, N. S. Compensatory mechanisms in the aging motor system. *Ageing Res. Rev.* **5,** 239–54 (2006).

185. Grafton, S. T., Schmitt, P., Van Horn, J. & Diedrichsen, J. Neural substrates of visuomotor learning based on improved feedback control and prediction. *Neuroimage* **39,** 1383–95 (2008).

186. Ryynänen, O. R. M., Hyttinen, J. a K., Laarne, P. H. & Malmivuo, J. a. Effect of electrode density and measurement noise on the spatial resolution of cortical potential distribution. *IEEE Trans. bio-medical Eng.* **51,** 1547–54 (2004).

187. Nunez, P. & Westdorp, A. The surface Laplacian, high resolution EEG and controversies. *Brain Topogr.* **6,** 221–6 (1994).

188. Srinivasan, R., Nunez, P. L. & Silberstein, R. B. Spatial filtering and neocortical dynamics: estimates of EEG coherence. *IEEE Trans. Biomed. Eng.* **45,** 814–26 (1998).

189. Engel, A. *et al.* Inter-individual differences in audio-motor learning of piano melodies and white matter fiber tract architecture. *Hum. Brain Mapp.* **35,** 2483–97 (2014).

190. Noohi, F. *et al.* Association of COMT val158met and DRD2 G>T genetic polymorphisms with individual differences in motor learning and performance in female young adults. *J. Neurophysiol.* (2013). doi:10.1152/jn.00457.2013

191. Schlaug, G., Knorr, U. & Seitz, R. Inter-subject variability of cerebral activations in acquiring a motor skill: a study with positron emission tomography. *Exp. brain Res.* **98,** 523–34 (1994).

192. Gaab, N., Gaser, C. & Schlaug, G. Improvement-related functional plasticity following pitch memory training. *Neuroimage* **31,** 255–63 (2006).

193. Van den Heuvel, M. P. & Hulshoff Pol, H. E. Exploring the brain network: a review on resting-state fMRI functional connectivity. *Eur. Neuropsychopharmacol.* **20,** 519–34 (2010).

194. Sharma, N., Baron, J. C. & Rowe, J. B. Motor imagery after stroke: relating outcome to motor network connectivity. *Ann. Neurol.* **66,** 604–616 (2009).

195. Ventura-Campos, N. *et al.* Spontaneous Brain Activity Predicts Learning Ability of Foreign Sounds. *J. Neurosci.* **33,** 9295–9305 (2013).

196. Zatorre, R. J. Predispositions and plasticity in music and speech learning: neural correlates and implications. *Science* **342,** 585–9 (2013).

197. Martin, A., Barnes, K. A. & Stevens, W. D. Spontaneous neural activity predicts individual differences in performance. *Proc. Natl. Acad. Sci. U. S. A.* **109,** 3201–2 (2012).

198. Van Wijk, B. C. M., Beek, P. J. & Daffertshofer, A. Neural synchrony within the motor system: what have we learned so far? *Front. Hum. Neurosci.* **6,** 252 (2012).

199. Jasper, H. & Penfield, W. Electrocorticograms in man: Effect of voluntary movement upon the electrical activity of the preeentral gyrus. *Arch. Psychiatr. Nervenkr.* **183,** 163–174 (1949).

200. Wu, J., Srinivasan, R., Kaur, A. & Cramer, S. Resting-state cortical connectivity predicts motor skill acquisition. *Neuroimage* **91,** 84–90 (2014).

201. Bischoff-Grethe, A., Goedert, K. M., Willingham, D. T. & Grafton, S. T. Neural substrates of response-based sequence learning using fMRI. *J. Cogn. Neurosci.* **16,** 127–38 (2004).

202. Oldfield, R. C. The assessment and analysis of handedness: The Edinburgh Inventory. *Neuropsychologia* **9,** 97–113 (1971).

203. Honda, M. *et al.* Dynamic cortical involvement in implicit and explicit motor sequence learning. A PET study. *Brain* **121 (Pt 1,** 2159–73 (1998).

204. George, J. S. *et al.* Dopaminergic therapy in Parkinson's disease decreases cortical beta band coherence in the resting state and increases cortical beta band power during executive control. *NeuroImage. Clin.* **3,** 261–70 (2013).

205. Muellbacher, W. *et al.* Early consolidation in human primary motor cortex. *Nature* **415,** 640–4 (2002).

206. Sanes, J. N. Neocortical mechanisms in motor learning. *Curr. Opin. Neurobiol.* **13,** 225–231 (2003).

207. Homan, R., Herman, J. & Purdy, P. Cerebral location of international 10-20 system electrode placement. *Electroencephalogr. Clin. Neurophysiol.* **66,** 376–382 (1987).

208. Andersson, C. A. & Bro, R. The N -way Toolbox for MATLAB. *Chemom. Intell. Lab. Syst.* **52,** 3–6 (2000).

209. McIntosh, A. R., Bookstein, F. L., Haxby, J. V & Grady, C. L. Spatial pattern analysis of functional brain images using partial least squares. *Neuroimage* **3,** 143–57 (1996).

210. Kang, L., Liu, A. & Tian, L. Linear combination methods to improve diagnostic/prognostic accuracy on future observations. *Stat. Methods Med. Res.* (2013). doi:10.1177/0962280213481053

211. Huang, X., Qin, G. & Fang, Y. Optimal Combinations of Diagnostic Tests Based on AUC. *Biometrics* **67,** 568–76 (2011).

212. Willingham, D. B. A neuropsychological theory of motor skill learning. *Psychol. Rev.* **105,** 558–84 (1998).

213. Grafton, S. T., Hazeltine, E. & Ivry, R. Functional Mapping of Sequence Learning in Normal Humans. *J. Cogn. Neurosci.* **7,** 497–510 (1995).

214. Kantak, S. S. & Winstein, C. J. Learning-performance distinction and memory processes for motor skills: a focused review and perspective. *Behav. Brain Res.* **228,** 219–31 (2012).

215. Wolf, S. L. *et al.* Effect of constraint-induced movement therapy on upper extremity function 3 to 9 months after stroke: the EXCITE randomized clinical trial. *J. Am. Med. Assoc.* **296,** 2095–104 (2006).

216. Jenkins, I. H., Brooks, D. J., Frackowiak, R. S. J. & Passingham, F. E. Motor Sequence Tomography Learning : A Study with Positron. *J. Neurosci.* **14,** (1994).

217. Bapi, R. S., Miyapuram, K. P., Graydon, F. X. & Doya, K. fMRI investigation of cortical and subcortical networks in the learning of abstract and effector-specific representations of motor sequences. *Neuroimage* **32,** 714–27 (2006).

218. Graydon, F. X., Friston, K. J., Thomas, C. G., Brooks, V. B. & Menon, R. S. Learning-related fMRI activation associated with a rotational visuo-motor transformation. *Brain Res.* **22,** 373–83 (2005).

219. Seitz, R., Roland, P., Bohm, C., Greitz, T. & Stone-Elanders, S. Motor learning in man: a positron emission tomographic study. *Neuroreport* 57–66 (1990).

220. Shadmehr, R. & Holcomb, H. H. Neural correlates of motor memory consolidation. *Science* **277,** 821–5 (1997).

221. Rathore, S. S., Hinn, A. R., Cooper, L. S., Tyroler, H. A. & Rosamond, W. D. Characterization of incident stroke signs and symptoms: findings from the atherosclerosis risk in communities study. *Stroke* **33,** 2718–2721 (2002).

222. Cramer, S. C. Repairing the human brain after stroke. II. Restorative therapies. *Ann. Neurol.* **63,** 549–60 (2008).

223. Zhu, L. L., Lindenberg, R., Alexander, M. P. & Schlaug, G. Lesion load of the corticospinal tract predicts motor impairment in chronic stroke. *Stroke* **41,** 910–915 (2010).

224. Johansen-Berg, H. *et al.* Correlation between motor improvements and altered fMRI activity after rehabilitative therapy. *Brain* **125,** 2731–42 (2002).

225. Schaechter, J. *et al.* Increase in sensorimotor cortex response to somatosensory stimulation over subacute poststroke period correlates with motor recovery in hemiparetic patients. *Neurorehabil. Neural Repair* **26,** 325–334 (2012).

226. Carter, A. R., Shulman, G. L. & Corbetta, M. Why use a connectivity-based approach to study stroke and recovery of function? *Neuroimage* **62,** 2271–80 (2012).

227. Grefkes, C. & Fink, G. R. Reorganization of cerebral networks after stroke: new insights from neuroimaging with connectivity approaches. *Brain* **134,** 1264–76 (2011).

228. Grefkes, C. *et al.* Cortical connectivity after subcortical stroke assessed with functional magnetic resonance imaging. *Ann. Neurol.* **63,** 236–246 (2008).

229. De Vico Fallani, F. *et al.* Evaluation of the brain network organization from EEG signals: a preliminary evidence in stroke patient. *Anat. Rec.* **292,** 2023–31 (2009).

230. Van Meer, M. *et al.* Recovery of sensorimotor function after experimental stroke correlates with restoration of resting-state interhemispheric functional connectivity. *J. Neurosci.* **30,** 3964–3972 (2010).

231. Sharma, N., Baron, J.-C. & Rowe, J. B. Motor imagery after stroke: relating outcome to motor network connectivity. *Ann. Neurol.* **66,** 604–16 (2009).

232. James, G. A. *et al.* Changes in resting state effective connectivity in the motor network following rehabilitation of upper extremity poststroke paresis. *Top Stroke Rehabil* **16,** 270–281 (2009).

233. Carey, L. M. *et al.* Evolution of brain activation with good and poor motor recovery after stroke. *Neurorehabil Neural Repair* **20,** 24–41 (2006).

234. Seitz, R. J. *et al.* Role of the premotor cortex in recovery from middle cerebral artery infarction. *Arch. Neurol.* **55,** 1081–8 (1998).

235. Mihara, M. *et al.* Near-infrared spectroscopy-mediated neurofeedback enhances efficacy of motor imagery-based training in poststroke victims: a pilot study. *Stroke* **44,** 1091–8 (2013).

236. Johansen-Berg, H. *et al.* The role of ipsilateral premotor cortex in hand movement after stroke. *Proc. Natl. Acad. Sci.* **99,** 14518–14523 (2002).

237. Loubinoux, I. *et al.* Correlation between cerebral reorganization and motor recovery after subcortical infarcts. *Neuroimage* **20,** 2166–2180 (2003).

238. Wei, W. *et al.* A longitudinal study of hand motor recovery after sub-acute stroke: a study combined FMRI with diffusion tensor imaging. *PLoS One* **8,** e64154 (2013).

239. See, J. *et al.* A Standardized Approach to the Fugl-Meyer Assessment and Its Implications for Clinical Trials. *Neurorehabil. Neural Repair* (2013).

240. Menzies, L. *et al.* Neurocognitive endophenotypes of obsessive-compulsive disorder. *Brain* **130,** 3223–3236 (2007).

241. Burke, E. *et al.* A multimodal approach to understanding motor impairment and disability after stroke. *J. Neurol.* (2014).

242. Dawes, H. *et al.* Walking performance and its recovery in chronic stroke in relation to extent of lesion overlap with the descending motor tract. *Exp. Brain Res.* **186,** 325–333 (2008).

243. Dodakian, L. *et al.* Targeted engagement of a dorsal premotor circuit in the treatment of post-stroke paresis. *NeuroRehabilitation* **33,** 13–24 (2013).

244. Saleh, S., Adamovich, S. V & Tunik, E. Resting state functional connectivity and task-related effective connectivity changes after upper extremity rehabilitation: a pilot study. in *Annu. Int. Conf. IEEE Eng. Med. Biol. Soc.* **2012,** 4559–62 (2012).

245. Wang, L. *et al.* Dynamic functional reorganization of the motor execution network after stroke. *Brain* **133,** 1224–1238 (2010).

246. Park, C. *et al.* Longitudinal changes of resting-state functional connectivity during motor recovery after stroke. *Stroke* **42,** 1357–62 (2011).

247. Ward, N. S., Brown, M. M., Thompson, A. J. & Frackowiak, R. S. Neural correlates of motor recovery after stroke: a longitudinal fMRI study. *Brain* **126,** 2476–2496 (2003).

248. Cramer, S. & Crafton, K. Somatotopy and movement representation sites following cortical stroke. *Exp. brain Res.* **168,** 25–32 (2006).

249. Marshall, R. S. *et al.* Early imaging correlates of subsequent motor recovery after stroke. *Ann. Neurol.* **65,** 596–602 (2009).

250. Murase, N., Duque, J., Mazzocchio, R. & Cohen, L. G. Influence of interhemispheric interactions on motor function in chronic stroke. *Ann. Neurol.* **55,** 400–409 (2004).

251. Jiang, T., He, Y., Zang, Y. & Weng, X. Modulation of functional connectivity during the resting state and the motor task. *Hum. Brain Mapp.* **22,** 63–71 (2004).

252. Chen, R., Gerloff, C., Hallett, M. & Cohen, L. G. Involvement of the ipsilateral motor cortex in finger movements of different complexities. *Ann. Neurol.* **41,** 247–254 (1997).

253. Yin, D. *et al.* Altered topological properties of the cortical motor-related network in patients with subcortical stroke revealed by graph theoretical analysis. *Hum. Brain Mapp.* **35,** 3343–59 (2014).

254. Pineiro, R., Pendlebury, S., Johansen-Berg, H. & Matthews, P. Functional MRI detects posterior shifts in primary sensorimotor cortex activation after stroke: evidence of local adaptive reorganization? *Stroke* **32,** 1134–9. (2001).

255. Várkuti, B. *et al.* Resting state changes in functional connectivity correlate with movement recovery for BCI and robot-assisted upper-extremity training after stroke. *Neurorehabil. Neural Repair* **27,** 53–62 (2013).

256. Bath, P. M. W. *et al.* Statistical Analysis of the Primary Outcome in Acute Stroke Trials. *Stroke* 1171–1178 (2012). doi:10.1161/STROKEAHA.111.641456

257. Sulzer, J. *et al.* Real-time fMRI neurofeedback: progress and challenges. *Neuroimage* **76,** 386–99 (2013).

258. Menezes, N. *et al.* The real estate factor: quantifying the impact of infarct location on stroke severity. *Stroke* **38,** 194–7 (2007).

259. Saver, J. *et al.* Infarct volume as a surrogate or auxiliary outcome measure in ischemic stroke clinical trials. The RANTTAS Investigators. *Stroke* **30,** 293–298 (1999).

260. Stinear, C. M. & Ward, N. S. How useful is imaging in predicting outcomes in stroke rehabilitation? *Int. J. stroke* **8,** 33–7 (2013).

261. Kerr, A. L., Cheng, S. Y. & Jones, T. A. Experience-dependent neural plasticity in the adult damaged brain. *J. Commun. Disord.* **44,** 538–548 (2011).

262. Di Piero, V., Chollet, F. M., MacCarthy, P., Lenzi, G. L. & Frackowiak, R. S. Motor recovery after acute ischaemic stroke: a metabolic study. *J. Neurol. Neurosurg. Psychiatry* **55,** 990–996 (1992).

263. Saur, D. *et al.* Early functional magnetic resonance imaging activations predict language outcome after stroke. *Brain* **133,** 1252–64 (2010).

264. Di Lazzaro, V. *et al.* Motor cortex plasticity predicts recovery in acute stroke. *Cereb. cortex* **20,** 1523–8 (2010).

265. Astrup, J., Symon, L., Branston, N. M. & Lassen, N. a. Cortical evoked potential and extracellular K+ and H+ at critical levels of brain ischemia. *Stroke* **8,** 51–7 (1977).

266. Tucker, D. Spatial sampling of head electrical fields: the geodesic sensor net. *Electroencephalogr. Clin. Neurophysiol.* **87,** 154–63 (1993).

267. Petrov, Y. *et al.* Ultra-dense EEG sampling results in two-fold increase of functional brain information. *Neuroimage* **90,** 140–5 (2014).

268. Giacino, J. T., Fins, J. J., Laureys, S. & Schiff, N. D. Disorders of consciousness after acquired brain injury: the state of the science. *Nat. Rev. Neurol.* **10,** 99–114 (2014).

269. Wu, J. *et al.* Connectivity measures are robust biomarkers of cortical function and plasticity after stroke. *Brain* (In press)

270. Finnigan, S. & van Putten, M. J. a M. EEG in ischaemic stroke: quantitative EEG can uniquely inform (sub-)acute prognoses and clinical management. *Clin. Neurophysiol.* **124,** 10–9 (2013).

271. Stradling, D. *et al.* Stroke care delivery before vs after JCAHO stroke center certification. *Neurology* **68,** 469–470 (2007).

272. Lyden, P., Claesson, L., Havstad, S., Ashwood, T. & Lu, M. Factor analysis of the National Institutes of Health Stroke Scale in patients with large strokes. *Arch Neurol* **61,** 1677–1680 (2004).

273. Jones, T. A. *et al.* Remodeling the brain with behavioral experience after stroke. *Stroke* **40,** S136–8 (2009).

274. Nudo, R. J. Neural bases of recovery after brain injury. *J. Commun. Disord.* **44,** 515–520 (2011).

275. Tecchio, F. *et al.* Outcome prediction in acute monohemispheric stroke via magnetoencephalography. *J. Neurol.* **254,** 296–305 (2007).

276. Platz, T. *et al.* Amphetamine fails to facilitate motor performance and to enhance motor recovery among stroke patients with mild arm paresis: interim analysis and termination of a double blind, randomised, placebo-controlled trial. *Restor Neurol Neurosci* **23,** 271–280 (2005).

277. Shuaib, A. *et al.* NXY-059 for the treatment of acute ischemic stroke. *N Engl J Med* **357,** 562–571 (2007).

278. Treig, T., Werner, C., Sachse, M. & Hesse, S. No benefit from D-amphetamine when added to physiotherapy after stroke: a randomized, placebo-controlled study. *Clin Rehabil* **17,** 590–599 (2003).

279. Diaconescu, A. O. *et al.* Distinct functional networks associated with improvement of affective symptoms and cognitive function during citalopram treatment in geriatric depression. *Hum. Brain Mapp.* **32,** 1677–91 (2011).

280. Lehmann, C. *et al.* Application and comparison of classification algorithms for recognition of Alzheimer's disease in electrical brain activity (EEG). *J. Neurosci. Methods* **161,** 342–50 (2007).

281. McKeown, M. & Sejnowski, T. Independent component analysis of fMRI data: examining the assumptions. *Hum. Brain Mapp.* **6,** 368–72 (1998).

282. O'Shea, J., Johansen-Berg, H., Trief, D., Göbel, S. & Rushworth, M. F. S. Functionally specific reorganization in human premotor cortex. *Neuron* **54,** 479–90 (2007).

APPENDIX

List of abbreviations and definitions

ANCOVA	analysis of covariance
ANOVA	analysis of variance
b	magnetic (induction) field in an MR system
beta	20-30 Hz frequencies
BSI	Brain Symmetry Index
C3	left M1 electrode
C4	right M1 electrode
CBF	cerebral blood flow
cc	cubic centimeter
CST	corticospinal tract
CST injury	percent of the CST affect by stroke
DAR	delta alpha ratio
dEEG	dense-array electroencephalography
delta	1-3 Hz frequencies
DTABR	delta theta alpha beta ratio
DWI	Diffusion Weighted Imaging
EEG	electroencephalography
EGI	Electrical Geodesics, Inc.
ER	emergency room
F3	left frontal-premotor electrode
fft	fast fourier transform

FM	upper extremity Fugl-Meyer assessment
fMRI	functional Magnetic Resonance Imaging
Fz	frontal electrode
gamma	31-50 Hz frequencies
GDS	Geriatric Depression Scale
Hz	hertz
ICA	independent component analysis
ICU	intensive care unit
IQR	inter-quartile range
lower beta	15-19 Hz frequencies
M1	primary motor cortex
MEG	magnetoencephalography
MMSE	Mini Mental Status Exam
MNI	Montreal Neurological Institute
MRI	Magnetic Resonance Imaging
ms	millisecond
mu	11-14 Hz frequencies
NIHSS	National Institute of Health Stroke Scale
PAR	left parietal operculum (Chapter 3)
PAR	ipsilesional parietal cortex (Chapter 4)
PARoperc	ipsilesional parietal operculum
PET	Positron Emission Tomography
PLS	partial least squares

PM	premotor cortex
P3	left parietal electrode
Pr	parietal cortex
Pz	parietal electrode
QEEG	quantitative EEG
ROI	region of interest
RP	rotor pursuit
r-tPA	recombinant tissue plasminogen activator
S1	left medial sensory region
SD	standard deviation
TE	echo time
theta	4-6 Hz frequencies
tPA	tissue plasminogen activator
TR	repetition time
WT	wrist targeting